

**THE DENSIFICATION AND SINTERING  
BEHAVIOUR OF MOLTEN SALT SYNTHESIZED  
HA WHISKER/HA COMPOSITES**

**A Thesis Submitted to  
The Graduate School of Engineering and Sciences of  
İzmir Institute of Technology  
in Partial Fulfillment of the Requirements for the Degree of**

**MASTER OF SCIENCE**

**in Materials Science and Engineering**

**by  
Suat Bahar BOZKURT**

**September 2005  
İZMİR**

We approve the thesis of **Suat Bahar BOZKURT**

**Date of Signature**

.....  
**Prof. Dr. Muhsin ÇİFTÇİOĞLU**  
Supervisor  
Department of Chemical Engineering  
Izmir Institute of Technology

**20 September 2005**

.....  
**Prof. Dr. Şebnem HARSA**  
Co-Supervisor  
Department of Food Engineering  
Izmir Institute of Technology

**20 September 2005**

.....  
**Assoc. Prof. Dr. Metin TANOĞLU**  
Department of Mechanical Engineering  
Izmir Institute of Technology

**20 September 2005**

.....  
**Assoc. Prof. Dr. Sedat AKKURT**  
Department of Mechanical Engineering  
Izmir Institute of Technology

**20 September 2005**

.....  
**Asst. Prof. Dr. Oğuz BAYRAKTAR**  
Department of Chemical Engineering  
Izmir Institute of Technology

**20 September 2005**

.....  
**Prof. Dr. Muhsin ÇİFTÇİOĞLU**  
Head of Materials Science and Engineering Program  
Izmir Institute of Technology

**20 September 2005**

.....  
**Assoc. Prof. Dr. Semahat Özdemir**  
Head of the Graduate School

## **ACKNOWLEDGEMENTS**

I would like to thank and express my deepest gratitude to Prof. Dr. Muhsin iftiođlu for his supervision, guidance and encouragement through my study. I also wish to thank to Prof. Dr. Őebnem Harsa for her valuable suggestions and comments about this thesis.

I am very grateful to specialist Rukiye iftiođlu for her endless help, support and tolerance in the laboratory work.

Thanks indeed to Center for Material Research staff for their cooperation and preservance during this study.

Special thanks to my dear roommates Alev GneŐ and Gzde Gen for their understanding, kindness and friendship.

Finally I would like to thank to my family members Asım, Azade, Pınar and Behet Bozkurt for their excellent support, encouragment and patience during this study.

## ABSTRACT

The hydroxyapatite (HA) whiskers were used as reinforcements in the HA powder/HA whisker (HAp/HAw) composites. The HAw was synthesized with molten salt synthesis method (MSS). NaCl, K<sub>2</sub>SO<sub>4</sub> and NaCl-K<sub>2</sub>SO<sub>4</sub> fluxes and HA powders were used for the synthesis of HA whiskers. The effects of various salt/HA ratios, heat treatment temperatures and time were investigated. In order to enhance the dispersibility and the elimination of the powder agglomerates ultrasonic treatment was applied to the HA-salt powder mixtures before heat treatment. Scanning electron microscopy (SEM) and X-ray diffraction (XRD) techniques were used for the examination of the whiskers.

The synthesized whiskers by using NaCl had a broad particle size range (0.25 to 40 μm in length and 0.2 to 20 μm in diameter) and similar morphologies. They had relatively larger diameters than those suitable for use as reinforcements in the HAp/HAw composites. The use of K<sub>2</sub>SO<sub>4</sub> resulted in the formation of relatively uniform and thinner HA whiskers. The length and diameter of the whiskers varied from 5 to 90 μm and 0.5 to 10 μm, respectively. The whiskers prepared from NaCl-K<sub>2</sub>SO<sub>4</sub> salt mixture were 12 to 110 μm in length and 0.5 to 25 μm in diameter. The HA whiskers, synthesized from NaCl-K<sub>2</sub>SO<sub>4</sub> salt mixture and HA powder at 850°C, were selected as reinforcements for the composites because of their uniform morphology and dimensional properties.

For the preparation of HAp/HAw composites, HA powder was ball milled and mixed with HAw in aqueous medium with the application of 2 h ultrasonic treatment. The HAp/ 0%-50% HAw composites were formed by dry pressing and slip casting techniques. Sintering was carried out at 1200-1350°C range for 2 h. Pure HA powder shrunk more than the composites at all sintering temperatures and attained to 98.5% theoretical density at 1350°C. Although the density increases with sintering temperature, the density increase relative to the green structures decreases with whisker content at each sintering temperature. This may be attributed to the low shrinkage rate due to the presence of whiskers at high temperatures. The HA whiskers could be observed as embedded in the fine HA matrix for both slip cast and dry pressed samples from the SEM images. It was observed that the whiskers generally aligned in one direction except the 50% HAw-50% HAp composites.

## ÖZET

Hidroksiapatit (HA) viskerleri, HA tozu ve HA viskerlerinden oluşan kompozitlerde mukavemetlendirici olarak kullanılmaktadır. HA viskerleri eriyik tuz yöntemiyle sentezlenmiştir. Bu metod için, NaCl, K<sub>2</sub>SO<sub>4</sub> ve NaCl - K<sub>2</sub>SO<sub>4</sub> tuz karışımı olmak üzere üç farklı çözücü malzeme denenmiştir. Hidroksiapatit ise çözünen madde olarak kullanılmıştır. Tuz ve HA karışımı, dağılım özelliklerini iyileştirmek ve aglomerasyonları önlemek amacıyla, ultrasonik muameleye tabi tutulmuştur. Taramalı elektron mikroskobu (SEM) ve X-ışın kırınımı (XRD) analizleri viskerlerin mikroyapılarını açığa çıkarmak için kullanılmıştır. NaCl tuzu kullanılarak sentezlenen viskerler geniş bir partikül dağılım aralığında (0.25-40 µm boy ve 0.2-20 µm çap) olup farklı morfolojilere göstermektedir. Bu viskerler HA tozu-HA visker kompozitleri için ideal olandan daha büyük çaplara sahiptir. K<sub>2</sub>SO<sub>4</sub> kullanımı sonucu nispeten daha ince ve birbirine benzer şekilde olan viskerler sentezlenmiştir. Oluşturulan bu viskerlerin boyu 5 ile 90 µm ve çapları da 0.5 ile 10 µm aralığındadırlar. NaCl-K<sub>2</sub>SO<sub>4</sub> tuzu kullanılarak hazırlanan viskerlerin boy ve çapları ise sırasıyla 12-110 µm ve 0.5-25 µm aralığında değişmektedir. Eriyik NaCl-K<sub>2</sub>SO<sub>4</sub> tuz karışımı ortamında oluşan ve 850°C'de ıslık işleme uğrayarak meydana gelen viskerler, uygun morfolojilerinden ve boyutsal özelliklerinden dolayı kompozitler için mukavemetlendirici olarak seçilmişlerdir.

Ufak toparlarla öğütülen HA tozu, 0%-50% hacimsel oranda HA viskeriyle karıştırılmış ve bu karışım sulu ortamda iki saat boyunca ultrasonik işleme tabi tutulmuştur. Oluşturulan HA - HA visker kompozitleri kuru presleme ve alçı döküm teknikleri ile şekillendirilmiştir. Sinterleme 1200-1350°C sıcaklık aralığında iki saatlik bekleme zamanıyla gerçekleştirilmiştir. Saf HA tozu, kompozitlere oranla her sıcaklıkta daha fazla büzülme göstermiş ve 1350°C'de %98.5'lik teorik yoğunluğa ulaşmıştır. Kompozit içinde visker miktarı artışının tüm sinterleme sıcaklıklarında göreceli yoğunluk azalışına yol açtığı görülmüştür. Yüksek sıcaklıklarda gerçekleşen bu durum visker varlığından kaynaklanan düşük büzülme oranına bağlanabilir. Gerek alçı döküm gerekse kuru presleme ile şekillendirilen kompozitlerde viskerlerin matriks içinde gömülü olduğu SEM fotoğraflarından gözlenmiştir. Ayrıca 50%HAw-50%HAp dışındaki kompozitlerde viskerlerin genellikle tek yönde dağılım gösterdikleri görülmüştür.

# TABLE OF CONTENTS

LIST OF FIGURES .....	vii
LIST OF TABLES .....	xi
CHAPTER 1. INTRODUCTION .....	1
CHAPTER 2. BIOMATERIALS .....	3
2.1. Bone .....	7
2.1.1. Structure of Bone .....	7
2.1.2 Mechanical Properties of Bone.....	9
CHAPTER 3. HYDROXYAPATITE BASED MATERIALS.....	11
3.1. Hydroxyapatite (HA) .....	11
3.2. Preparation of HA Powder.....	12
3.3. Production of HA Whiskers.....	13
3.3.1. Molten Salt Synthesis (MSS).....	14
3.4. Formation Techniques of HA Ceramics .....	20
3.4.1 Slip Casting of HA Ceramics.....	20
3.5. Densification and Sintering Behaviour of Pure HA Ceramics .....	21
3.5.1. Densification and Sintering Behaviour of HAp/Haw Composites.....	24
CHAPTER 4. EXPERIMENTAL.....	24
4.1. Materials .....	25
4.2. Methods .....	25
4.2.1. Synthesis of HA .....	25
4.2.2. Molten Salt Synthesis of HA Whiskers .....	25
4.3. Formation of HAp/HAw Composites .....	27
4.3.1. Slip Casting of HAp/HAw Composites .....	27
4.3.2. Dry Pressing of HAp/HAw Composites.....	28
4.4. Characterization of HA Whiskers and HAp/HAw Composites.....	29

CHAPTER 5. RESULTS AND DISCUSSION.....	30
5.1. Characterization of HA Powder and HA Whiskers .....	30
5.2. The Densification and Sintering Behaviour of Pure HA and HAp/HAw Composites .....	63
5.3. Characterization of Pure HA and HAp/HAw Composites .....	67
 CHAPTER 6. CONCLUSIONS .....	 76
 REFERENCES .....	 78

## LIST OF FIGURES

<u>Figure</u>	<u>Page</u>
Figure 2.1. Microscopic structure of bone .....	8
Figure 2.2. Stress-strain curve of human compact bone according to (a) strain rate (b) tension-compression test .....	9
Figure 3.1. Crystal structure of hydroxyapatite.....	11
Figure 3.2. Schematic illustration of MSS process for the formation of perovskite phase with increasing temperature .....	15
Figure 3.3. SEM photograph of needle-like mullite particles heated at 1100°C for 3 h.....	16
Figure 3.4. SEM photograph of carbonate apatite single-crystal obtained at 1400°C for 1 h at 55 MPa and exposed to oscillation.....	16
Figure 3.5. SEM of BaNd <sub>2</sub> Ti <sub>4</sub> O <sub>12</sub> powder prepared at (a)1100°C (b)1450°C.....	17
Figure 3.6. SEM micrographs of CaSiO <sub>3</sub> whiskers prepared from (a) NaCl (b) KCl (c) NaCl+KCl fluxes (scale bar=10µm) treated at 900°C for 24 h.....	18
Figure 3.7. (a) HA whiskers from K <sub>2</sub> SO <sub>4</sub> at 1300°C for 9 h (b) HA crystals from KCl at 880°C for 3 h (c) HA whiskers from K <sub>2</sub> SO <sub>4</sub> at 1100°C for 0.5 h.....	19
Figure 5.1. XRD pattern of commercial HA powder.....	30
Figure 5.2. SEM image of commercial HA powder .....	31
Figure 5.3. XRD patterns of NW4, NW5, NW6 whiskers where NaCl/HA ratio during preparation was 1/1 .....	33
Figure 5.4. XRD patterns of NW7, NW8 and NW9 whiskers where NaCl/HA ratio during preparation was 3/1 .....	33
Figure 5.5. SEM image of NW1 whiskers synthesized at 800°C where NaCl/HA ratio during preparation was 1/3.....	34

Figure 5.6.	SEM image of NW2 whiskers synthesized at 1000°C where NaCl/HA ratio during preparation was 1/3 .....	35
Figure 5.7.	SEM image of NW5 whiskers synthesized at 1000°C where NaCl/HA ratio during preparation was 1/1 .....	35
Figure 5.8.	SEM image of NW8 whiskers synthesized at 1000°C where NaCl/HA ratio during preparation was 3/1 .....	36
Figure 5.9.	SEM image of NW6 whiskers synthesized at 1100°C where NaCl/HA ratio during preparation was 1/1 .....	38
Figure 5.10.	SEM image of NW3 whiskers synthesized at 1100°C where NaCl/HA ratio during preparation was 1/3 .....	38
Figure 5.11.	The XRD patterns of HA-K <sub>2</sub> SO <sub>4</sub> whiskers at 1100°C (K <sub>2</sub> SO <sub>4</sub> /HA:3/1) .....	39
Figure 5.12.	SEM image of dry mixed KW1 whiskers synthesized at 1100°C where K <sub>2</sub> SO <sub>4</sub> /HA ratio during preparation was 1/1 .....	41
Figure 5.13.	SEM image of dry mixed KW2 whiskers synthesized at 1100 where K <sub>2</sub> SO <sub>4</sub> /HA ratio during preparation was 2/1 .....	41
Figure 5.14.	SEM image of dry mixed KW3 whiskers synthesized at 1100°C where K <sub>2</sub> SO <sub>4</sub> /HA ratio during preparation was 3/1 .....	42
Figure 5.15.	SEM image of dry mixed KW4 whiskers synthesized at 1100°C where K <sub>2</sub> SO <sub>4</sub> /HA ratio during preparation was 4/1 .....	42
Figure 5.16.	The XRD pattern of synthesized HA powder .....	43
Figure 5.17.	EDX image of wet mixed commercial HA powder KW7 whiskers synthesized at 1150°C where K <sub>2</sub> SO <sub>4</sub> /HA ratio during preparation was 3/1 .....	45
Figure 5.18.	EDX image of wet mixed commercial HA powder KW7 spherical particle synthesized at 1150°C where K <sub>2</sub> SO <sub>4</sub> /HA ratio during preparation was 3/1 .....	45
Figure 5.19.	SEM image of wet mixed commercial powder KW7 sample agglomerate synthesized at 1150°C where K <sub>2</sub> SO <sub>4</sub> /HA ratio during preparation was 3/1 .....	46
Figure 5.20.	SEM image of wet mixed commercial powder KW7 sample agglomerate synthesized at 1150°C where K <sub>2</sub> SO <sub>4</sub> /HA ratio during preparation was 3/1 .....	46

Figure 5.21.	SEM image of wet mixed commercial HA powder KW5 whiskers synthesized at 1100°C where K <sub>2</sub> SO <sub>4</sub> /HA ratio during preparation was 3/1 .....	48
Figure 5.22.	SEM image of wet mixed synthesized HA powder KW6 whiskers synthesized at 1100°C where K <sub>2</sub> SO <sub>4</sub> /HA ratio during preparation was 3/1 .....	48
Figure 5.23.	SEM image of wet mixed commercial HA powder KW7 whiskers synthesized at 1150°C where K <sub>2</sub> SO <sub>4</sub> /HA ratio during preparation was 3/1 .....	49
Figure 5.24.	SEM image of wet mixed synthesized HA powder KW8 whiskers synthesized at 1150°C where K <sub>2</sub> SO <sub>4</sub> /HA ratio during preparation was 3/1 .....	49
Figure 5.25.	XRD patterns of KNW1, KNW2, KNW3,KNW4, KNW5 .....	52
Figure 5.26.	a) SEM image of KNW1 whiskers synthesized at 800°C for 2 h where salt mixture/HA ratio during preparation was 3/1 .....	53
Figure 5.26.	b) SEM image of KNW1 whiskers synthesized at 800°C for 2 h where salt mixture/HA ratio during preparation was 3/1 .....	53
Figure 5.27.	a) EDX results of KNW2 whiskers synthesized at 850°C for 3 h where salt mixture/HA ratio during preparation was 3/1 .....	54
Figure 5.27.	b) SEM image of KNW2 whiskers synthesized at 850°C for 3 h where salt mixture/HA ratio during preparation was 3/1 .....	55
Figure 5.27.	c) SEM image of KNW2 whiskers synthesized at 850°C for 3 h where salt mixture/HA ratio during preparation was 3/1 .....	55
Figure 5.28.	a) EDX results of KNW3 whiskers synthesized at 825°C for 5 h where salt mixture/HA ratio during preparation was 3/1 .....	56
Figure 5.28.	b) SEM image of KNW3 whiskers synthesized at 825°C for 5 h where salt mixture/HA ratio during preparation was 3/1 .....	57
Figure 5.28.	c) SEM image of KNW3 whiskers synthesized at 825°C for 5 h where salt mixture/HA ratio during preparation was 3/1 .....	57
Figure 5.29.	a)SEM image of KNW4 whiskers synthesized at 875°C for 2 h where salt mixture/HA ratio during preparation was 3/1 .....	58

Figure 5.29.	b) SEM image of KNW4 whiskers synthesized at 875°C for 2 h where salt mixture/HA ratio during preparation was 3/1 .....	58
Figure 5.30.	a) SEM image of KNW5 whiskers synthesized at 900°C for 2 h where salt mixture/HA ratio during preparation was 3/1 .....	60
Figure 5.30.	b) SEM image of KNW5 whiskers synthesized at 900°C for 2 h where salt mixture/HA ratio during preparation was 3/1 .....	60
Figure 5.31.	a) EDX results of KNW6 whiskers synthesized at 850°C for 2 h where salt mixture/HA ratio during preparation was 5/1 .....	61
Figure 5.31.	b) SEM image of KNW6 whiskers synthesized at 850°C for 2 h where salt mixture/HA ratio during preparation was 5/1 .....	62
Figure 5.31	c) SEM image of KNW6 whiskers synthesized at 850°C for 2 h where salt mixture/HA ratio during preparation was 5/1 .....	62
Figure 5.32.	The variation of the green densities of slip cast composites with different whisker contents.....	64
Figure 5.33.	Densities of slip cast composites with different whisker content after sintering .....	64
Figure 5.34.	The variation of the green densities of dry pressed composites with different whisker contents.....	66
Figure 5.35.	Densities of dry pressed composites with different whisker contents after sintering.....	66
Figure 5.36.	XRD patterns of pure HA powder and WDP composites with different whisker contents sintered at 1200°C.....	68
Figure 5.37.	XRD patterns of pure HA powder and WDP composites with different whisker contents sintered at 1250°C .....	68
Figure 5.38.	XRD patterns of pure HA powder and WDP composites with different whisker contents sintered at 1300°C .....	69
Figure 5.39.	XRD patterns of pure HA powder and WDP composites with different whisker contents sintered at 1350°C .....	69
Figure 5.40.	SEM image of 30WSC sample sintered at 1250°C for 2 h.....	70
Figure 5.41.	SEM image of 30WDP' sample sintered at 1250°C for 2 h .....	71
Figure 5.42.	SEM image of 40WSC sample sintered at 1250°C for 2 h.....	72
Figure 5.43.	SEM image of 40WDP' sample sintered at 1250°C for 2 h .....	72

Figure 5.44.	SEM image of 50WSC sample sintered at 1250°C for 2 h.....	73
Figure 5.45.	SEM image of 50WDP' sample sintered at 1250°C for 2 h .....	73
Figure 5.46.	SEM image of 50WSC sample sintered at 1250°C for 2 h.....	75
Figure 5.47.	SEM image of 50WDP' sample sintered at 1250°C for 2 h .....	75

## LIST OF TABLES

<b><u>Table</u></b>		<b><u>Page</u></b>
Table 2.1.	Selected biomaterial types and properties .....	4
Table 2.2.	Mechanical properties of human compact bone .....	10
Table 4.1.	Properties of materials used in this study .....	24
Table 4.2.	Heat treatment steps of HA whiskers produced from HA- K <sub>2</sub> SO <sub>4</sub> .....	26
Table 5.1.	2θ values of XRD pattern of HA .....	31
Table 5.2.	Synthesis conditions and dimensional properties of HA whiskers prepared by using NaCl .....	32
Table 5.3.	Synthesis conditions and dimensional properties of HA whiskers prepared by using K <sub>2</sub> SO <sub>4</sub> .....	40
Table 5.4.	Preparation parameters and dimensional properties of HA whiskers prepared by using NaCl- K <sub>2</sub> SO <sub>4</sub> salt mixture .....	51
Table 5.5.	Relative densities of slip cast composites at various sintering temperatures.....	63
Table 5.6.	Relative densities of drey pressed composites at various sintering temperatures.....	65

# CHAPTER 1

## INTRODUCTION

Thousands of patients around the world have improved the quality of their lives with the aid of some types of implanted devices. Diseases and accidents cause damages in the human bodies. Biomaterials, the functional components of medical devices, are used extensively in the treatment of disease, trauma and disability. The very breadth of this field precludes a comprehensive, in-depth projection in all areas of biomaterials, which currently include orthopaedics, cardiovascular, neurological, drug delivery, and other applications. Projected future applications include the use of micro robotic devices for disease detection, drug delivery, and neurological applications (Helmus et al. 1991).

Bone failures and damages are still very serious health problems throughout the world. In the field of orthopaedics surgery, bone substitutes are commonly required to replace damaged tissue due to disease, trauma or surgery. Current bone substitutes do not show the physiological and mechanical characteristics of the real bone. The development of artificial bone would seem to solve these problems, although it may cause other problems. Materials options include metals, ceramics and polymers. Unfortunately, conventional materials are used that were not specifically developed for biological applications. Interaction between biomaterials and natural tissues is an important subject for biomaterial science (Hench et al. 1993).

Metals have been widely used for major load-bearing orthopaedics applications. There are, however, various problems related to metallic materials in the human body due to corrosion, wear, and/or negative tissue reaction. Therefore, several ceramic materials have been clinically applied. Among them,  $ZrO_2$  and  $Al_2O_3$  exhibit high mechanical strength and good biocompatibility. However, like metals, they are bioinert materials, which show non-toxicity but do not form interfacial bond between the implant and tissue. Polymeric materials are also used in biomedical applications, whereas their physical and mechanical properties are not sufficient for an implant and can cause some problems (Helmus et al. 1991).

There is an escalating interest in calcium phosphates, particularly apatites, which seems to be driven mainly by the requirements for the development, understanding and manufacture of biomaterials. Appropriate hard tissue replacement implants should be

bioactive, have modulus equal to that of bone, and be even tougher than the bone. Hydroxyapatite (HA) seems to be the most suitable ceramic material for hard-tissue replacement. Hydroxyapatite ceramics do not exhibit any cytotoxic effects, show excellent biocompatibility with hard tissues and also with skin and muscle tissues (Helmus et al. 1991).

However, because of poor mechanical properties, HA based ceramics can not be used for heavy load-bearing applications. Although studies for the improvement of mechanical properties of these materials began a long time ago, HA ceramics of proper strength characteristics have not yet been produced. Various reinforcements (ceramic, metallic or polymer) have been used in order to enhance the reliability of HA ceramics. Fibrous HA is a very promising material for the preparation of composites, because it should act as a bioactive phase and reinforcement. In contrast to the other available fibrous materials, HA whiskers should not be a health hazard due to their perfect biocompatibility and relatively better chemical durability. Hydrothermal method is a very common technique for the synthesis of HA whiskers. The HA whiskers produced with this technique have uniform shapes, high crystallinity and single phase. However, non-stoichiometry (e.g., calcium deficiency) and low thermal stability (e.g. decomposition to  $\alpha$  or  $\beta$  tricalcium phosphate) influence the composite structures negatively (Suchanek et al. 1995).

Molten salt synthesis (MSS) is a simple method for the processing of whiskerlike, platelike or needlelike ceramic bodies with complex stoichiometry. The low melting solvents like alkali chlorides, sulfates, carbonates or hydroxides are used as the mediums of crystal growth in this technique. The MSS method has been used with different alkali salts to prepare ferrites, titanates and niobates (Taş. 2001).

The subject of this work can be divided into two parts. The effects of various parameters on the synthesis of uniform and stable HA whiskers with MSS technique for the preparation of HA powder/HA whisker (HAp/HAw) composites and the sintering and densification behaviour of these composites with different whisker contents were investigated.

## CHAPTER 2

### BIOMATERIALS

There have been significant advances in the “biomaterial” science for the last couple of decades. Scientists are trying to improve these materials so that they are able to interact with the biological systems properly. Biomaterials are used for performing or supporting the functions of living tissues. These materials can be obtained either naturally or synthetically and they are generally in contact with the body fluids (Hench et al. 2002).

Biomaterials are used in various parts of the human body that have different conditions. For example, in the daily activities, our bones and tendons are subjected to 4 MPa and 80 MPa stresses, respectively. Therefore, the biomaterials should be strong enough to perform hard activities.

According to the clinical experiences, under specific conditions, some materials can be accepted by the human body; however, the same materials can also be rejected under various other conditions. For the last three decades researchers have obtained vital information about the biomaterial/tissue interactions (Hench et al. 2002).

The terms “biofunctionality” and “biocompatibility” are used in order to specify the biological performance of biomaterials. Biofunctionality may be considered in relation to a set of properties which allow a device to perform a function. Biocompatibility can be defined as the absence of any undesirable reactions from the immune system (Park et al. 1992).

Biomaterials are classified under four major groups like polymers, metals, ceramics and composites according to the type of material utilized.

*Metals* are widely used as biomaterials because of their superior mechanical properties. Metals are especially employed as artificial joint prosthesis, tooth implants, vascular grafts and artificial heart valves. The most commonly used metals are stainless steels, Co-Cr alloys, gold and titanium alloys (Park et al. 1992).

The human body has a corrosive environment for metallic biomaterials. The metallic corrosion products penetrate into the tissue and damage the body cells. In spite of their excellent mechanical properties, metallic materials lead to some undesired

problems such as young modulus mismatch with host tissue, no active bonding to the tissue, low biocompatibility, causing allergic reactions that generally restrict the life of implant and make surgical removal of the implant necessary (Park et al. 2002).

Table 2.1. Selected biomaterial types and properties.

(Source: Suchanek 1998)

<b>Materials</b>	<b>Advantages</b>	<b>Disadvantages</b>	<b>Applications</b>
<b>Polymers</b> Nylon Silicones	Resilient Easy fabrication Bioresorbable Bioinert	Insufficient properties for heavy loading Degradation	Blood vessels Hip socket Ear Nose
<b>Metals</b> Titanium Co-Cr Alloy Gold Stainless Steel	High strength Tough Ductile	Corrosive Dense	Joint replacement Bone plates Dental implant
<b>Ceramics</b> Alumina Carbon Hydroxyapatite	Biocompatible Inert High compressive strength Wear resistant Bioactive	Brittle Difficult production High modulus	Dental implants Hip socket
<b>Composites</b>	High strength Controllable mechanical properties and microstructure	Difficult production	Joint implants Heart valves

*Ceramics* are refractory, polycrystalline compounds, commonly inorganic, including silicates, metallic oxides, carbides and various refractory hydrides, sulfides etc. Specially designed ceramics for the repair, reconstruction and replacement of diseased or damaged parts of the body are defined as “bioceramics”. Polycrystalline ceramics (alumina and hydroxyapatite), bioactive glasses, bioactive glass ceramics and bioactive composites (polyethylene-hydroxyapatite) are the most common types of bioceramics. Especially, ceramics are oftenly employed in dentistry as dental crowns because of their inertness to the body fluids, high compressive strength and esthetic appearance (Hench et al. 1993).

The bioceramics can be divided into three types according to the interaction between the ceramic implant and tissue: bioinert, bioactive and bioresorbable. Bioinert ceramics (alumina, zirconia) lead to the fibrous tissue formation in the interface. On the

other hand, if the material is bioactive (hydroxyapatite, bioactive glasses, glass ceramics), a kind of bonding is formed on the implant interface. A bioresorbable implant (tricalciumphosphate) dissolves in the body, thus the surrounding tissue replaces the implant. Applications contain replacement for hips, knees, teeth, tendon and ligaments; repairing for periodontal disease, maxillofacial reconstruction, augmentation and stabilization of the jaw bone, spinal fusion and bone repair after tumor surgery (Hench et al. 1993). A different ceramic material is designed for a specific application with the necessary responses.

Bioceramics are classified into three groups according to their structural properties which are oxide ceramics, calcium phosphate ceramics, glass & glass ceramics.

1) *Oxide Ceramics*: These ceramics have polycrystalline structure and exhibit bioinert behaviour. Most common examples of oxide ceramics are alumina and zirconia. High purity and density, corrosion resistance, high strength and bioinertness are the superior properties of these materials. Due to these advantages, they have been used as dental implants and hip prosthesis.

2) *Calcium Phosphate Ceramics*: These ceramics are present with different calcium/phosphate molar ratios. Hydroxyapatite, tricalciumphosphate, octacalciumphosphate are examples to various calcium phosphate phases. HA based ceramics are currently used as biomaterials for many applications in especially dentistry and orthopedics because they form a real bond with the surrounding bone tissue when implanted.

3) *Glass & Glass Ceramics*: Silica ( $\text{SiO}_2$ ) is the main component of these kinds of ceramics. Glass ceramics are the compositions of lithium/aluminium or magnesium/aluminium crystals. Glass and glass-ceramics are used in the repair and regeneration of hard tissues (Hench et al).

There are some specific limitations for the application of bioceramics such as brittleness, low fracture toughness, fabrication difficulty, low mechanical reliability, lack of resilience and high density (Helmus et al. 2001).

*Polymer* is a kind of substance that is composed of molecules characterized by the multiple repetition of one or more species of atoms (constitutional repeating units)

linked to each other in amounts sufficient to provide some specific properties which do not change markedly with the addition of one or a few of the atoms constitutional repeating units (Bonfield et al. 1998).

Polymeric materials are commonly used because they are available in different types of compositions, properties and also they can be easily fabricated into many forms such as fibres, textiles, films, rods and viscous liquids. Polymers have a close similarity with natural polymeric tissue components like collagen. Certain types of bonds may form between the synthetic polymers and natural tissue polymers (Bonfield et al. 1998).

Synthetic polymeric materials are employed in dental materials, implant, dressing, encapsulate, polymeric delivery system, orthopedic devices and medical disposable supplies. Polymers can be categorized into two groups which are resorbable (polyglycolic acid, polylactic acid and chitosan) and non resorbable (polypropylene, polyethylene and polymethylmetacrylate) polymers. There are some requirements for a polymeric material to be used as a biomaterial like biocompatibility, non-toxicity, sufficient mechanical properties and sterility. In terms of structural and mechanical compatibility, polymeric materials are oftenly used for soft tissue applications different from the other kinds of biomaterials. As a composite material component, polymers are widely used in the biomaterial industry (Ramakrishna et al. 2001).

*Composite materials* are considered to be combinations of materials differing in composition or form on a macroscale. The constituents retain their identities in the composite. They do not dissolve or otherwise merge completely into each other. The components can be physically identified and exhibit an interface between one another (Bonfield et al. 1998).

Since the composites are non-homogeneous, the resulting properties will be the combination of the properties of the constituent materials. The different type of loading may call on different component of the composite to take the load. This implied that the material properties of composite materials may be different in tension and in compression as well as in bending (Bonfield et al. 1998).

Today, the most common man-made composites can be divided into three main groups which are metal matrix composites (MMC), polymer matrix composites (PMC) and ceramic matrix composites (CMC).

The mechanical properties of composites are strongly dependent on the reinforcement and interfacial compatibility of the composite system. In the development of a medical implant, the mechanical properties in terms of elastic modulus, toughness

and tensile strength are major factors for design. Other aspects such as biocompatibility and stability of the implant in a biological environment have also great importance (Cheanga et al. 2002).

The improvement of composites has been investigated by the aim of creating a composite structure which mimics the natural bone. This generally involves a hard reinforcement phase within a soft matrix. The blending of the appropriate amount of reinforcement is often used to achieve the desired mechanical property. Bioceramics such as bioglass and hydroxyapatite (HA) are preferred reinforcements because of their stiffness, density, and bioactivity (Suchanek et al. 1998).

Hydroxyapatite (HA) is a useful bioceramic, because of its superior biocompatibility. For bone and teeth repairs, biomaterials with both good biocompatibility and reliable mechanical properties for long periods are needed. However, the nature of the HA bonding results in low fracture toughness and fracture energy, similar to those of glasses. The fracture toughness and fracture energy of monolithic HA are reported to be approximately  $0.7\text{--}1.0 \text{ MPam}^{1/2}$  and  $1 \text{ J/m}^2$ , respectively. The disadvantage of such poor intrinsic properties makes clinical and orthopedic applications difficult. It is possible to improve the fracture properties of HA by the addition of a secondary phase while keeping its biocompatibility characteristics.

Many ceramic materials such as  $\text{ZrO}_2$ ,  $\text{Al}_2\text{O}_3$  and SiC are widely used as reinforcements in HA due to their corrosion and wear resistance as well as minimal tissue reaction. However, partially stabilized zirconia (PSZ) degrades in wet environments and eventually lowers the strength of implants (Suchanek et al. 1998).

## **2.1. Bone**

Bone injuries and fractures are the leading medical problems throughout the world and yet there is still much research required for a better understanding of the physical, chemical and mechanical properties human bone. There is an increasing demand for the use of artificial bone implants for the stabilization of fractured bones.

### **2.1.1. Structure of Bone**

Bone is a composite material. The main components of bone are collagen (20 wt%), calcium phosphate (69 wt%) and water (9 wt%). Some organic materials like

proteins, polysaccharides and lipids are present in small quantities. Collagen which is in the form of small microfibrils, is the matrix constituent of the bone. The diameter of the collagen microfibrils vary from 100-2000 nm. Calcium phosphate in the form of crystallized hydroxyapatite (HA) and/or amorphous calcium phosphate (ACP) provides stiffness to the bone. The HA crystals, present in the form of plates or needles, are about 40–60 nm long, 20 nm wide, and 1.5–5 nm thick. They are deposited parallel to the collagen fibers, such that the larger dimension of crystals is along the long axis of the fiber (Suchanek et al. 1998).

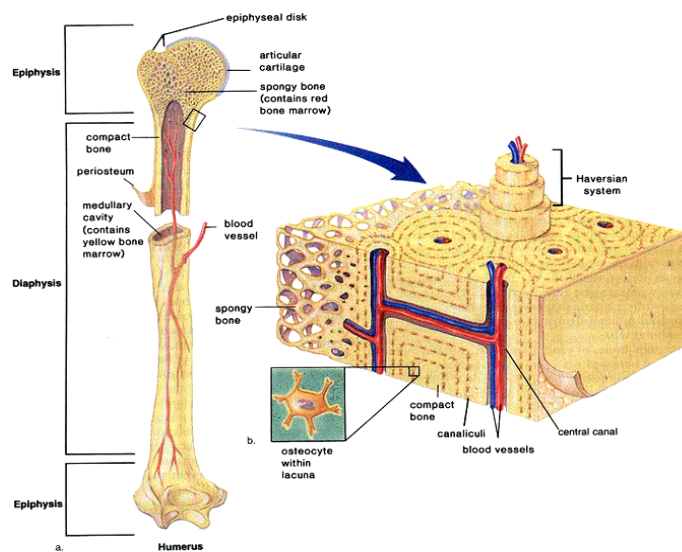


Figure 2.1. Microscopic structure of bone.

(Source: [www.uic.edu/depts/bioe/courses/Fall05/BioE515/BioE515Lecture2.ppt](http://www.uic.edu/depts/bioe/courses/Fall05/BioE515/BioE515Lecture2.ppt))

Long bone consists of cortical and trabecular bone as shown in Figure 2.1. Cortical (compact/dense) bone is placed on the exterior part of the bone and shows semi-brittle, viscoelastic and anisotropic material behaviour. Its properties are mainly influenced by porosity, mineralization level and the organization of the solid matrix. Trabecular (cancellous/porous) bone is placed in the interior part of the bone. Cancellous bone is active metabolically and is remodeled more often than cortical bone, therefore the mechanical properties of the bone change with age. The mechanical properties depend on the direction of loading, pore density and rate of loading. The proportion of cortical and trabecular bone is different at various locations in the skeleton (Suchanek et al. 1998).

## 2.1.2. Mechanical Properties of Bone

Organic components of bone (mainly collagen) would behave as a compliant material with high toughness, low modulus, and other properties characteristic for polymers. Inorganic components (HA crystals) provide appropriate stiffness to the bone. As a ceramic-organic composite, bone exhibits high toughness and relatively high modulus. High toughness is related not only to the presence of collagen, but also to the complicated fibrous microstructure.

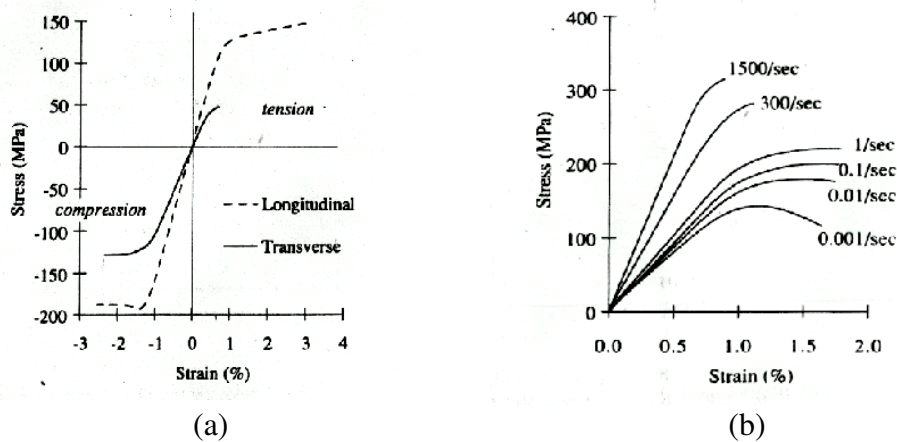


Figure 2.2. Stress-strain curve of human compact bone (a) tension-compression test  
(b) strain rate dependence.

(Source: Suchanek et al. 1998)

Natural bone has strength and resilience that is difficult to match artificially. The compressive strength of bone is higher than the tensile strength as seen in Figure 2.2 (a). The toughness of bone is higher in longitudinal direction than in transverse direction.

In Figure 2.2 (b), a linear elastic region is present up to ~0.8% strain in the stress-strain curve of bone. The toughness of the bone is very high at low strain rates, however, it fails more like a brittle material at high strain rates. The stiffness of the bone increases with increasing mineral content. Bone shows excellent toughness at low strain rates mostly due to its hierarchical structure, which stops cracks after little propagation. The mechanical properties of compact bone are given in Table 2.2 (Suchanek et al. 1998).

Table.2.2. Mechanical properties of human compact bone.

(Source: Suda 1994)

Mechanical properties	Test directions related to bone axis	
	Parallel	Normal
Tensile strength (MPa)	124-174	49
Compressive strength (MPa)	170-193	133
Bending strength (MPa)	160 <sup>a</sup>	
Shear strength (MPa)	54	
Young's modulus (GPa)	17-18.9	11.5
Work of fracture at low strain rates (J/m <sup>2</sup> )	6000	
Work of fracture at high strain rates (J/m <sup>2</sup> )	98	
Fracture toughness (Mpa..m <sup>1/2</sup> )	2-12 <sup>a</sup>	
Ultimate tensile strain	0.014-0.031	0.007
Ultimate compressive strain	0.0185-0.026	0.028
Yield tensile strain	0.007	0.004
Yield compressive strain	0.010	0.011

<sup>a</sup>:Direction is not specified

## CHAPTER 3

### HYDROXYAPATITE BASED COMPOSITES

#### 3.1. Hydroxyapatite

Hydroxyapatite is one of the main phases of calcium phosphates that have been studied extensively and used clinically because of its excellent biocompatibility and bioactivity. It has a hexagonal crystal structure, a stoichiometric chemical formula of  $\text{Ca}_{10}(\text{PO}_4)_6(\text{OH})_2$  and weight percentages of 39.9 %Ca, 18.5 %P, 38.22 %O and 3.38 % OH. The crystal structure of hydroxyapatite is shown in Figure 3.1. Hydroxyapatite (HA) belongs to the hexagonal system, with a space group  $\text{P6}_3/\text{m}$ . This space group is characterized by a six-fold c-axis perpendicular to three equivalent a-axes ( $a_1, a_2, a_3$ ) at angles  $120^\circ$  to each other. The dimensions of the unit cell of HA are a-axis=0.9422nm, c-axis=0.6880nm (Hench et al. 1998). At present, applications for synthetic hydroxyapatite are restricted to dynamic load bearing applications because HA has low fracture toughness. The major requirements for bioceramics either in dense or in porous form are good biocompatibility, high mechanical strength, good thermal stability at high temperatures and ease of application under operating conditions. Many researchers focus on the investigation of the reinforcement of HA ceramics. A common technique to improve toughness and reliability of ceramic materials is the addition of short fibres and whiskers (Kakihana et al. 1995).

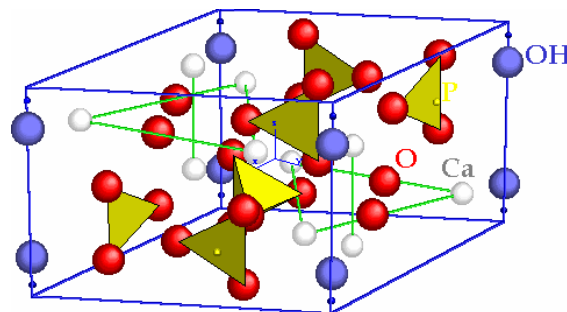


Figure 3.1. Crystal structure of hydroxyapatite.

Source: ([http://www.bupa.co.uk/wellness/asp/factsheets/bone\\_marrow.asp](http://www.bupa.co.uk/wellness/asp/factsheets/bone_marrow.asp))

Metals, partially stabilized zirconia (PSZ), alumina and fibres/whiskers can be added to the HA materials for enhancing the reliability of HA ceramics. However, biocompatibility and bioactivity of HA ceramics decrease with the addition of bioinert ceramics and metal reinforcements. The presence of foreign materials in the HA matrix causes the decomposition of HA ceramics with the formation of new phases like tricalcium phosphate (TCP) which affects the densification negatively. Another undesired effect related with most reinforcements is the increase of elastic modulus of the material. Higher load is carried by the implant when mismatch of elastic modulus of implant and bone gets larger. This leads to a decrease in strength of the healed bone (Suchanek et al. 1998).

### **3.2. Preparation of HA Powder**

Various methods have been reported in the literature for the preparation of HA powders. Solid state and wet synthesis are the two major techniques for the preparation of HA powders. The wet methods can be categorized into three main groups which are precipitation, hydrothermal technique, and hydrolysis of other calcium phosphates. Depending upon the technique, powders with various morphology, stoichiometry, and level of crystallinity can be obtained. Solid state methods usually give a stoichiometric and well-crystallized product but they require relatively high temperatures and long heat-treatment times. Sinterability of such powders is usually low.

In the precipitation technique the temperature does not exceed 100°C and nanometer-size crystals can be obtained. They are in the shape of blades, needles, rods, or equiaxed particles. However, their crystallinity and Ca/P ratio depend strongly on the preparation conditions and in many situations, these properties are lower than that of well-crystallized stoichiometric HA. The hydrothermal technique usually gives HA powders with a high degree of crystallinity and with a Ca/P ratio close to the stoichiometric value. Their crystal size is in the range of nanometers to millimeters.

Hydrolysis of tricalcium phosphate, monetite, brushite, or octacalcium phosphate requires low temperatures (usually below 100°C) and results in HA needles or blades with the size of microns. In most cases, the hydrolysis product is highly nonstoichiometric (Ca/P ratio in the range of 1.50–1.71). Another issue related to wet

methods is the presence of carbonate ions and/or other impurities in the lattice of the crystallized HA.

There are also alternative techniques for the preparation of HA powders such as sol-gel, flux method, electrocrystallization, spray-pyrolysis, freeze-drying, microwave irradiation, mechano-chemical method, or emulsion processing (Suchanek et al. 1998).

### **3.3. Production of Hydroxyapatite Whiskers**

Reinforcement by HA whiskers has been considered as a means of improving the fracture toughness of pure HA bioceramics. In contrast to the other available fibrous materials, HA whiskers are not health hazardous due to the perfect biocompatibility, bioactivity and relatively low chemical durability. HA whiskers can be used as biocompatible and bioactive reinforcements due to these properties (Suda et al. 1999).

There have been several studies about the synthesis techniques of whiskerlike or needlelike crystals of HA. Preparation techniques for HA whiskers can be categorized into two major groups: (1) *homogeneous precipitation method* and (2) *the decomposition of chelating agents*. The first technique benefits a continuous increase of pH in the solution including calcium and phosphate ions at high temperature using urea. In the second synthesis method, chelating agents like EDTA, lactic acid or citric acid are used. Ca complexes with chelating agents decompose during heat treatment under hydrothermal conditions and HA whiskers precipitate (Suchanek et al. 1998).

HA whisker-like materials by the homogeneous precipitation method using urea was prepared. However, these materials were contaminated with large quantities of carbonate ions and they have not been verified to be single crystals like whiskers. The length and diameter of the carbonate ion containing whiskers were reported to be about 50  $\mu\text{m}$  and 0.5-5  $\mu\text{m}$  respectively in another work by using the same technique (Suchanek et al. 1995).

Needle-like HA crystals with dimensions of 0.5  $\mu\text{m}$   $\times$  10  $\mu\text{m}$  and Ca/P stoichiometric ratio of about 1.50 were prepared in another work. Traces of some carbonate ions were detected in the lattice of the crystal. It was possible to prepare the needle-like HA crystals by the hydrolysis of brushite and monetite. The decomposition of urea at high temperature also accelerated the reaction (Suchanek et al. 1995).

Suchanek and co-workers reported on other HA powders prepared under hydrothermal conditions formed from fine needle-like crystals and whiskers. These crystals had a length of 30-100  $\mu\text{m}$  and a diameter of 0.1-5  $\mu\text{m}$ . The molar ratio of Ca/P was in the range of 1.59-1.63 and the crystal structure did not contain larger quantities of carbonate ions (Suchanek et al. 1995).

The synthesis methods that are explained above suffer from nonstoichiometry (i.e. calcium deficiency) and low thermal stability (i.e. partially decomposition into  $\beta$ -TCP phase even after 1 h of heating at 1100°C). Furthermore, Suchanek and co-workers have reported that in the HA composites reinforced with hydrothermally synthesized HA whiskers (~30 vol% whiskers), the whiskers disappear within the HA matrixes at sintering temperatures above 1000°C and turn themselves into large, equiaxed grains (Suchanek et al. 1996).

### **3.3.1. Molten Salt Synthesis**

The molten salt synthesis (MSS) is one of the simplest methods for the preparation of ceramic powder bodies with whiskerlike, needlelike or platelike morphology. This synthesis technique is a well established process of forming a desirable compound in a flux of low melting point. Molten salt synthesis offers a significant reduction in the formation temperature when compared to that required in a conventional solid state reaction. It also provides control on the particle size and morphology of the resulting powders (Yoon et al. 1998).

Molten salt synthesis method is based on the use of low-melting point solvents like alkali chlorides, sulfates, carbonates or hydroxides, for the synthesis of the ceramics. There are many studies about the MSS technique which involves the preparation of ferrites, titanates, niobates, mullite, aluminium borate, wollastonite and carbonated apatite with various alkali salts. The selection of a proper salt has a major importance in terms of obtaining desirable powder morphology and characteristics. Two important criteria for the selection of the salt is important. The melting point of the salt should be low and appropriate for the syntesis of the required phase. The salt should have sufficient aqueous solubility that it will be eliminated easily by simple washing after synthesis (Taş. 2001).

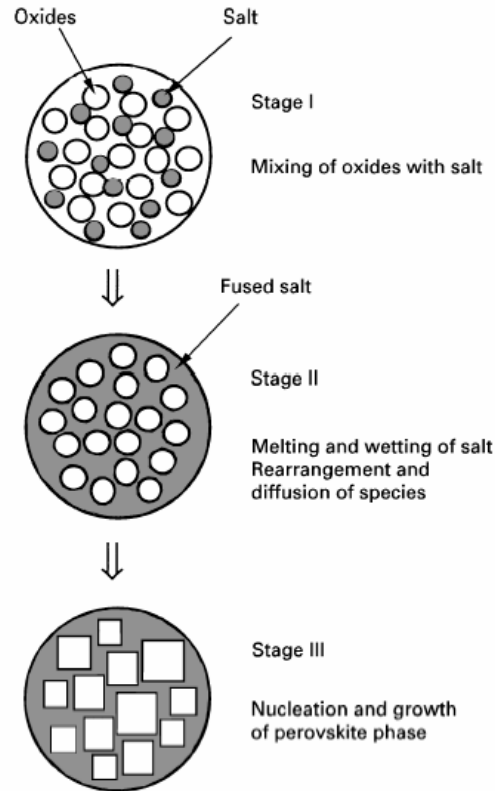


Figure 3.2. Schematic illustration of MSS process for the formation of perovskite phase with increasing temperature. (Source: Yoon et al. 1998)

K1 Hyun Yoon and his co-workers showed the main processing steps of MSS method with the increasing temperature in the case of lead-based relaxors as shown in Figure 3.2. Oxides corresponding to a lead-based compound were mixed with one or two types of salt and then fired at a temperature above the melting point of the salt in order to form a flux of the salt composition. At this temperature, the oxides were rearranged and then diffused rapidly in a liquid state of the salt. With further heating, perovskite phase particles formed during the nucleation and growth process (Yoon et al. 1998).

Hashimito et al synthesized needlelike mullite particles by using potassium sulfate flux for the fabrication of aluminium borate whiskers as seen in Figure 3.3. These mullite particles were obtained by heating a powder mixture consisting of  $\text{Al}_2(\text{SO}_4)_3$ ,  $\text{SiO}_2$  and  $\text{K}_2\text{SO}_4$  in an alumina crucible covered with a lid. When the powder mixture consisting of 24.5 mol % of  $\text{Al}_2(\text{SO}_4)_3$ , 48 mol %  $\text{K}_2\text{SO}_4$  and 27.5 mol % of  $\text{SiO}_2$  was heated at  $1100^\circ\text{C}$  for 3 h fine and long mullite particles were obtained. Their length and diameters were 2-5  $\mu\text{m}$  and 0.2-0.5  $\mu\text{m}$ , respectively (Hashimito et al. 2000).

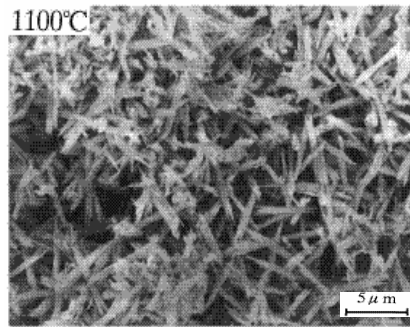


Figure 3.3. SEM image of needlelike mullite particles heated at 1100°C for 3 h.  
(Source: Hashimoto et al. 2000)

Y. Suetsugu et al. studied on the single carbonate apatite crystal growth. The dry mixture of TCP and  $\text{CaCO}_3$  were mixed and apatite crystals were grown with Ar gas pressure.  $\text{CaCO}_3$  flux was employed without water for the elimination of hydroxide ions from the apatite crystals. Both temperature oscillation and slow cooling were tried in order to grow large crystals as shown in Figure 3.4. The most promising crystals were prepared at 1400°C for 1 h at 55 MPa and oscillated 11 times between 1200 and 1300°C with a hexagonal symmetry (Suetsugu et al. 1999).

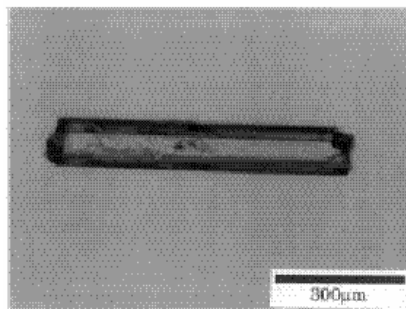


Figure 3.4 SEM image of carbonate apatite single-crystal obtained at 1400°C for 1h at 55 MPa and exposed to oscillation. (Source: Suetsugu et al. 1999)

Katayama et al. synthesized  $\text{BaNd}_2\text{Ti}_4\text{O}_{12}$  (BNT4) powder by MSS technique. Single phase BNT4 powder with a longitudinal shape could be formed by using KCl as shown in Figure 3.5. The temperature and duration of heating and the amount of KCl salt largely affected the formation of the single-phase BNT4 powder. The BNT4 powder particles sintered at 1100°C were in a longitudinal shape and formed aggregates. At

1200 and 1300°C the BNT4 powder had similar particle forms but aggregation decreased with increasing temperature. Fully dense ceramics were obtained at 1450 or 1500°C without changing the particle shape. The single-phase BNT4 powder with a lesser degree of aggregation showed excellent sinterability and resulted in the formation of dense ceramics (Katayama et al. 1999).

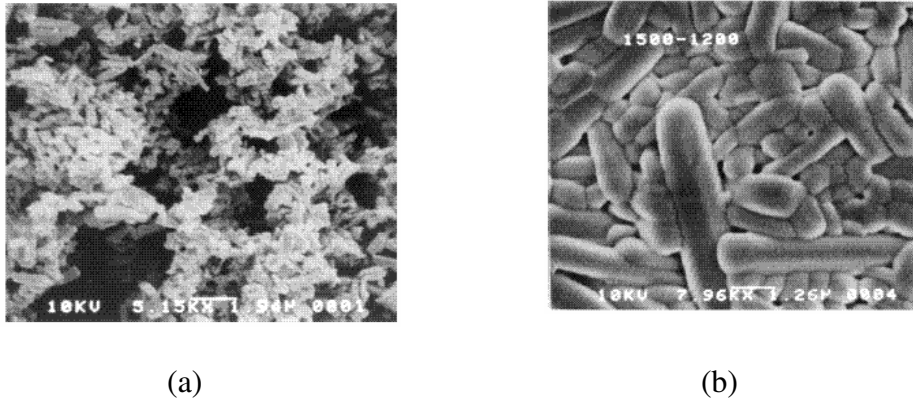


Figure 3.5 SEM images of  $\text{BaNd}_2\text{Ti}_4\text{O}_{12}$  powder prepared at (a) 1100°C (b) 1450°C.

(Source: Katayama et al. 1999)

Hayashi et al prepared  $\text{CaSiO}_3$  whiskers from fine  $\text{CaSiO}_3$  powder by using alkali halide fluxes, NaCl, KCl, and their mixture, starting from  $\text{CaSiO}_3$  fine powder prepared by the coprecipitation method as shown in Figure 3.6. The  $\text{CaSiO}_3$  powder and the flux were mixed and heated at temperatures from 850 to 1000°C for 1 to 48 h. Their length, diameter, and aspect ratio ranged from 3.24 to 10.45 mm, 0.33 to 1.12 mm, and 7.1 to 21.7, respectively (Hayashi et al. 2000). The length of the whiskers was expected to be affected by the mobility of components in the flux, which might be related to the diffusion rate of components and/or the viscosity of the flux during heating. The mobility of the components in the NaCl+KCl flux might be larger because the temperature difference between the synthesis temperature and the melting point of the flux was much larger in the NaCl+KCl flux than in the others; the melting points of NaCl, KCl and NaCl+KCl (1:1) fluxes are 801, 774 and 645°C respectively.

In general, the starting material completely dissolves in the flux during the heat treatment time and the synthesized crystals are obtained during the cooling process in the usual 'flux method'. The solubility of  $\text{CaSiO}_3$  in the alkali halide fluxes might be

very low so that the starting material was considered not to dissolve completely into the flux in the above work (Hayashi et al. 2000). This suggested that the whiskers might mainly grow by an Ostwald ripening mechanism, i.e., the dissolving of fine particles and the depositing of components on larger particles. The whiskers in this mechanism grew not during the cooling process but grew in the melt. The dissolution rate of the material depends on the properties of the starting material like particle size and/or chemical activity which may have a strong effect on the growth of whiskers when Ostwald ripening is the dominant mechanism.

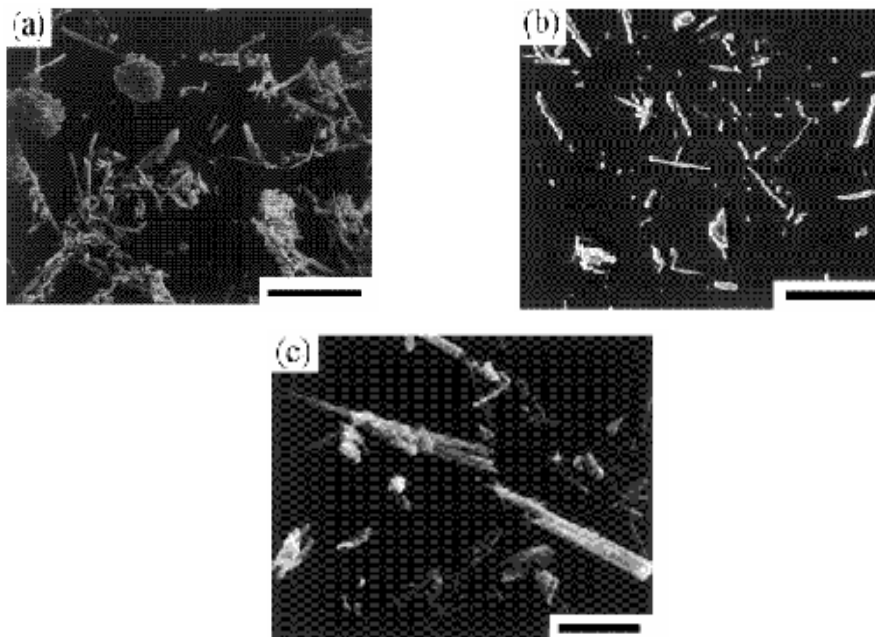
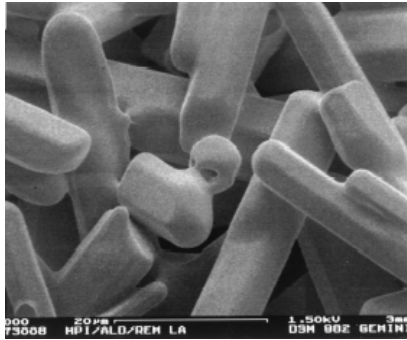


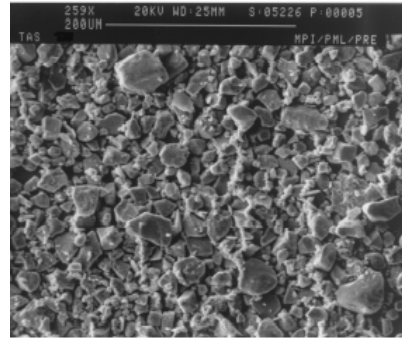
Figure 3.6. SEM micrographs of  $\text{CaSiO}_3$  whiskers prepared from (a) NaCl (b) KCl (c) NaCl+KCl fluxes, treated at  $900^\circ\text{C}$  for 24 h (scale bar= $10\mu\text{m}$ ). (Source: Hayashi et al. 2000)

Taş synthesized (HA) whiskers and crystals by the route of molten salt synthesis (MSS). The  $\text{K}_2\text{SO}_4$  as flux and HA powder as starting material were used in this method. Single-phase HA whiskers were synthesized in the  $1080\text{-}1190^\circ\text{C}$  temperature range. The salt/HA ratios in the initial mixture varied between 1.2 and 3 without significantly affecting the microstructure. The synthesized HA whiskers obtained by the  $\text{K}_2\text{SO}_4$  flux retained their initial shape and dimensions when even heated at  $1300^\circ\text{C}$  for 9 h as shown in Figure 3.7 (a). At that temperature, decomposition of HA crystals were observed. Also, different types of fluxing agents such as KCl, KBr,  $\text{CaCl}_2$  and  $\text{Na}_2\text{SO}_4$

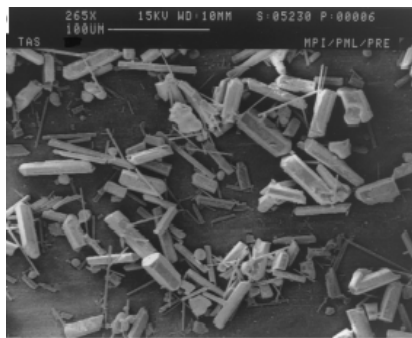
were used instead of  $K_2SO_4$ . However, the products were in the shape of large equiaxed HA crystals and their average particle size were about  $25\ \mu m$  rather than HA whiskers in the range of  $850-1000^\circ C$  (Figure 3.7.b) (Taş. 2001).



(a)



(b)



(c)

Figure 3.7 (a). HA whiskers from  $K_2SO_4$  heated at  $1300^\circ C$  for 9 h (b) HA crystals from KCl synthesized at  $880^\circ C$  for 3 h (c) HA whiskers from  $K_2SO_4$  synthesized at  $1080^\circ C$  for 0.5 h. (Source: Taş 2001)

C.Taş obtained the HA whiskers with the highest aspect ratio at the lowest temperature ( $1080^\circ C$ ) and time (0.5 h) combination where the  $K_2SO_4/HA$  was chosen as 3/1 (Figure 3.7. c).

The following process for HA crystal growth was proposed as a result of the  $K_2SO_4$  flux HA synthesis experiments (Taş 2001):

1) The initial ceramic raw material is first dissolved by the liquid phase of molten  $K_2SO_4$  during the MSS process.

2) With further heating, the apatite phase particles are formed through the nucleation and growth processes.

3) Rapid crystallization occurs along the preferred growth axes of the ceramic phase while passing through its melting point down to room temperature.

4) During MSS, HA whisker growth occurred by a sequential “dissolution–crystallization–whisker-growth” process.

5) Solubility of the ceramic raw material in the molten flux (which is a function of temperature) must have a great importance in terms of the crystallization process.

6) The extent of superheating of the molten flux must be also very effective on the resultant aspect ratio of the formed whiskers.

7) The morphology of the whiskers growing out of the cooling molten salt bath must be strongly dependent on soaking time at the soaking temperature.

### **3.4. Formation Techniques of HA Ceramics**

Several techniques like dry pressing, slip casting, tape casting, injection molding, viscous plastic processing or centrifugal settling are used for the consolidation of HA ceramics. Slip casting and dry pressing are the most common and relatively easy methods for the formation of HA based composites.

#### **3.4.1. Slip Casting of HA Ceramics**

Slip casting has been known as a very old shaping/forming process for ceramic products. This technique has emerged as one of the major forming processes for the large scale fabrication of both monolithic and composite ceramic components having either simple or complicated shapes. Colloidal processing methods that affect the deflocculation and stabilization behaviour of powder particle dispersions in a liquid medium have been established. The use of a stable colloidal dispersion provides a control over packing density variations in a green compact and, thus, the improvement of the desired microstructures in the sintered product (Rodriguez et al. 2001).

Only conventional dry powder compaction followed by sintering has been performed as a processing route for HA based ceramic consolidation. There have been limited studies about the use of colloidal methods for HA ceramic preparation. Slip

casting of a synthetic HA powder was reported as an appropriate formation technique for a high density body. The dispersion behaviour of mechanochemically synthesized HA powders in water by using various dispersing agents was investigated in the literature. Although pH modification had a negligible effect for all dispersions, anionic polyelectrolytes at considerably high concentrations ( $\geq 3\text{wt}\%$ ) effectively stabilized the suspensions through an electrosteric mechanism.

Anionic polyelectrolytes were found as the most effective dispersing agents for HA between the various (anionic, cationic or nonionic) dispersing agents. Such a suspension, solids loaded to 73 wt% with a precipitated and calcined (at 800-900°C) HA powder was slip cast and sintered to density  $\geq 96\%$ . The calcination temperature affected both the morphology and the chemical nature of the surface of the particles, with the optimum calcination temperature  $\geq 800^\circ\text{C}$ . The colloidal stability of commercial HA powder and its calcined version as a function of pH and deflocculant concentration was also studied in another work. The high solids-loaded slips could be sintered to up to  $\geq 99\%$  of theoretical density (Ramachandro et al. 2001).

In the study of Ramachandro et al. (2001), the HA powders synthesized by a high-temperature solid-state reaction between TCP and  $\text{Ca}(\text{OH})_2$  were highly agglomerated/ flocculated when dispersed in an aqueous medium. Alteration of the pH of the medium had no effect on the dispersion of the HA powder. Two dispersing agents, studied for their influence on the deagglomeration and dispersion of HA powders in aqueous media, were only effective when used at higher concentrations, in the range of 2–4 wt% of HA. A well-dispersed slip with optimum amounts of dispersing agents showed near-Newtonian flow behavior up to a solids loading of 45 wt% and non-Newtonian behavior for solids loadings of 50 wt%. With the use of optimum amounts of dispersing agents and conditioning by ball milling HA slips having 60–67 wt% of solids loading could be slip cast into compacts having 50%–58% green density, which in turn sintered to 90%–93% density in the temperature range 1300°–1400°C

### **3.5. Densification and Sintering Behaviour of Pure HA Ceramics**

Preparation of pure, dense HA ceramics with superior mechanical properties is possible if the starting HA powder is stoichiometric (Ca/P molar ratio of 1.67). If the Ca/P molar ratio of the HA exceeds the value of 1.67, CaO forms during sintering.

Existence of CaO is reported to decrease strength and may even cause decohesion of the whole material. If the Ca/P molar ratio of HA is lower than 1.67,  $\beta$ - or  $\alpha$ -tricalcium phosphate (TCP) forms. The decomposition process itself may have a negative effect on the densification of the HA ceramics due to formation of a new phase and evaporation of water, decreasing in consequence the strength. Many of the HA powders can be pressurelessly sintered up to theoretical density at moderated temperatures 1000-1200°C (Thangamani et al. 2002).

Processing at higher temperatures may lead to exaggerated grain growth and/or decomposition of HA and subsequently to strength degradation. Hot pressing (HP), hot isostatic pressing (HIP), or HIP-postsintering makes it possible to decrease the temperature of the densification process, decrease the grain size, and achieve higher densities. This leads to finer microstructures, higher thermal stability of HA, and subsequently better mechanical properties of the prepared HA ceramics. (Suchanek et al. 1998).

### **3.5.1. Densification and Sintering Behaviour of HAp/HAw Composites**

In the study of Suchanek et al, hydrothermally prepared HA whiskers were used as reinforcements for the HA ceramics. HA/0-30 HA whisker composites were fabricated by three types of formation techniques which were pressureless sintering, hot pressing (HP) and hot isostatic pressing (HIP).

Powder mixtures that contained HA fine crystals with 0%, 10%, 20%, 30% of HA whiskers (HAw) were isostatically pressed under 350 MPa. These pellets were subsequently sintered in the range of 1000-1400°C for 3 h (heating rate was 10°C/min in all cases). The HAp/HAw composites that were prepared by pressureless sintering achieved full density at 1400°C for 3h, whereas the nonreinforced HA matrix achieved full density after sintering at 1100°C for 3h.

Open porosity in the sintered Hap/10 HAw composites disappeared at 1200°C. The composites sintered at 1200-1400°C had sufficiently high relative density (92%-99%). However, when the sintering temperature increased to 1150°C, significant grain growth occurred and HA whiskers disappeared in the composites. HA partially decomposed into  $\beta$ - or  $\alpha$ -TCP after 1250°C.

The composites that contained with 0%, 10%, 20%, 30% of HA<sub>w</sub> in the HA matrix were hot pressed at 1000-1100°C for 1-2 h under a pressure of 30 MPa. Relative densities of these composites were in the range of 92.5%-95%, in comparison with 97% for the nonreinforced HA matrix. The density of the composite decreased as the content of the HA whiskers increased.

The HA/0-30 HA<sub>w</sub> composites were fabricated by HIP at 1000, 1050 and 1100°C for 2 h under a pressure of 190 MPa and the relative densities of such prepared composites were in the range of 97%-99.5% (Suchanek et al. 1998).

## CHAPTER 4

### EXPERIMENTAL

#### 4.1. Materials

In this thesis, two types of hydroxyapatite powders were used. Commercial hydroxyapatite (HA) powder was purchased from Sigma-Aldrich (Catalog no: 23,093-6) and HA powder was also synthesized in the laboratory. NaCl and K<sub>2</sub>SO<sub>4</sub>, purchased from Merck, were used in order to synthesize HA whiskers with molten salt synthesis method (MSS) that was previously reported in the literature. In this study, the whiskers were synthesized by using three types of mixtures: K<sub>2</sub>SO<sub>4</sub>-HA mixture, NaCl-HA mixture and K<sub>2</sub>SO<sub>4</sub>-NaCl-HA mixture. These mixtures were heat treated at different temperatures which were in the range of 800°C to 1100°C for 1 to 5 hours. Hydroxyapatite whiskers were recovered by washing of the salts. HA/HA whisker composite pellets were prepared by dry pressing and slip casting routes. Commercially known Darvan-C purchased from Vanderbilt was used for the preparation of stable suspensions for the slip casting of HAp/HAw (HA powder/HA whisker composites). Some of the chemical properties of materials used in this study are given in Table 4.1.

Table 4.1. Properties of materials used in this study.

	<b>Chemical Formula</b>	<b>Molecular Weight (g/mol)</b>	<b>Density (g/cm<sup>3</sup>)</b>	<b>Purity (%)</b>	<b>Melting Point (°C)</b>
<b>Hydroxyapatite</b>	Ca <sub>10</sub> (PO <sub>4</sub> ) <sub>6</sub> (OH) <sub>2</sub>	1004.6	3.16	99	-----
<b>Sodium Chloride</b>	NaCl	58.44	2.16	99.5	801
<b>Potassium Sulphate</b>	K <sub>2</sub> SO <sub>4</sub>	174.27	2.66	99.5	1069
<b>Calcium Nitrate</b>	Ca(NO <sub>3</sub> ).4H <sub>2</sub> O	236.2	-----	99.1	-----
<b>Ammonia Hydrogen Phosphate</b>	(NH <sub>4</sub> ) <sub>2</sub> HPO <sub>4</sub>	132.05	-----	Analytical Grade	-----

## 4.2. Methods

The experimental study in this thesis can be separated into two main sections: production of the hydroxyapatite whiskers (HAW) and the production of HAp/HAW composites. The HA whiskers were obtained with MSS method by using NaCl, K<sub>2</sub>SO<sub>4</sub> and NaCl- K<sub>2</sub>SO<sub>4</sub> mixture as the medium of reaction.

### 4.2.1. Synthesis of Hydroxyapatite

Hydroxyapatite was synthesized by precipitation method. A batch mixture with Ca/P=1.67 molar ratio was prepared using Ca(NO<sub>3</sub>).4H<sub>2</sub>O and (NH<sub>4</sub>)<sub>2</sub>HPO<sub>4</sub> as starting materials. For the preparation of HA, 39.445 gr (0.167 M) Ca(NO<sub>3</sub>).4H<sub>2</sub>O was dissolved in 1000 ml deionised water and also 13.206 gr (0.1 M) (NH<sub>4</sub>)<sub>2</sub>HPO<sub>4</sub> was dissolved in 1000 ml deionised water. Aqueous solution of Ca(NO<sub>3</sub>).4H<sub>2</sub>O was slowly added (6 ml/min) into (NH<sub>4</sub>)<sub>2</sub>HPO<sub>4</sub> solution while stirring. The pH values of starting solutions were adjusted to about 10-11 with NH<sub>4</sub>OH addition and the precipitation was performed at room temperature. Precipitation medium pH was held above 10 by the addition of ammonium hydroxide along the process.

The precipitate solution was stirred for 24 h at 60°C and was further filtered by using fritted glass Buchner funnel. The filtered cake was washed three times with deionised water in order to eliminate ammonia. The centrifuged cake was dried in oven (Binder) at 90°C overnight.

### 4.2.2. Molten Salt Synthesis of HA Whiskers

In the initial stages of the study, NaCl (as flux) and commercial HA were used for the synthesis of HA whiskers. The HA to NaCl weight ratios were fixed at 1/3, 1/1 and 3/1. Hydroxyapatite and NaCl were mixed together in an agate mortar according to their weight ratios. These mixtures were put into ceramic crucibles and placed inside a muffle furnace (Carbolite-CW1300). Samples were heat treated at 800, 1000 and 1100°C for 2 h with a heating rate of 5°C/min and they were cooled to room temperature by shutting off the furnace. The whiskers were separated from the mass of solidified salt by washing several times in hot (~90°C) deionised water to ensure

complete removal of the flux. “NW” was the code of NaCl-HA whiskers where N and W represent “NaCl” and “whisker”, respectively.

After these preliminary experiments with NaCl, the HA whiskers were synthesized by using  $K_2SO_4$  in order to investigate the differences in the whisker growth behaviour. Both commercial and synthesized HA powders were used for these experiments. The  $K_2SO_4$ -HA weight ratios were varied in the 1/1 to 4/1 range. Hydroxyapatite and  $K_2SO_4$  were mixed both in dry and wet conditions. The dry blending of as received  $K_2SO_4$  and HA was accomplished in an agate mortar.

In order to eliminate the foreign nucleation sites, recrystallized  $K_2SO_4$  was used for the wet mixing of the two components. For the preparation of HA whiskers recrystallized  $K_2SO_4$  was dissolved in deionised water and then suitable amount of commercial HA was added. The suspension was mixed with a magnetic stirrer for 1 h and subsequently treated ultrasonically with glass balls for 2 h in order to enhance the dispersion of the powder particles in the flux and elimination of the agglomerates. “KW” was the code of  $K_2SO_4$ -HA whiskers where K represents “ $K_2SO_4$ ” and W stand for “whisker”.

Hydroxyapatite and  $K_2SO_4$  suspension was left in an oven at 90°C until it dried. The dried mixture was ground by means of an agate mortar and was subjected to heat treatment. The heat treatment temperatures and time were selected as 1100°C, 1150°C and 1 hour, respectively. The heat treatment schedules are given in Table 4.2.

Table 4.2. Heat treatment steps of HA whiskers produced from HA- $K_2SO_4$

<b>For 1100°C</b>	<b>For 1150°C</b>
RT-1000°C: 10°C/min	RT-1000°C:10°C/min
1050°C: 5°C/min	1000-1050°C: 5°C/min
1050-1100°C: 2°C/min	1050-1150°C: 2°C/min
Duration at 1100°C for 1h.	Duration at 1150°C for 1h.
1100-1050°C: 2°C/min	1150-1050°C: 2°C/min
1050-RT: furnace cooled (20°C/min)	1050-RT: furnace cooled (20°C/min)

$K_2SO_4$  was removed from the whiskers and the other particles by washing the solidified salt and whisker mass several times with deionised water. Washing was repeated until the specific conductance of the decanted liquid was  $\leq 10\text{-}15 \mu\text{S}$  which was measured by using a conductance meter (Inolab-WTW), knowing that the conductance of deionised water was  $1.5 \mu\text{S}$ . Finally, the washed whiskers were dried in the oven at  $100^\circ\text{C}$  overnight.

The last HA whisker synthesis process in this study was carried out by using a mixture of NaCl, recrystallized  $K_2SO_4$  and commercial HA powder. Although the exact melting point of the salt mixture was not present in the literature, it was observed that it melted at around  $700^\circ\text{C}$ . The weight ratio of NaCl/ $K_2SO_4$  was chosen as 1:1 and (NaCl+ $K_2SO_4$ )/HA ratios were determined as 3:1 and 5:1. These components were wet mixed. The whisker preparation steps were similar with the molten salt synthesis of  $K_2SO_4$ -HA route except that the soaking temperature and the time which were varied from  $800^\circ\text{C}$  to  $900^\circ\text{C}$  and 2 to 5 h, respectively. The heating and cooling rates were determined as  $5^\circ\text{C}/\text{min}$  for all of the samples in this part. “KNW” was the code of NaCl- $K_2SO_4$ -HA whiskers where K, N and W stand for “ $K_2SO_4$ ”, “NaCl” and “whisker”, respectively.

### **4.3. Formation of HAp/HAw Composites**

The synthesized HA whisker/commercial HA powder composites were consolidated by slip casting and dry pressing methods. Both consolidation techniques are widely used in the ceramic industry. The consolidation technique utilized for the formation of the composites may influence the compact microstructure significantly. The particle size and particle size distribution may have great importance especially for the slip casting method. Both slip cast and dry pressed samples were sintered under similar conditions in order to observe differences in their densification behaviours.

#### **4.3.1. Slip Casting of HAp/HAw Composites**

Slip casting method was used for the production of HAp/HAw composites. The slurries with different HA contents (25%, 30%, 35% and 40% by volume) were prepared by mixing the HA powder with water and Darvan-C (as dispersant). Slip

castable suspensions were prepared after 1 h of ultrasonic treatment except the 40% vol/vol suspension. The HAp + HA<sub>w</sub> content was chosen as 35% vol/vol for the preparation of composites. The HA<sub>w</sub> content of the composites was further selected as 0, 10%, 20%, 30%, 40% and 50%.

The HA powder suspension was ball milled for 6 h with 3 mm diameter zirconia balls in order to break down the agglomerates. This stock suspension was further used for the preparation of composite suspensions. The necessary amount of HA whisker was added to the HA powder suspensions after ball milling. The composite suspensions were treated ultrasonically for 2 h with momentary mechanical mixing. These composite suspensions were dried in the oven at 70°C until they were brought to the desired water content and they were ultrasonically treated again for about 1 h. Darvan-C was added dropwise into the suspensions gradually in order to obtain a desirable slip during ultrasonic treatment. The addition of Darvan-C decreased the viscosity and improved the flow behaviour of the suspensions. These slips were poured into cylindrical moulds which were further closed with lids in order to prevent excessive evaporation and contamination from the laboratory environment. The composites were cast overnight and they were dried in the oven at 60°C for 12 h.

The green densities of the HAp/HA<sub>w</sub> composites were calculated by using their approximate dimensions. All the samples were sintered at 1200, 1250, 1300 and 1350°C for 2 hours with a heating rate of 10°C/min and cooling rate of 20°C/min (Carbolite-CW1300 furnace). The density values of the sintered composites were determined by means of the Archimedes' method (Sartorius density measurement kit).

### **4.3.2. Dry Pressing of HAp/HA<sub>w</sub> Composites**

Dry pressing (uniaxial press) is a very common method for the formation of HA based materials. Some of the slip cast compacts were ground to the powder form without damaging the whisker structures. Composite powders with different whisker contents were dry pressed (Carver Hydraulic Press) with a 10 mm diameter die at 160 MPa pressure. They were further sintered under similar conditions with the slip cast composites and their densities were determined by means of the Archimedes' method.

#### **4.4. Characterization of HA Whiskers and HAp/HAw Composites**

The sizes, size distribution and the morphologies of the HA whiskers produced by using different salts (NaCl, K<sub>2</sub>SO<sub>4</sub> and NaCl-K<sub>2</sub>SO<sub>4</sub> mixture) and the microstructure of the composites were investigated by using a scanning electron microscope (SEM) equipped with an energy dispersive X-ray (EDX) probe for the determination of the approximate elemental compositions of the samples (Philips XL 30S FEG).

X-Ray diffraction (XRD) analysis were performed on the HA whiskers and HAp/HAw composites in order to investigate the phase structure of the samples (Philips XPERT PRO).

## CHAPTER 5

### RESULTS AND DISCUSSION

In this study, the densification and sintering behaviour of HAp/HAw composites were investigated. Molten salt synthesis (MSS) technique was used for the preparation of HA whiskers with different types of salts such as NaCl, K<sub>2</sub>SO<sub>4</sub> and NaCl-K<sub>2</sub>SO<sub>4</sub> mixture. The effects of MSS parameters such as the starting HA powder properties, synthesis temperature / time, salt, salt/HA powder ratio and the degree of mixing of the starting phases on the sizes and the morphologies of the whiskers were analysed. The densification behaviour of composites with various HA whisker contents was investigated

#### 5.1. Characterization of Pure HA Powder and HA Whiskers

The XRD patterns (CuK<sub>α</sub> radiation: 1.542) of commercial hydroxyapatite powder used in this study is given in Figure 5.1. The major reference HA XRD peaks tabulated in Table 5.1 (JCPDS card no: 73-0294) can be seen in the HA powder pattern given in Figure 5.1.

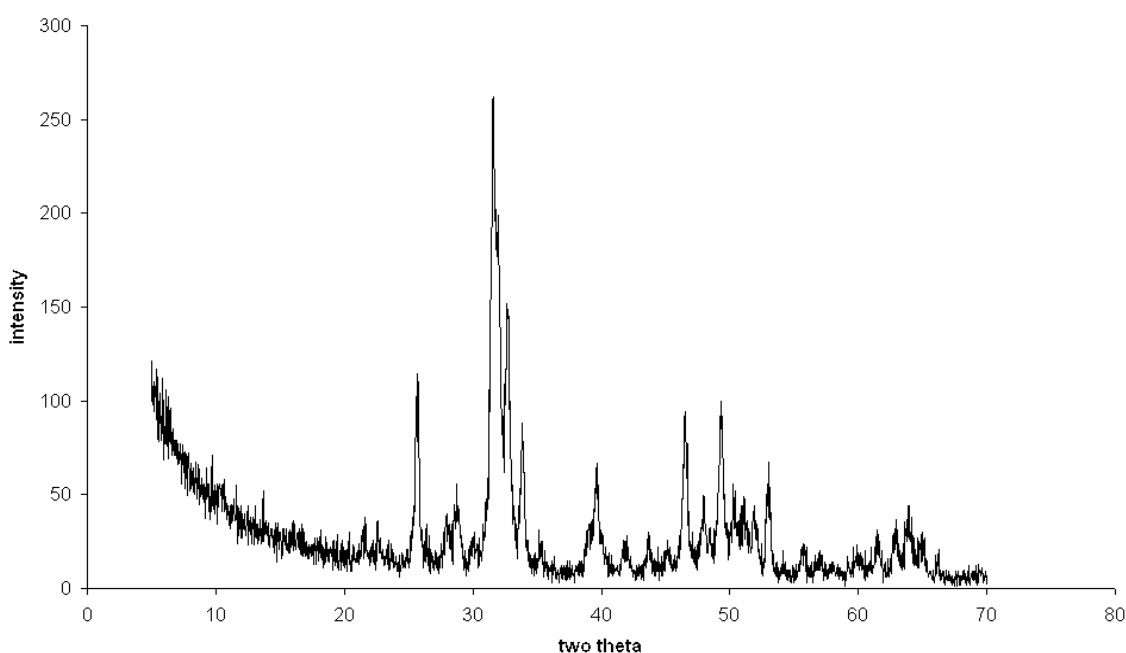


Figure 5.1. XRD pattern of commercial HA powder.

Table 5.1.  $2\theta$  values of XRD pattern of reference HA.

$2\theta$	10.82	16.83	18.80	21.74	22.84	25.33	25.87	28.12	28.89	31.74	32.17	32.86	34.04
Intensity	171	46	24	66	63	24	362	89	161	999	515	615	212

$2\theta$	35.42	38.13	39.17	39.75	40.40	40.83	41.95	42.29	43.85	44.32	45.30	46.34	46.66
Intensity	39	2	51	206	18	4	56	11	45	11	35	7	283

$2\theta$	48.04	48.54	49.46	50.43	51.20	52.03	53.20	54.46	55.81	56.26	57.09	57.97	58.13
Intensity	122	41	309	162	115	114	138	10	60	2	38	15	11

$2\theta$	58.24	58.68	59.86	60.34	61.51	61.67	25.87	62.92	63.34	63.96	64.11	64.93	66.36
Intensity	10	8	43	31	31	54	362	79	16	74	89	70	20

$2\theta$	67.32	68.42	68.91	69.16	69.61	70.04	70.44	70.74	71.33	71.52	71.67	72.15	72.40
Intensity	1	4	2	1	20	4	1	2	5	37	20	28	16

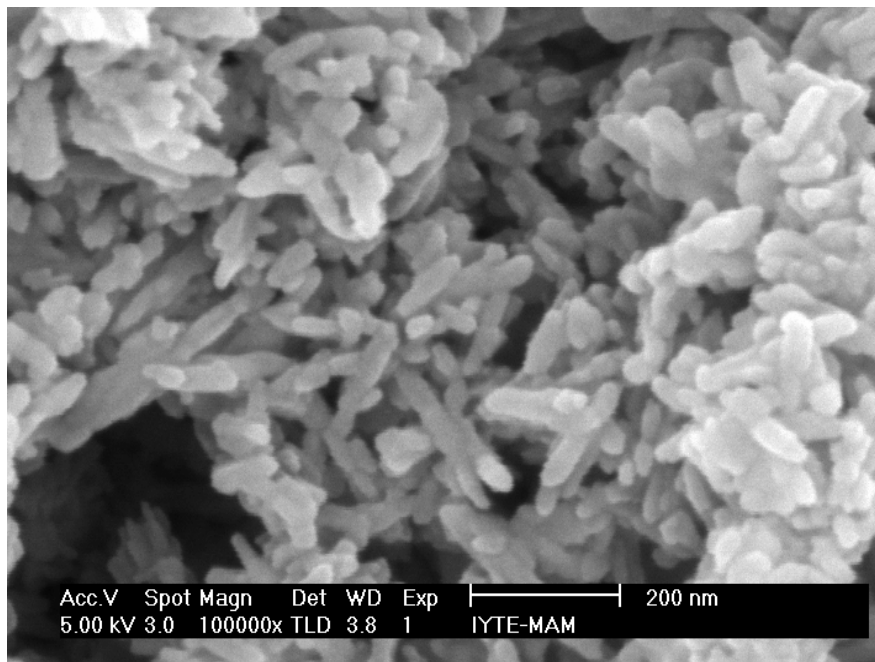


Figure 5.2. SEM image of commercial HA powder.

The morphology of commercial HA powder is seen in Figure 5.2. The fine HA powder particles have rod-like morphology. The length and diameters of the particles were in the range of 50-220 nm and 20-50 nm, respectively.

The characteristics of NaCl-HA whiskers synthesized at different temperatures are given in Table 5.2. N and W represent “NaCl” and “whisker”, respectively, in the sample coding. The dimensional and morphological properties were investigated by SEM analysis.

Table 5.2. Synthesis conditions and dimensional properties of HA whiskers prepared by using NaCl.

<b>Sample Name</b>	<b>NaCl/HA Ratio (weight)</b>	<b>Heat Treatment Temp.(°C)</b>	<b>Whisker Length (µm)</b>	<b>Whisker Diameter (µm)</b>	<b>Aspect Ratio</b>
NW1	1/3	800	0.2-3	0.10-1	2-5
NW2	1/3	1000	0.5-20	0.3-8	2-5
NW3	1/3	1100	1-20	0.5-5	2-8
NW4	1/1	800	0.25-3	0.15-1.25	2-5
NW5	1/1	1000	5-45	2-15	2-7
NW6	1/1	1100	5-45	2-20	2-8
NW7	3/1	800	0.25-5	0.15-1.25	2-5
NW8	3/1	1000	5-40	2-15	2-7
NW9	3/1	1100	5-40	2-20	2-8

Figure 5.3 and 5.4 show the XRD graphs of whiskers from NW4 to NW9. The XRD patterns of first three whiskers (NW1, NW2 and NW3) exhibited close resemblance with the NW4, NW5 and NW6. The whisker patterns in Figure 5.3 show that HA is the dominant phase for all of the samples. It seems that the different heat treatment temperatures did not influence the peak sharpness. The major peaks mentioned in Table 5.1 were also seen in HA whisker patterns. The intensities of major peaks at 31.7° and 32.86° displayed increase in Figure 5.4 when compared with those in the XRD pattern of reference HA powder. On the other hand, the width of these major peaks and other minor peaks decreased as the preparation temperature increased. The increase in sharpness and intensities of these peaks at 1000 and 1100°C indicates that the crystal size becomes larger. The major phase is mainly HA in all of these whiskers where no peaks related with other impurity phases were detected.

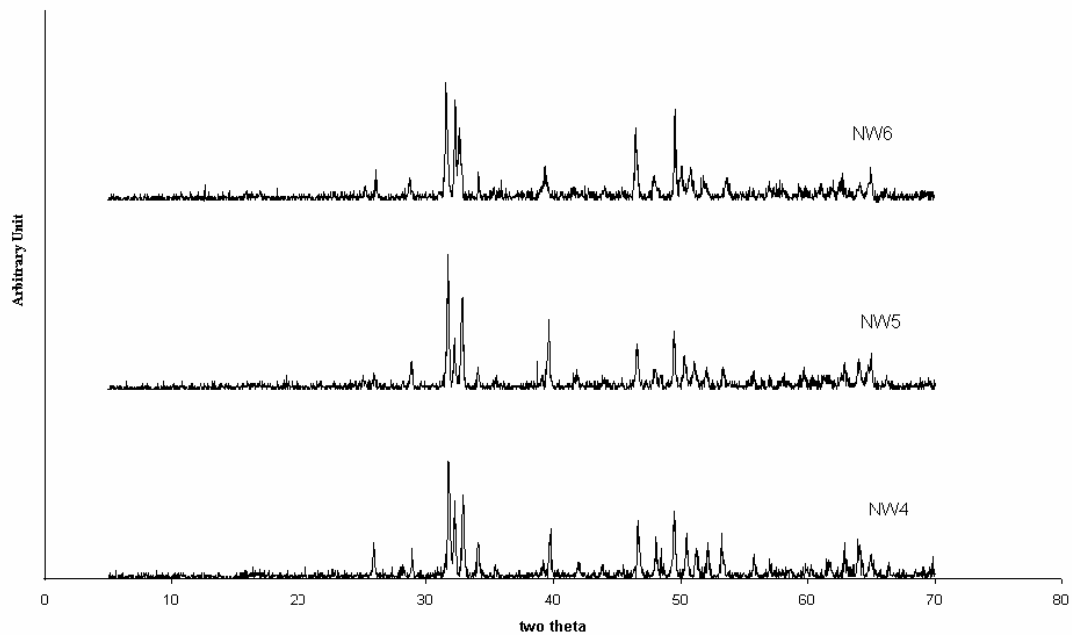


Figure 5.3. XRD patterns of NW4, NW5, NW6 whiskers where NaCl/HA ratio during preparation was 1/1.

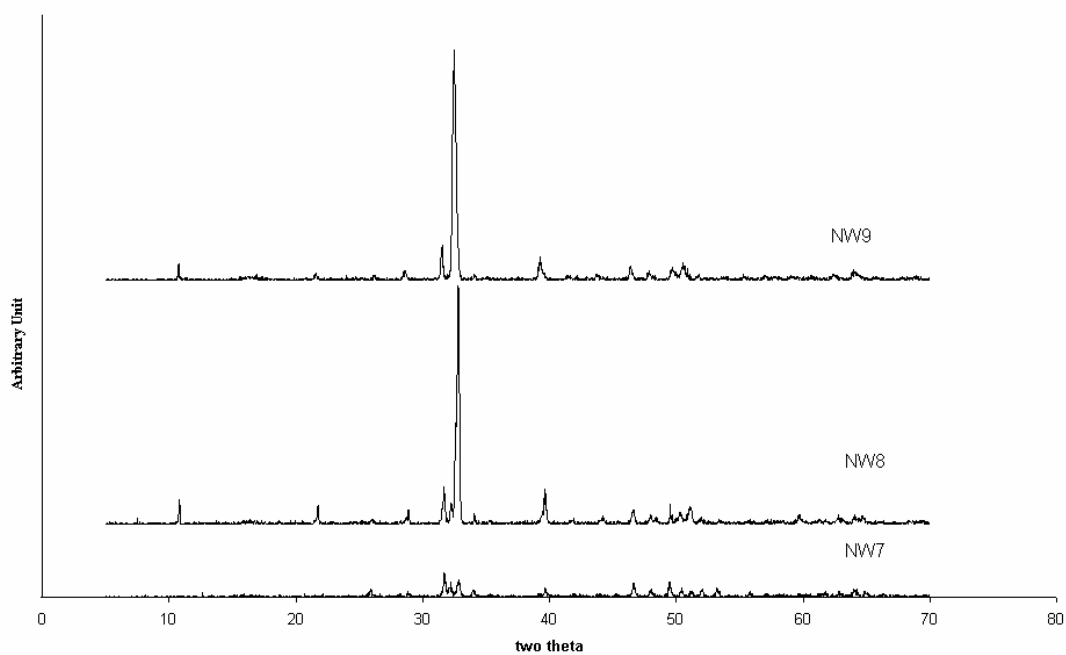


Figure 5.4. XRD patterns of NW7, NW8 and NW9 whiskers where NaCl/HA ratio during preparation was 3/1.

The morphology and sizes of NaCl-HA whiskers synthesized at 800°C is shown in Figure 5.5. The whiskers that have different NaCl/HA ratios, almost exhibited the same microstructure at this temperature. The presence of fine whiskers was most likely due to the fact that the preparation temperature was about equal to the melting point of NaCl (801°C). The forms of the salt/whisker mixture obtained after heat treatment at 800°C have shown that the salt melted during whisker synthesis. However, it is likely that the synthesis temperature/time was not high enough for molten salt viscosity/mass transport processes and/or enhanced crystal growth kinetics of HA whiskers. Therefore, the length and diameters of whiskers were in the range of 0.2-3  $\mu\text{m}$  and 0.1-1  $\mu\text{m}$ , respectively. Rarely, relatively larger whiskers can be seen among the small ones.

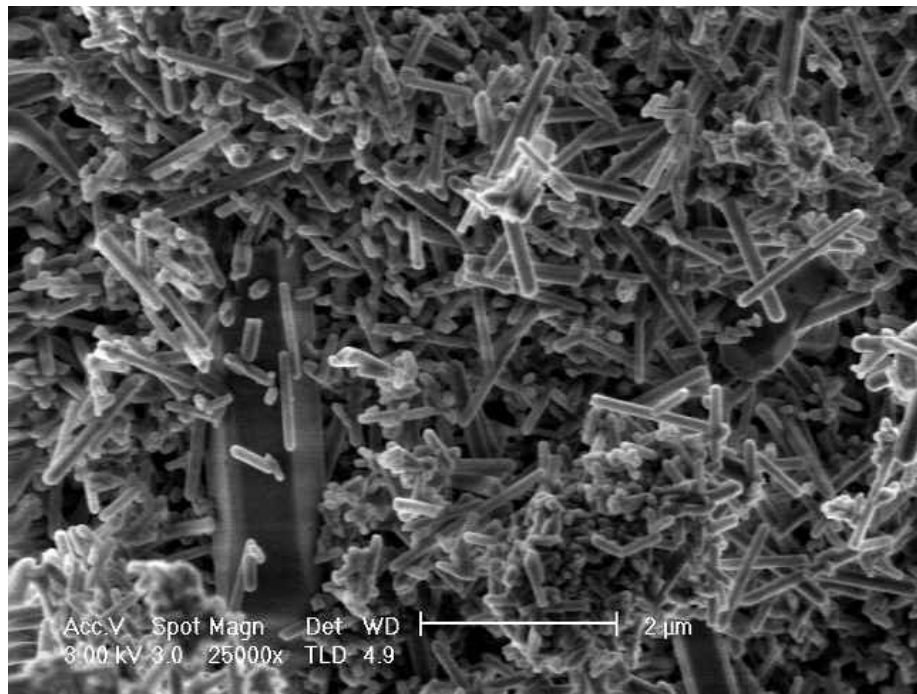


Figure 5.5. SEM image of NW1 whiskers synthesized at 800°C where NaCl/HA ratio during preparation was 1/3.

The NW2 whiskers shown in Figure 5.6 are relatively thick compared to the previous NW1 whiskers. In some regions of the SEM samples agglomerates were observed. These agglomerates contained very small and thin whiskers. The length and diameter of the whiskers were determined to be in a wide range and varied from 0.2-20  $\mu\text{m}$  and 0.1-8  $\mu\text{m}$ , respectively because of the presence of fine whiskers as agglomerates and on the surfaces of bigger whiskers.

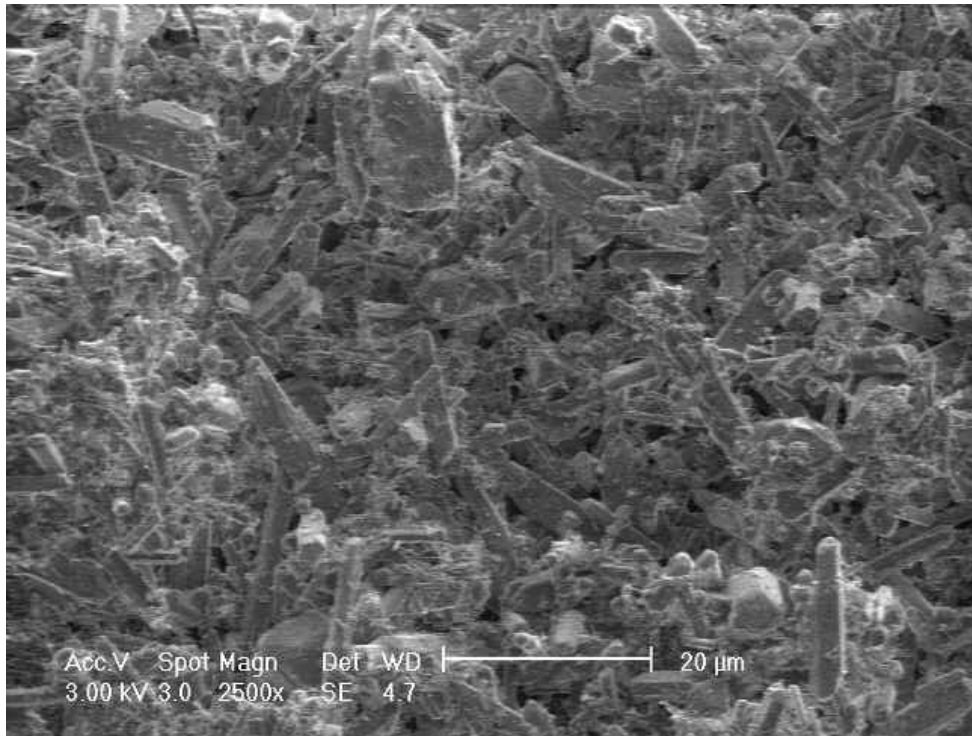


Figure 5.6. SEM image of NW2 whiskers synthesized at 1000°C where NaCl/HA ratio during preparation was 1/3.

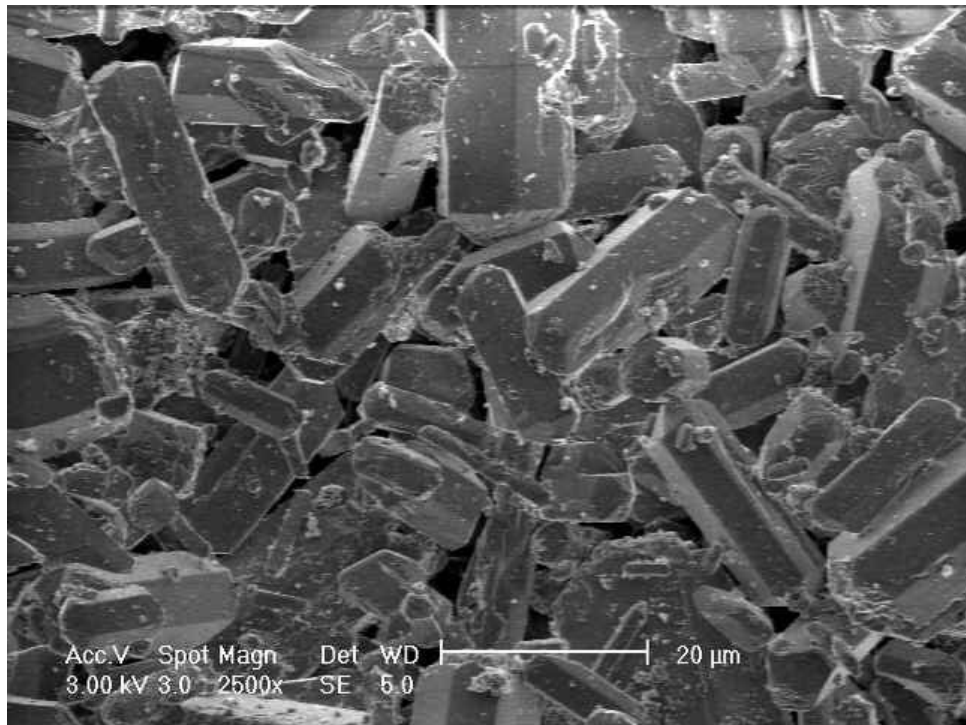


Figure 5.7. SEM image of NW5 whiskers synthesized at 1000°C where NaCl/HA ratio during preparation was 1/1.

The morphology/size of the NW5 whiskers are shown in Figure 5.7. The dimensions of the whiskers are significantly different when compared with the NW2 whiskers. The presence of three times more salt for the synthesis at the same temperature enhanced crystal growth kinetics and caused the formation of whiskers with larger diameters. The length, diameter and aspect ratio of NW5 whiskers generally varied from 5 to 45  $\mu\text{m}$ , 2 to 15  $\mu\text{m}$  and 2 to 7, respectively.

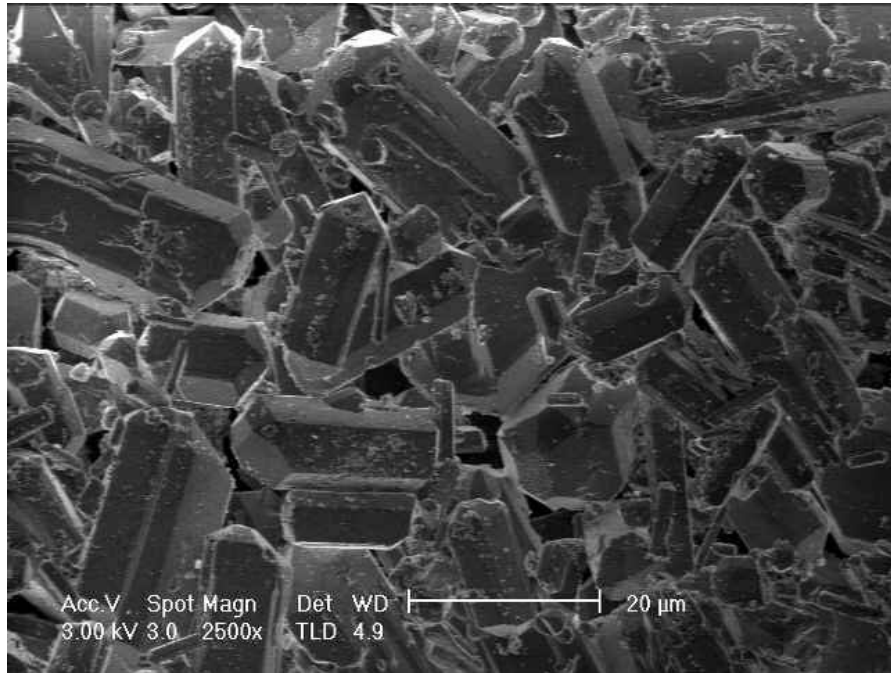


Figure 5.8. SEM image of NW8 whiskers synthesized at 1000°C where NaCl/HA ratio during preparation was 3/1.

The morphology/size of the NW8 whiskers given in Figure 5.8 are similar to NW5 whiskers. The further increase in the NaCl/HA powder ratio above 1/1 to 3/1 did not affect the morphological properties significantly. This indicates the presence of a limiting salt amount to use during whisker synthesis. Synthesized NW8 whiskers all had hexagonal crystal structures where their length diameter and aspect ratio were in the range of 5 to 40  $\mu\text{m}$  and 2 to 15  $\mu\text{m}$  and 2-7, respectively.

The morphology/size of the NW6 whiskers is given in Figure 5.9 which also resembles closely with the NW9 whiskers. These synthesized particles have a broad particle size range and different morphologies. Although some particles retained their cylindrical shapes, a significant amount formed close to equiaxed particles which were fused together at the points of mutual contact. The length and diameters of the whisker like particles were in the range of 5-45 and 2-20  $\mu\text{m}$ , respectively. The aspect ratio of the whiskers varied from 2-8.

Unlike the NW6 crystals, numerous thin and small whiskers were present in the NW3 sample shown in Figure 5.10. The sizes and shapes of the crystals varied in a broad range.

The experiments performed by using NaCl salt in three different weight ratios and heat treatment temperatures revealed that the whiskers were not very uniform in size/morphology and had relatively large diameters than those suitable for use as reinforcements in the HAp/HAw composites. Although the whiskers synthesized at 800°C were uniform, the sizes/aspect ratios of those whiskers may not be large enough for use as reinforcements.

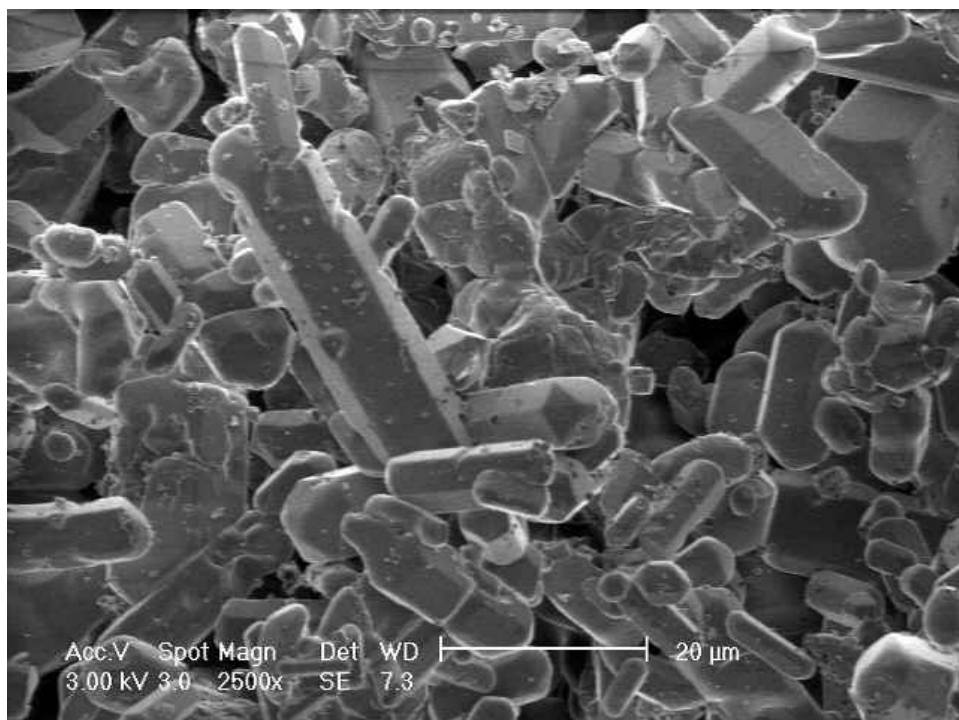


Figure 5.9. SEM image of NW6 whiskers synthesized at 1100°C where NaCl/HA ratio during preparation was 1/1.

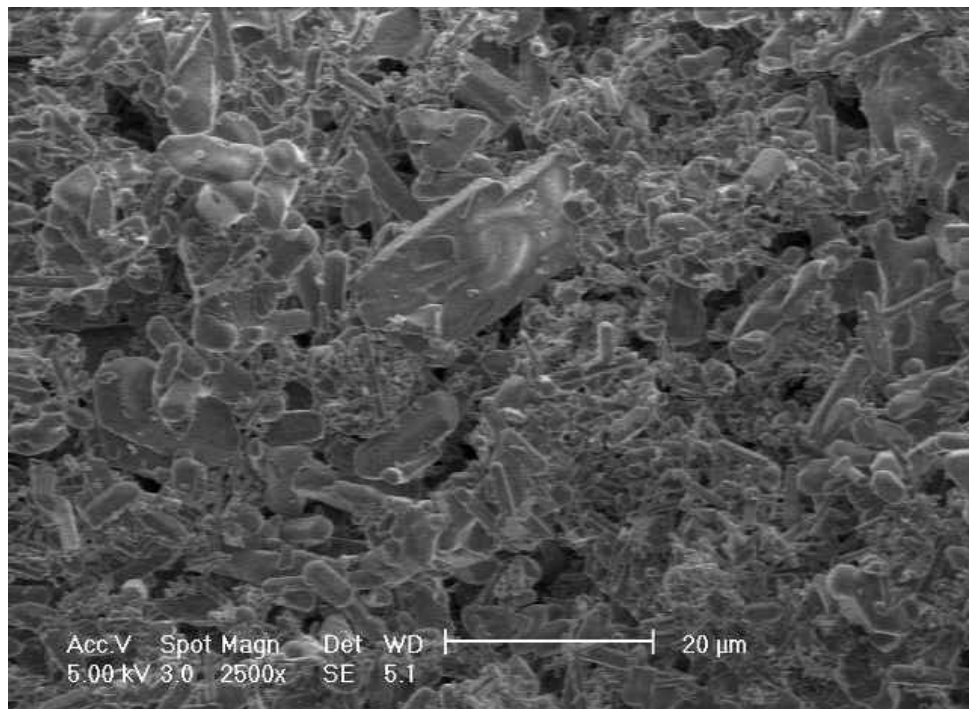


Figure 5.10. SEM image of NW3 whiskers synthesized at 1100°C where NaCl/HA ratio during preparation was 1/3.

$K_2SO_4$  was used as the second flux for synthesizing HA whiskers. The preparation conditions and codes of these HA whiskers are tabulated in Table 5.3. The XRD pattern of KW5 whiskers is shown in Figure 5.11. The peaks tabulated previously in Table 5.1 for HA are mainly present in the KW5 HA whisker XRD pattern. The intensity of KW5 whisker peak located at  $32.86^\circ$  is higher than that of the peak at  $31.7^\circ$  in contrary to that observed in the reference HA powder XRD pattern. The broadness of those peaks and several other minor peaks decreased.

It can be stated that the phase structure is mainly HA and other impurity phases are not present. Both the increase in sharpness and intensities and the smaller peak width are indications of the increase in crystal size.

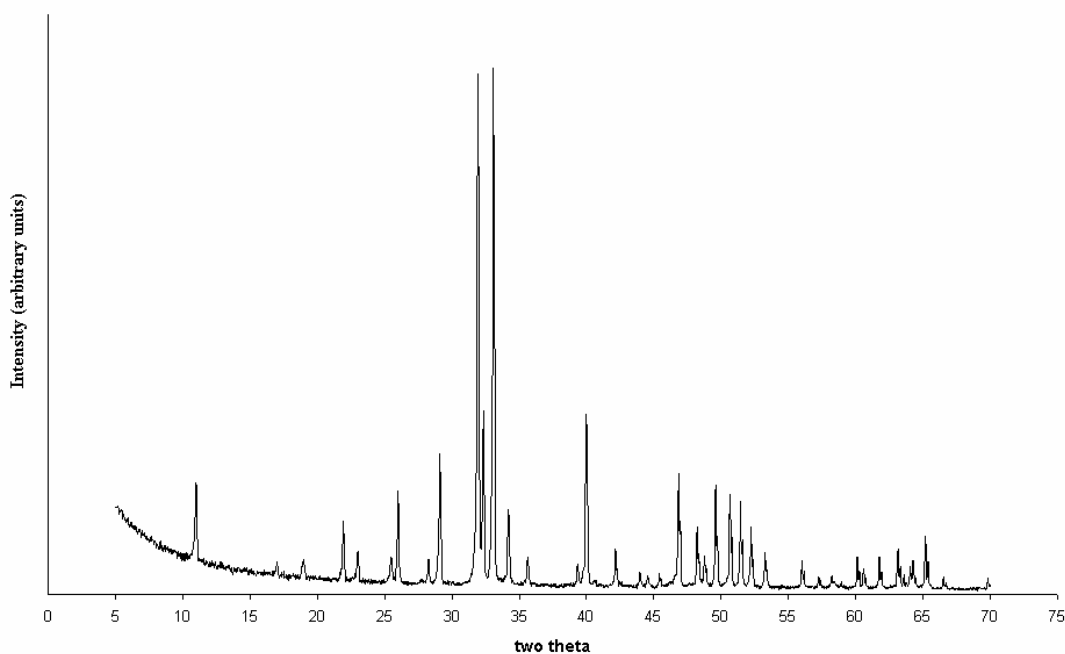


Figure 5.11. The XRD pattern of KW5 whiskers at  $1100^\circ\text{C}$  ( $K_2SO_4/HA$ : 3/1)

The synthesis conditions and characteristics of  $K_2SO_4$ -HA whiskers are given in Table 5.3. K and W stand for “ $K_2SO_4$ ” and “whisker”, respectively in the sample coding. The dimensional and morphological properties were investigated by SEM analysis.

Table 5.3. Synthesis conditions and dimensional properties of HA whiskers prepared by using  $K_2SO_4$

Sample Name	HA powder type	Mixing Type	$K_2SO_4/HA$ (weight)	Heat Treat. Temp. ( $^{\circ}C$ )	Whisker Length ( $\mu m$ )	Whisker Diameter ( $\mu m$ )	Aspect Ratio
KW1	commercial	dry	1/1	1100	5-10	0.5-1	10
KW2	commercial	dry	2/1	1100	5-30	1.5-2.5	10-15
KW3	commercial	dry	3/1	1100	7-25	0.8- 4	6-15
KW4	commercial	dry	4/1	1100	10-20	1-3	10
KW5	commercial	wet	3/1	1100	15-75	1-5	10-30
KW6	synthesized	wet	3/1	1100	10-30	0.8-5	6-10
KW7	commercial	wet	3/1	1150	5-90	1-10	10
KW8	synthesized	wet	3/1	1150	5-30	1-4	5-8

As can be seen from Table 5.3, the samples from KW1 to KW4 were mixed in the dry medium and heat treated at  $1100^{\circ}C$  for 1h. The morphologies of these whiskers are shown in Figures 5.12 to 5.15. Some small and thin whisker agglomerates can be detected especially in Figures 5.12 and 5.13. The length and diameter of the KW1-KW4 whiskers were determined to be in a wide range and varied from 5-30  $\mu m$  and 0.5-4  $\mu m$ , respectively. Some spherical particles with 4 $\mu m$  diameter were observed in KW3 and KW4 microstructures (Figures 5.14 and 5.15). Smaller particles were observed in KW1 sample which may be due to the insufficient amount of  $K_2SO_4$  for the growth of HA whiskers. The increase in  $K_2SO_4$  amount for the synthesis at the same temperature enhanced crystal growth kinetics and caused the formation of whiskers with relatively larger diameters. KW2 and KW3 whiskers have larger dimensional properties like length, diameter and aspect ratio when compared with KW1 and KW4 samples as can be seen in Table 5.3.

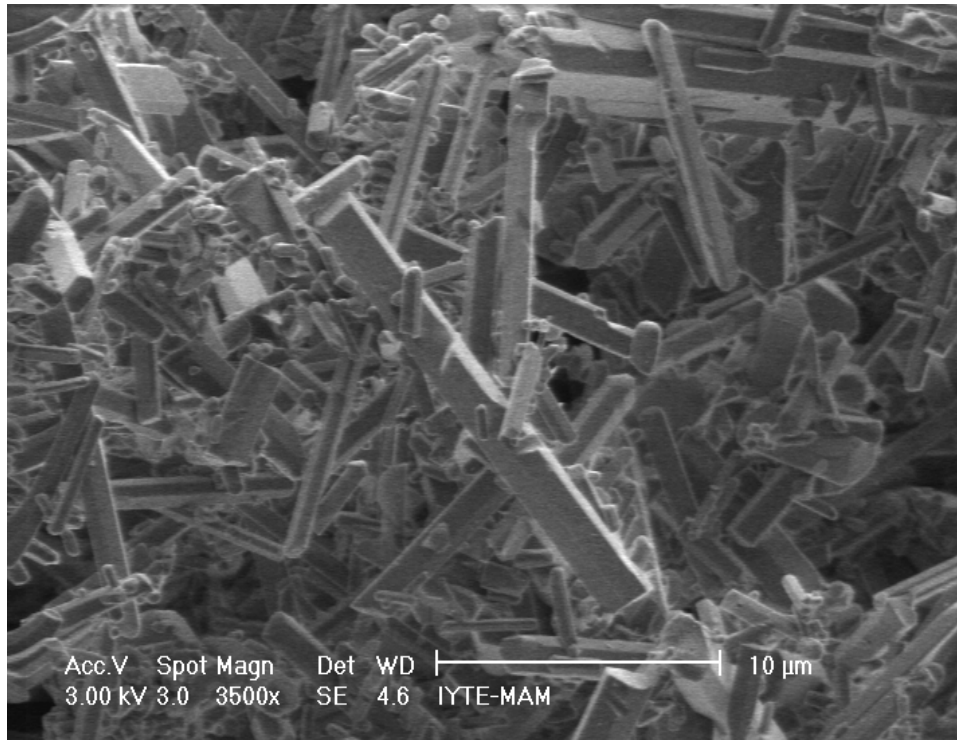


Figure 5.12. SEM image of dry mixed KW1 whiskers synthesized at 1100°C where  $K_2SO_4/HA$  ratio during preparation was 1/1.

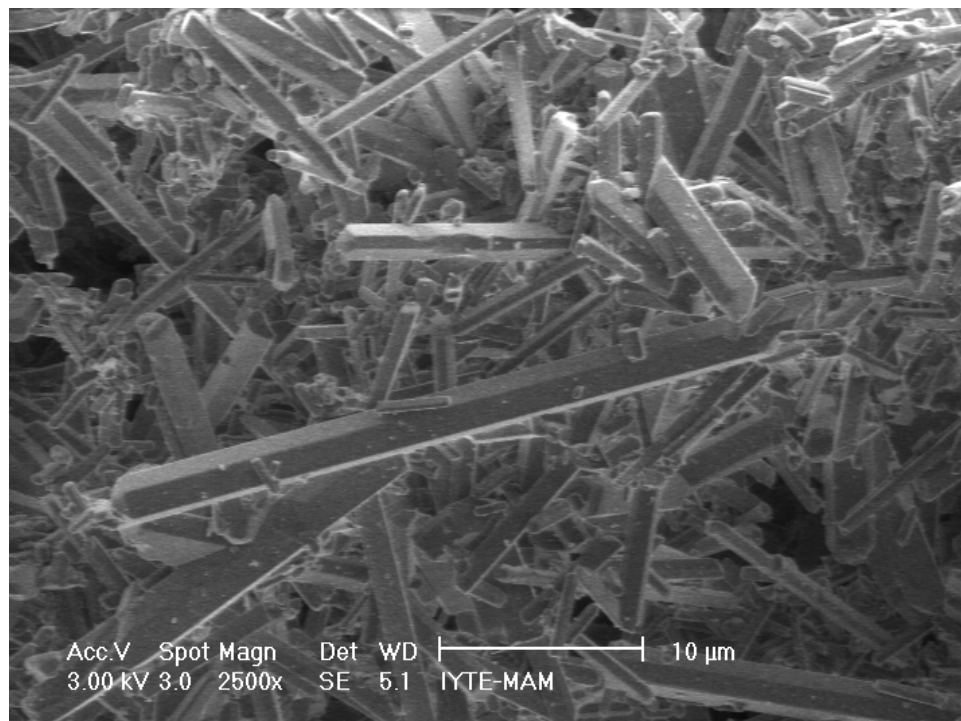


Figure 5.13. SEM image of dry mixed KW2 whiskers synthesized at 1100°C where  $K_2SO_4/HA$  ratio during preparation was 2/1.

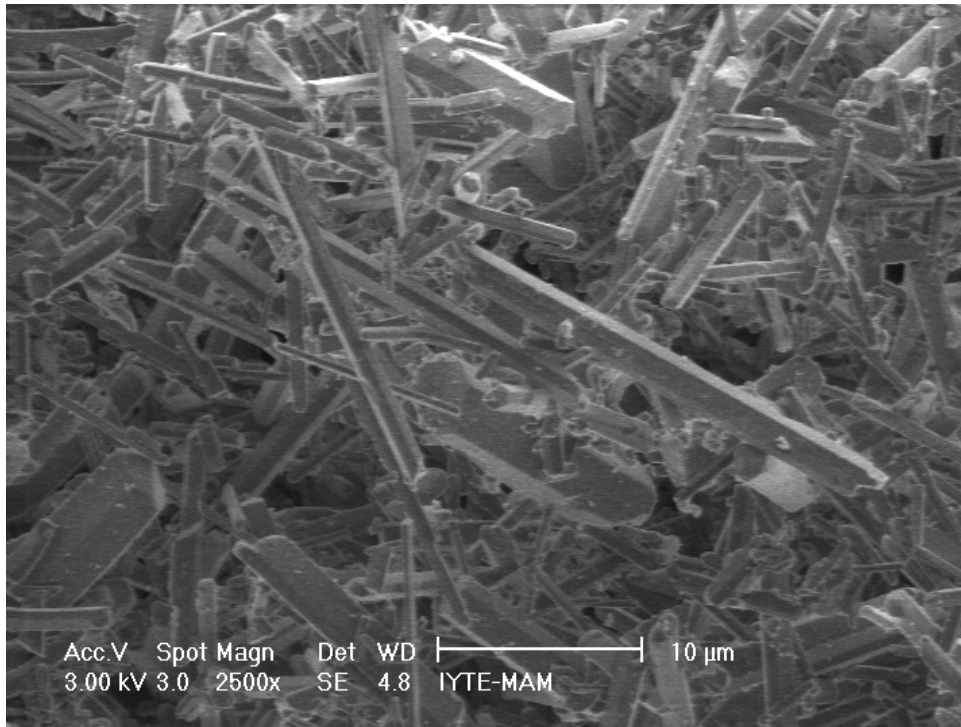


Figure 5.14. SEM image of dry mixed KW3 whiskers synthesized at 1100°C where  $K_2SO_4/HA$  ratio during preparation was 3/1.

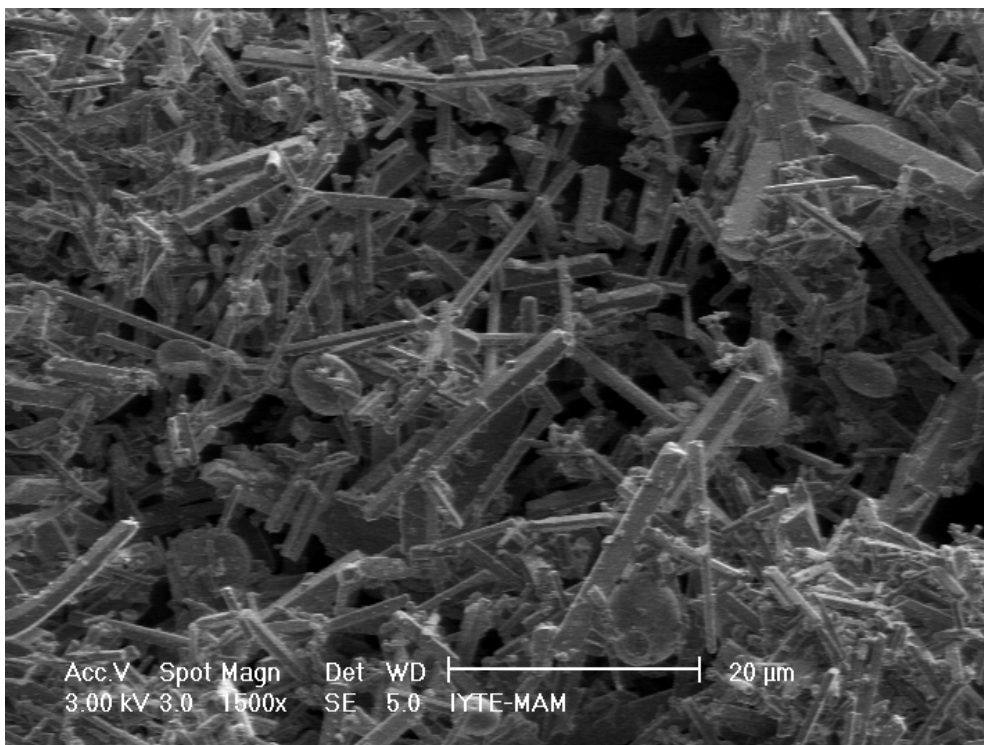


Figure 5.15. SEM image of dry mixed KW4 whiskers synthesized at 1100°C where  $K_2SO_4/HA$  ratio during preparation was 4/1.

Some process steps like ball milling and ultrasonic treatment were added to the preparation of HA whiskers in order to obtain better whisker morphology. The  $K_2SO_4$  to HA ratio of KW5, KW6, KW7 and KW8 samples was selected as 3/1. In those experiments, both commercial and synthesized HA powders were used. The XRD patterns of commercial HA powder and synthesized HA powder ( $CuK_{\alpha}$  radiation: 1.542) were similar and no impurity phases were detected in the  $5-70^{\circ} 2\theta$  range (Figure 5.16). Similar processing conditions were applied to all salt-HA powder mixtures other than the heat treatment temperature.

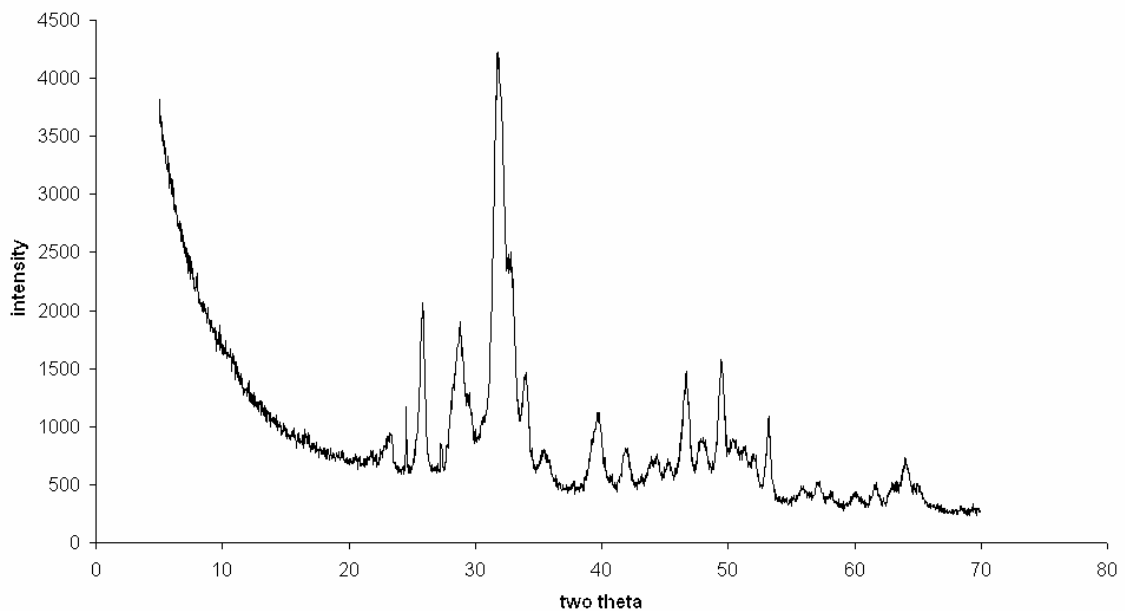


Figure 5.16. The XRD pattern of synthesized HA powder.

The KW5 whiskers made of commercial HA powder and KW6 whiskers obtained from the synthesized HA powder were treated at 1100°C for 1 hour. The distributions of these whiskers seem more uniform compared to the KW1-KW4 whiskers. The KW5 whiskers exhibited the formation of relatively uniform and thinner HA whiskers with an aspect ratio of 30 and a typical diameter and length of 2.5  $\mu\text{m}$  and 60  $\mu\text{m}$ , respectively. Unlike the KW1-KW4 samples, no spheres were observed in the SEM pictures of KW5. However, the subsequent samples prepared by applying the same processing steps of KW5 did not exhibit similar morphology and contained spherical particles with the diameters in 4-7  $\mu\text{m}$  range. The dissolution/recrystallization/crystal growth and sintering of particles occur simultaneously at 1100-1150°C. Significantly higher levels of potassium was detected on the spherical particles by SEM-EDX analysis compared to the whiskers. This may be due to the penetration of potassium into the HA particles during heat treatment (Figures 5.17 and 5.18). Also, some fine HA particles formed agglomerates and densified significantly at that temperature. The presence of a sintered microstructure with relatively large grains on these spherical particles may also be due to the enhanced densification processes caused by the presence of a liquid phase (Figures 5.19 and 5.20).

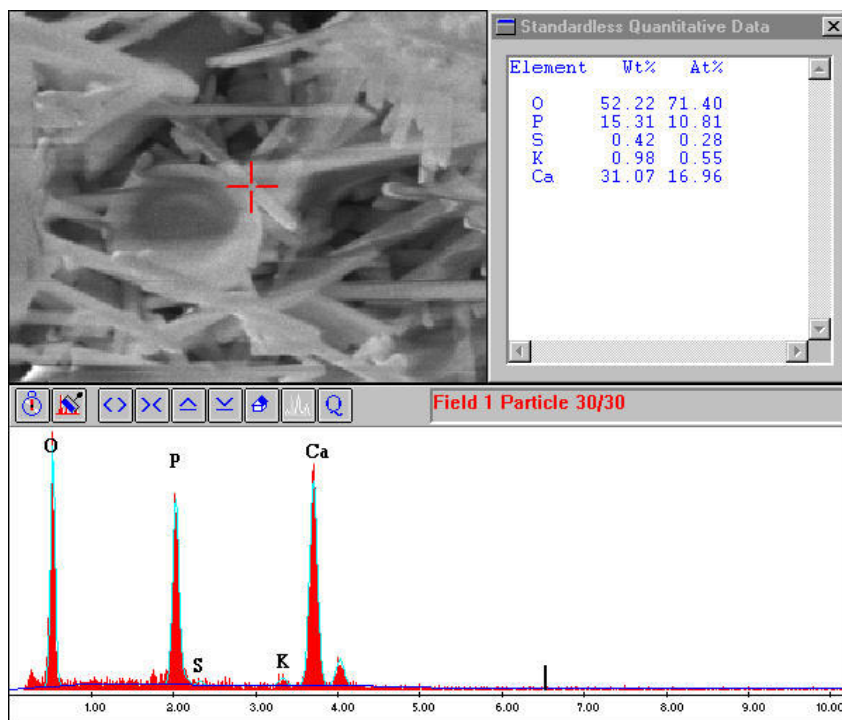


Figure 5.17. EDX image of wet mixed commercial HA powder KW7 whisker synthesized at 1150°C where  $K_2SO_4/HA$  ratio during preparation was 3/1.

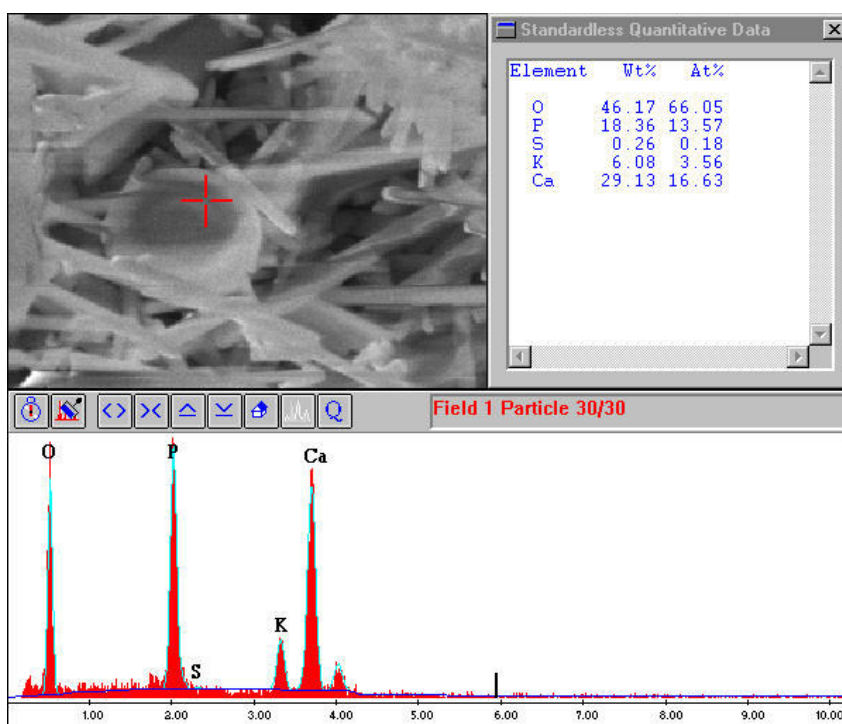


Figure 5.18. EDX image of wet mixed commercial HA powder KW7 spherical particle synthesized at 1150°C where  $K_2SO_4/HA$  ratio during preparation was 3/1.

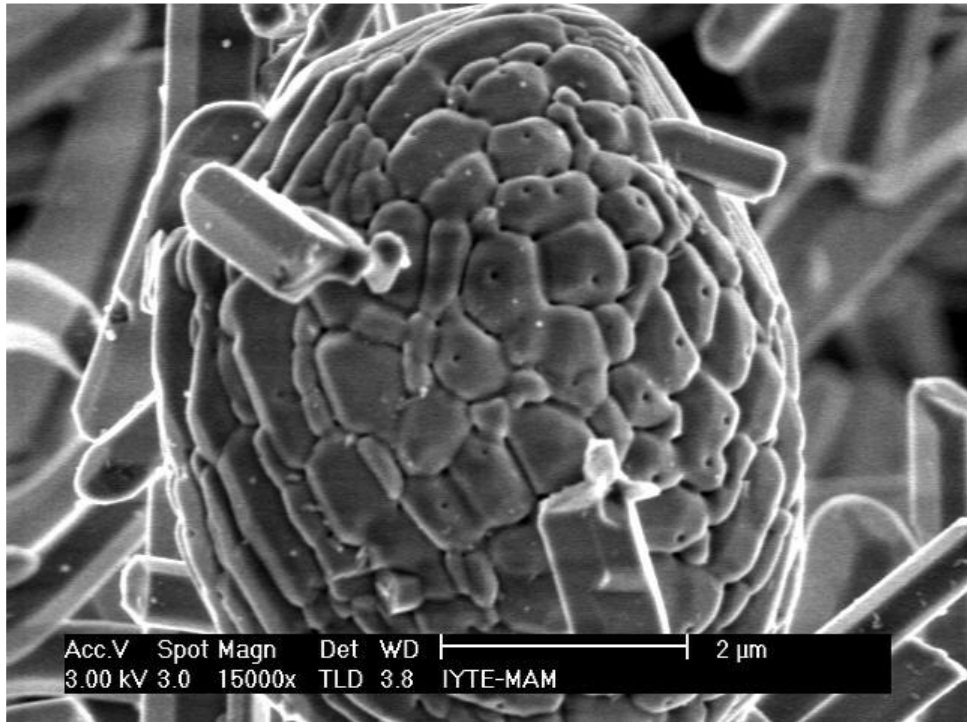


Figure 5.19. SEM image of wet mixed commercial powder KW7 sample agglomerate synthesized at 1150°C where  $K_2SO_4/HA$  ratio during preparation was 3/1.

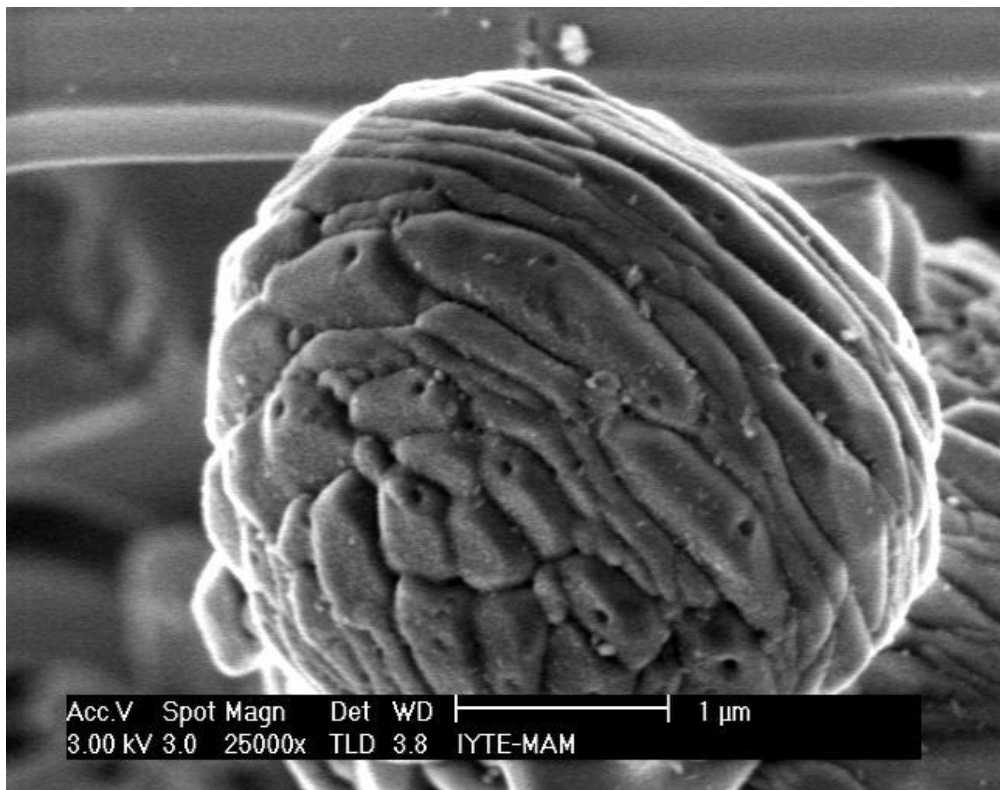


Figure 5.20. SEM image of wet mixed commercial powder KW7 sample agglomerate synthesized at 1150°C where  $K_2SO_4/HA$  ratio during preparation was 3/1.

Although the morphologies of KW5 and KW6 samples were similar, the diameters of KW6 whiskers were smaller than KW5 whiskers (Figures 5.21 and 5.22). The length, diameter and aspect ratio of KW6 whiskers were in the range of 10-30  $\mu\text{m}$ , 0.8-5  $\mu\text{m}$  and 6-10, respectively. Some spheres were also observed in the SEM pictures of KW6 samples with diameter in the range of 3-8  $\mu\text{m}$ .

The KW6 and KW8 samples (synthesized powder derived) exhibited close similarity in terms of the whisker dimension distribution as shown in Figures 5.22 and 5.24, respectively. The length, diameter and aspect ratios of KW8 whiskers varied from 5-30  $\mu\text{m}$ , 1-4  $\mu\text{m}$  and 5-8, respectively. However, the KW7 whiskers were not as long as the KW5 whiskers (both samples derived from commercial HA) and their aspect ratios decreased. Higher sphere content in the KW7 sample was also observed (Figure 5.23).

Neither heat treatment temperature (1100 or 1150°C) nor starting HA powder properties influenced the morphologies of the  $\text{K}_2\text{SO}_4/\text{HA}$  whiskers significantly. The  $\text{K}_2\text{SO}_4$  amount increase at a constant temperature led to the enhanced crystal growth kinetics and caused the formation of whiskers with larger diameters.

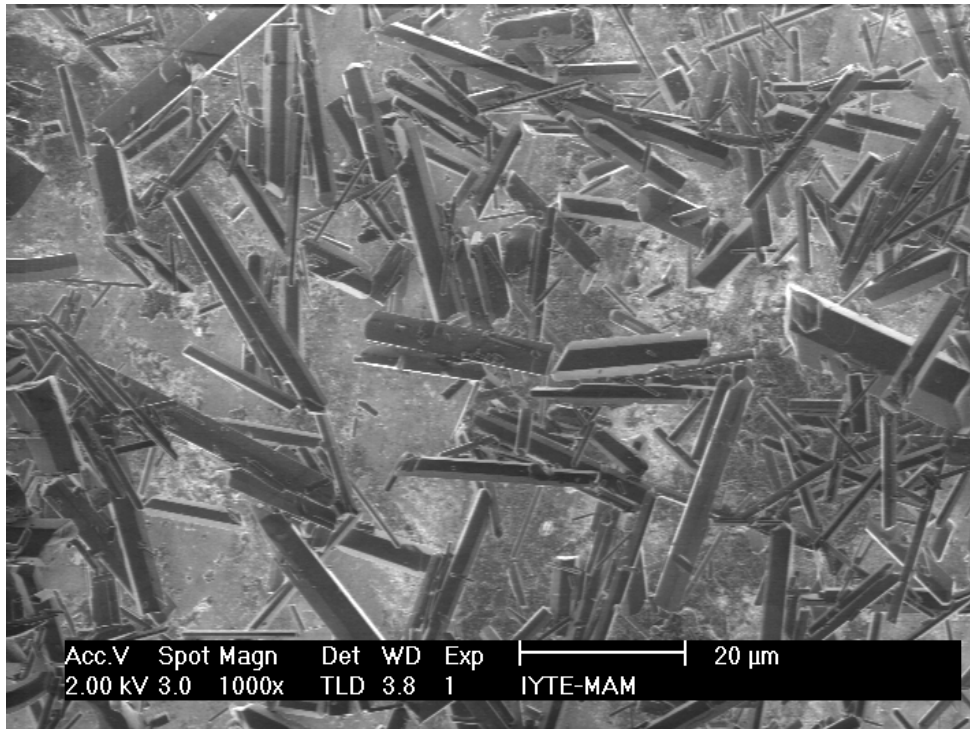


Figure 5.21. SEM image of wet mixed commercial HA powder KW5 whiskers synthesized at 1100°C where  $K_2SO_4/HA$  ratio during preparation was 3/1.

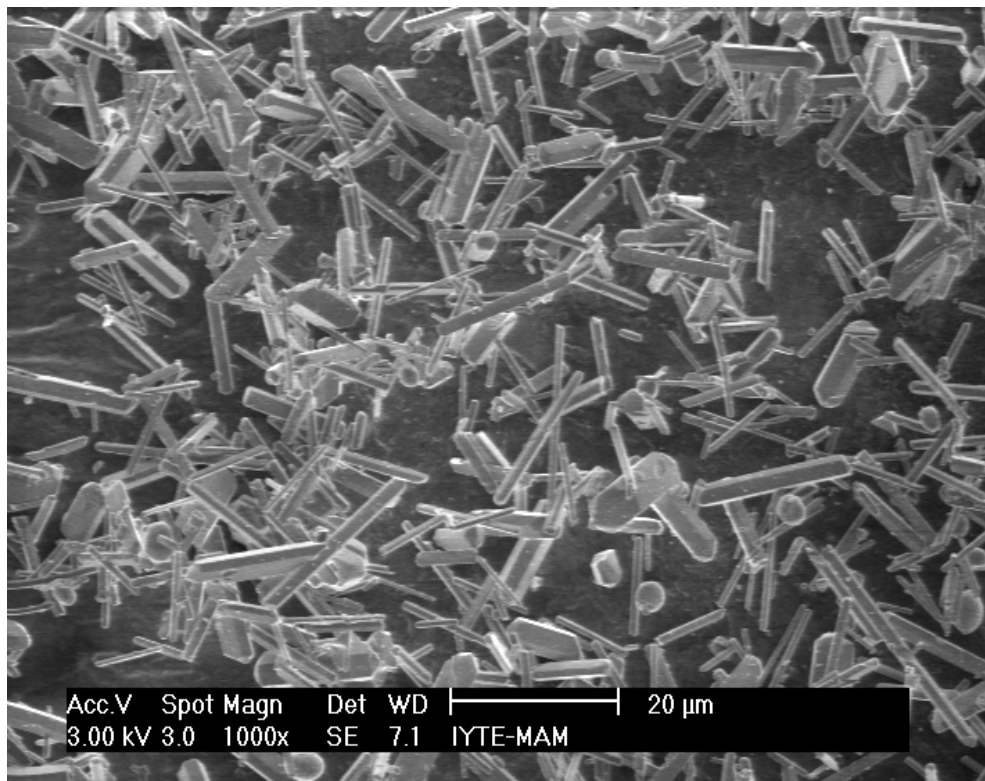


Figure 5.22. SEM image of wet mixed synthesized HA powder KW6 whiskers synthesized at 1100°C where  $K_2SO_4/HA$  ratio during preparation was 3/1.



Figure 5.23. SEM image of wet mixed commercial HA powder KW7 whiskers synthesized at 1150°C where  $K_2SO_4/HA$  ratio during preparation was 3/1.

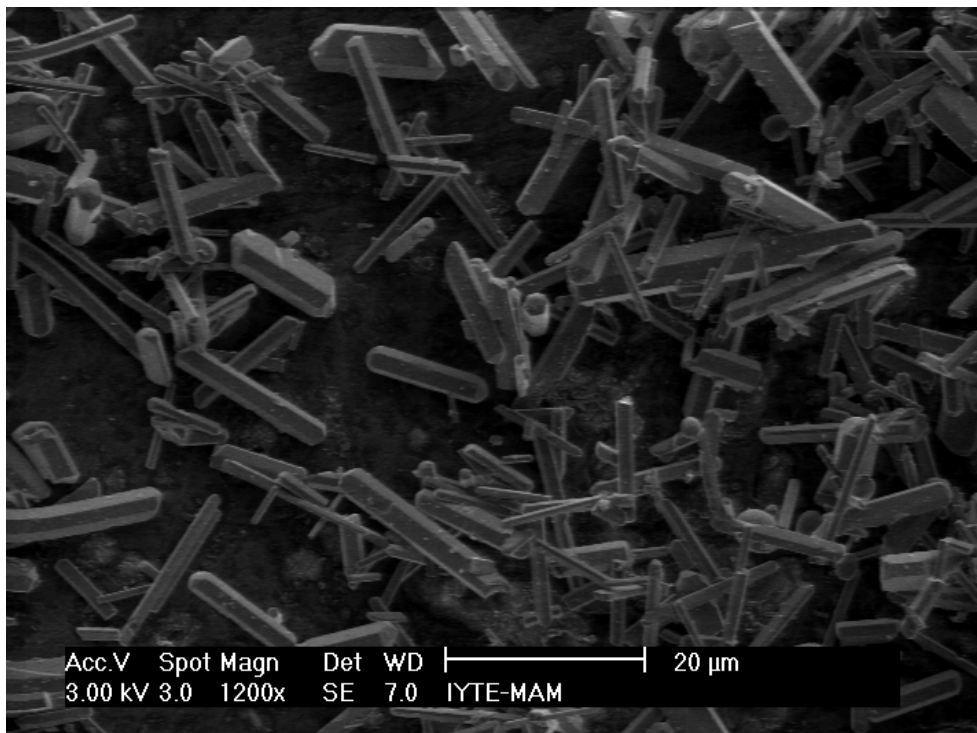


Figure 5.24. SEM image of wet mixed synthesized HA powder KW8 whiskers synthesized at 1150°C where  $K_2SO_4/HA$  ratio during preparation was 3/1.

Whiskers were finally synthesized by using  $K_2SO_4$ -NaCl salt mixture as flux and commercial HA powder as the starting HA source. The crystals could be also synthesized by using a salt mixture (Hayashi et al. 2000). As the difference between the heat treatment temperature and the melting point of the salt mixture increases, the morphology of the whiskers varies. The  $K_2SO_4$ - NaCl salt mixture was used in order to improve the whisker morphology. The  $K_2SO_4$  to NaCl ratio was fixed as 1:1 and all of the salt-HA samples were prepared in aqueous medium. The characteristics of NaCl- $K_2SO_4$ -HA whiskers synthesized at different temperatures are given in Table 5.4. K, N and W stand for “ $K_2SO_4$ ”, “NaCl” and “whisker”, respectively in sample coding. The dimensional and morphological properties were investigated by SEM analysis.

The KNW samples contained relatively long whiskers with hexagonal shape. The size distribution was very wide, the lengths varied from 12 to 110  $\mu m$  and the diameters were in the range of 0.5 to 25  $\mu m$ . Numerous small and thin whiskers were observed to be attached onto the surface of the long whiskers. Many of them were also in the form of coagulates and clusters. It may be said that some HA particles nucleate and form the first generation of crystals when supersaturation is obtained for the first time. As they begin to grow and form whiskers, other generations of HA particles nucleate and start growing. It is apparent that this event occurs repeatedly during the 2-5 hours of heat treatment time. During cooling when the temperature decreases, small HA whiskers precipitate out and are partially attached onto the surface of the larger whiskers without getting enough time for their growth. It is also likely that this crystal growth process proceeds without the need for the formation of new nuclei where original powder particles act as heterogenous nucleation sites.

Table 5.4. Preparation parameters and dimensional properties of HA whiskers prepared by using NaCl- K<sub>2</sub>SO<sub>4</sub> salt mixture.

Sample Name	Salt/HA Ratio (weight)	Heat Treatment Time (h)	Heat Treatment Temp. (°C)	Whisker Length (µm)	Whisker Diameter (µm)	Aspect Ratio
KNW1	3/1	2	800	20-80	0.7-8	10-25
KNW2	3/1	3	850	17-100	0.5-8.5	10-25
KNW3	3/1	5	825	25-95	0.8-7	10-25
KNW4	3/1	2	875	10-95	0.7-10	10-15
KNW5	3/1	2	900	12-100	0.8-25	4-25
KNW6	5/1	2	850	13-110	0.5-8	15-25

The XRD patterns of HA whiskers at various temperatures are given in Figure 5.25. The location of the peaks of the HA whiskers were close to those listed in Table 5.1 for reference HA. However, the intensity of the peaks located at 32.86° were much higher than the reference hydroxyapatite peak intensity at 31.7°. This may be attributed to the whisker orientation. This result was also observed earlier for hydrothermally synthesized HA whiskers (Yoshimura et al. 1994). The KNW5 whiskers had sharper peaks compared to the KNW1-KNW4 samples. The width of all peaks are lower than those of the original commercial HA powder. All of the KNW whiskers were totally transparent like the NW and KW whiskers when examined by optical microscopy.

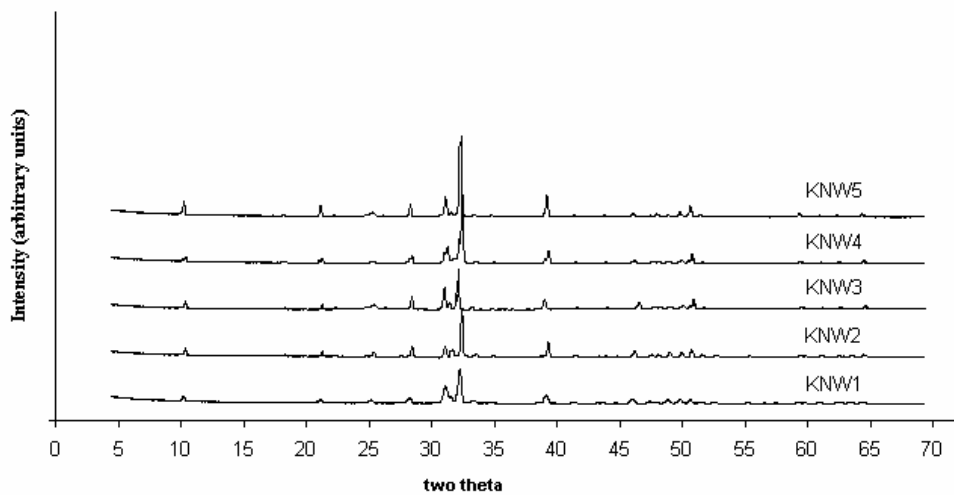


Figure 5.25. XRD patterns of KNW1, KNW2, KNW3, KNW4, KNW5.

The whisker synthesis temperature decreased compared to the experiments with NaCl or  $K_2SO_4$ . The KNW1 whiskers obtained at  $800^\circ\text{C}$  are shown in Figure 5.26 (a) and (b). The length, diameter and aspect ratios were in the range of 20-80  $\mu\text{m}$ , 0.7-8  $\mu\text{m}$  and 10-25, respectively. However, the quantities of whiskers were relatively low and many small crystals were present around the HA whiskers.

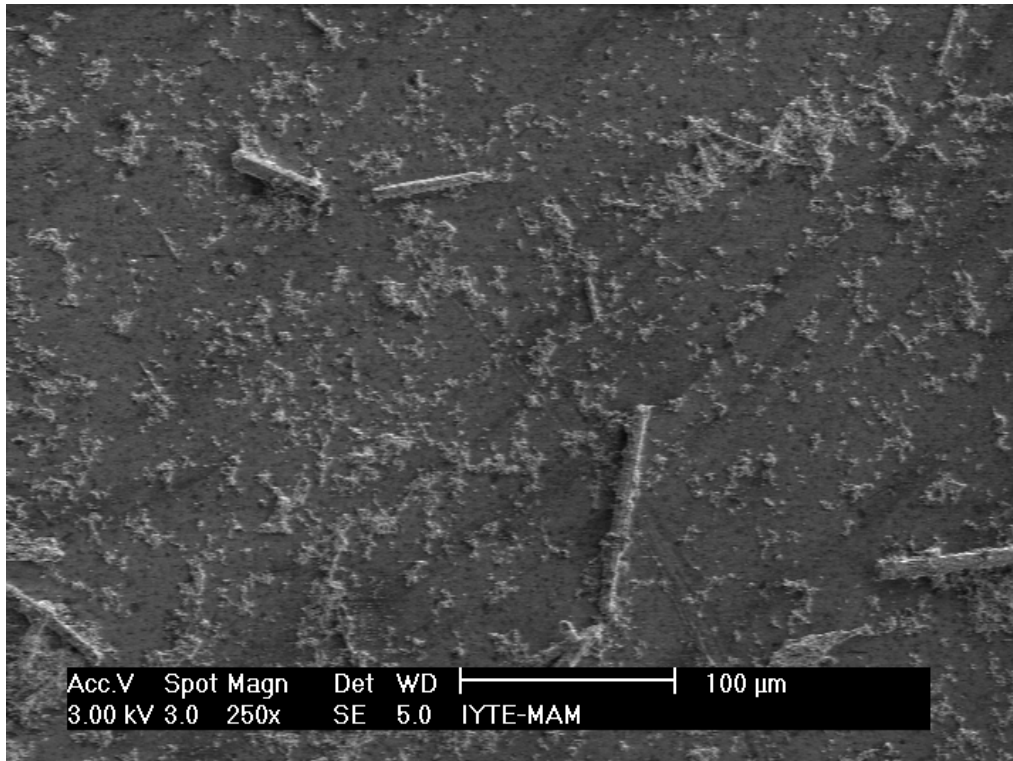


Figure 5.26 (a). SEM image of KNW1 whiskers synthesized at 800°C for 2 h where salt mixture/HA ratio during preparation was 3/1.

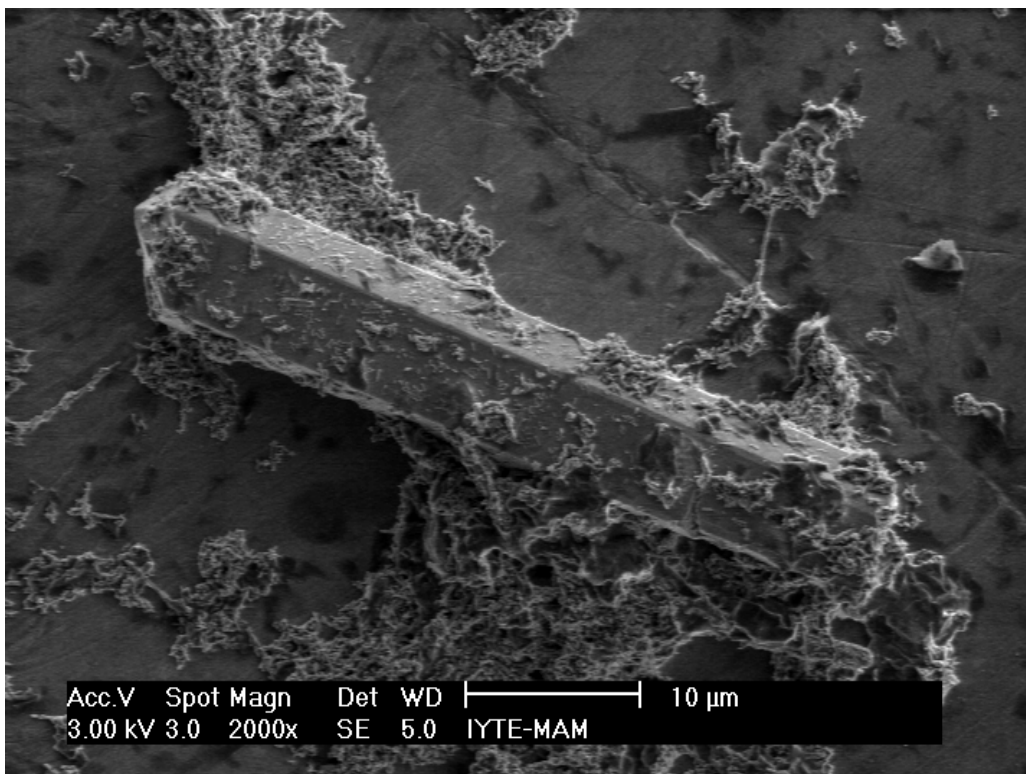


Figure 5.26 (b). SEM image of KNW1 whiskers synthesized at 800°C for 2 h where salt mixture/HA ratio during preparation was 3/1.

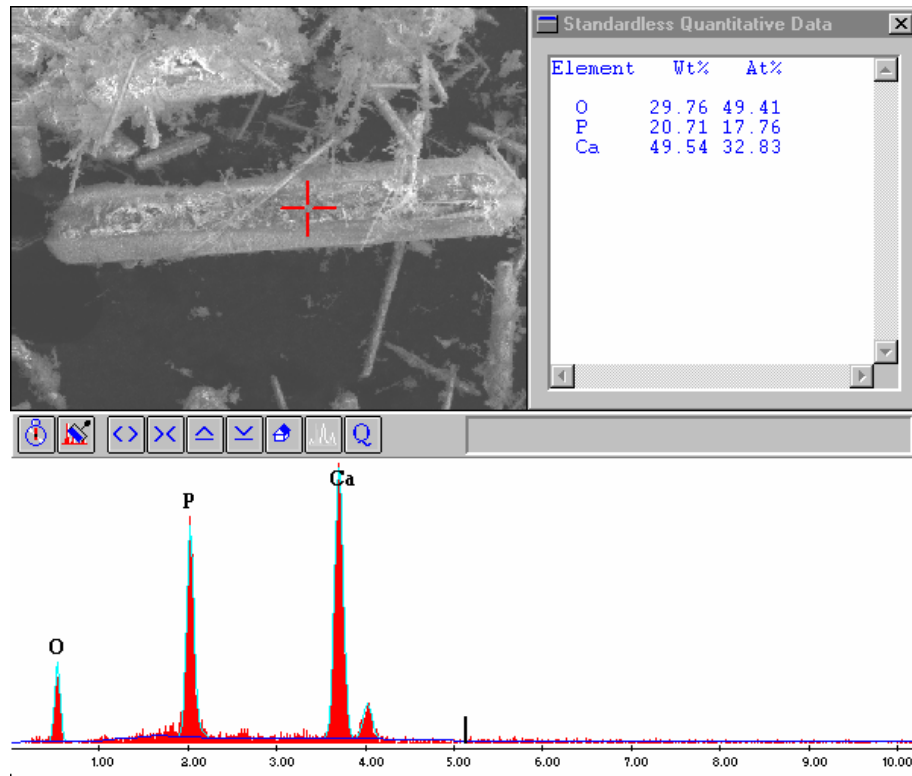


Figure 5.27 (a). EDX results of KNW2 whiskers synthesized at 850°C for 3 h where salt mixture/HA ratio during preparation was 3/1.

Hydroxyapatite whiskers synthesized at 850°C for 3 h, are seen in Figure 5.27 (a), (b) and (c). At this temperature, the quantities of formed whiskers were greater than the KNW1 whiskers. Ideal thin and long whiskers existed in the microstructure. The Ca/P ratio of KNW2 was found as approximately 1.84 according to the EDX result. Also, the length, diameter and aspect ratio of whiskers changed from 17-100  $\mu\text{m}$ , 0.5-8.5  $\mu\text{m}$  and 10-25, respectively.

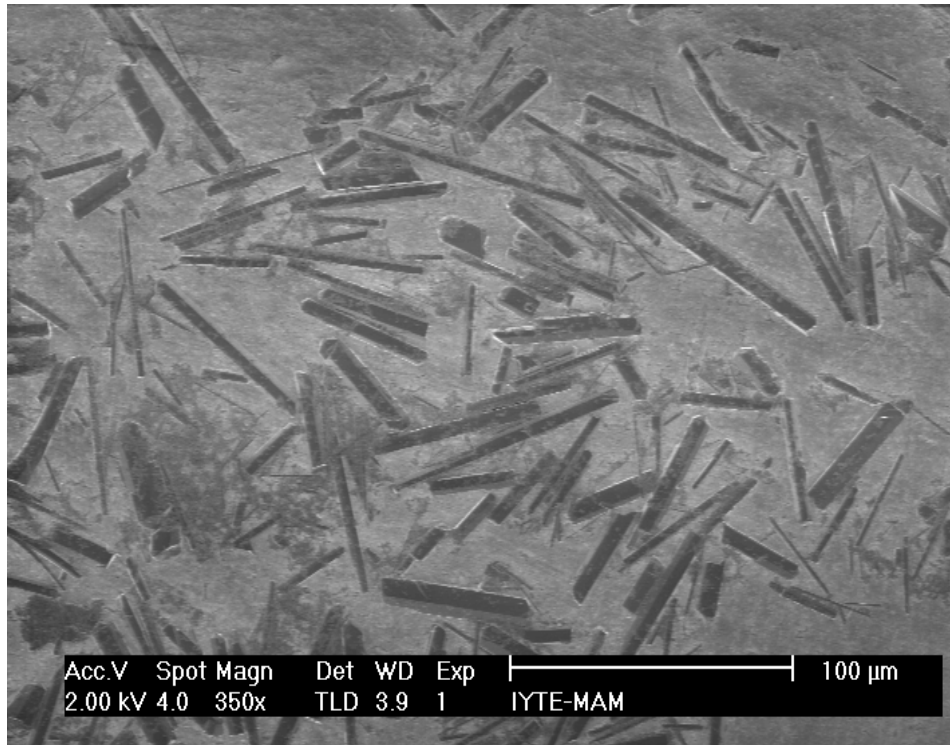


Figure 5.27 (b). SEM image of KNW2 whiskers synthesized at 850°C for 3 h where salt mixture/HA ratio during preparation was 3/1.

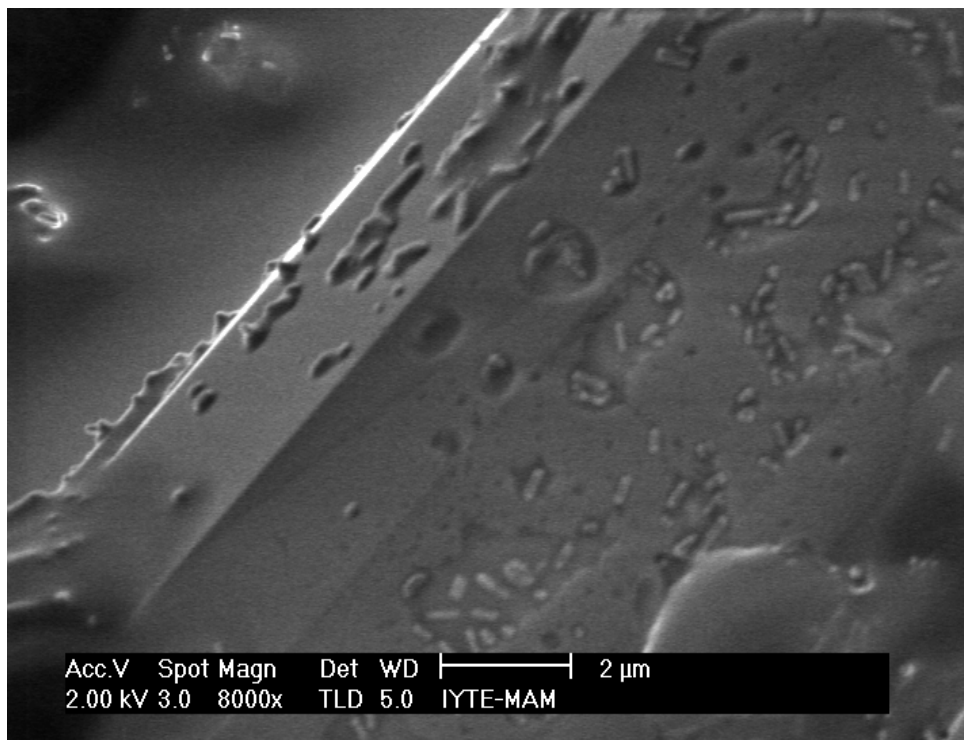


Figure 5.27 (c). SEM image of KNW2 whiskers synthesized at 850°C for 3 h where salt mixture/HA ratio during preparation was 3/1.

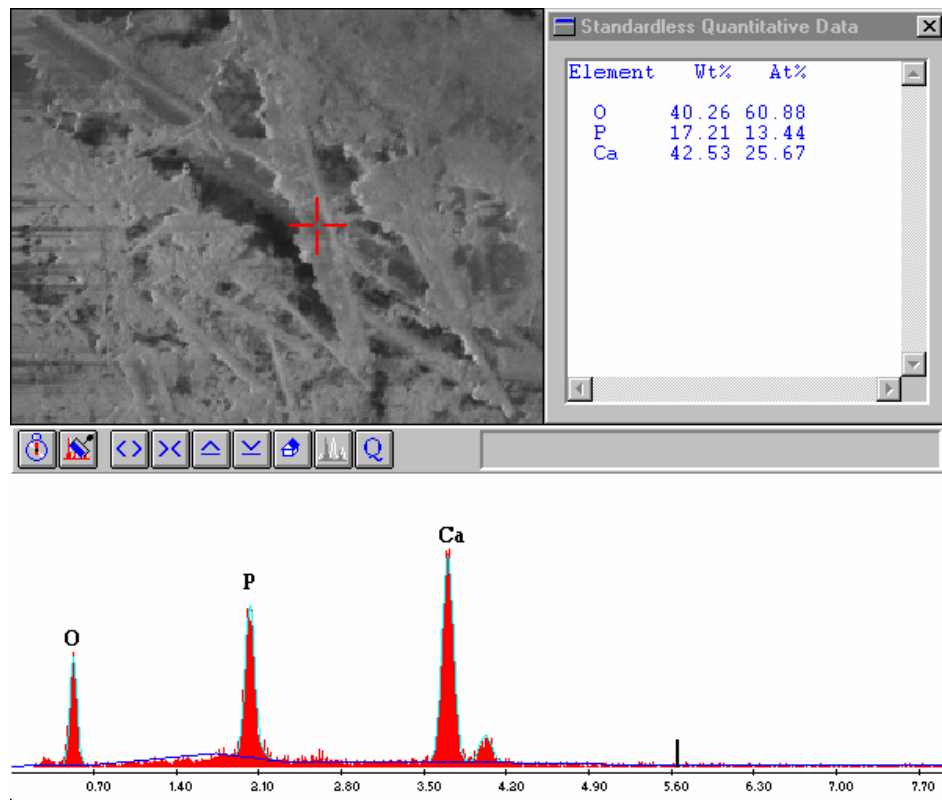


Figure 5.28 (a). EDX results of KNW3 whiskers synthesized at 825°C for 5 h where salt mixture/HA ratio during preparation was 3/1.

In order to remove the small crystals from the microstructure, the soaking temperature and time parameters were changed as 825°C and 5 h, respectively. However, no significant improvement was observed. The Ca/P ratio was found as approximately 1.9 from the EDX result. The morphology of KNW3 whiskers are shown in Figures 5.28 (b) and (c). The average length and diameters were distributed from 25 to 95  $\mu\text{m}$  and 0.8 to 7  $\mu\text{m}$ , respectively. The aspect ratios varied from 10 to 25.

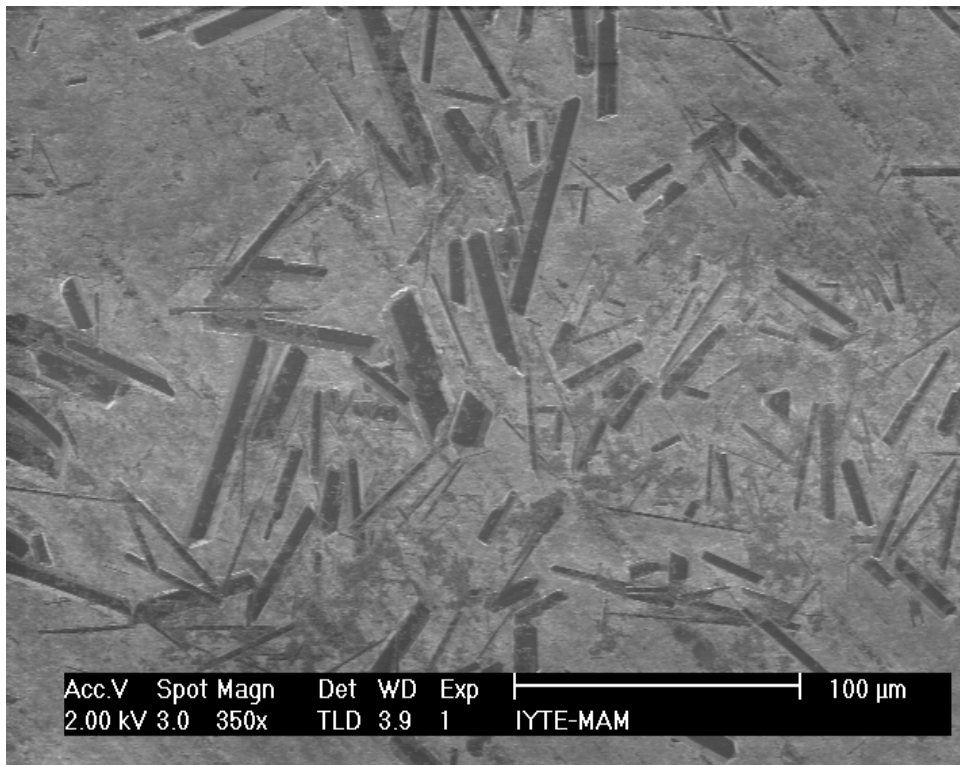


Figure 5.28 (b). SEM image of KNW3 whiskers synthesized at 825°C for 5 h where salt mixture/HA ratio during preparation was 3/1.

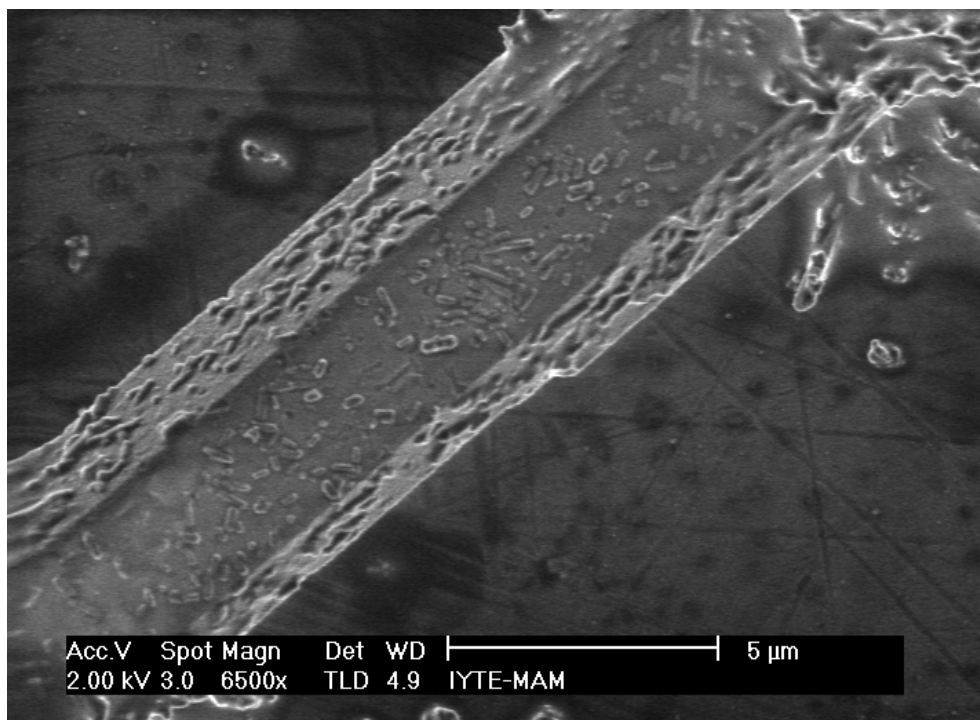


Figure 5.28 (c). SEM image of KNW3 whiskers synthesized at 825°C for 5 h where salt mixture/HA ratio during preparation was 3/1.

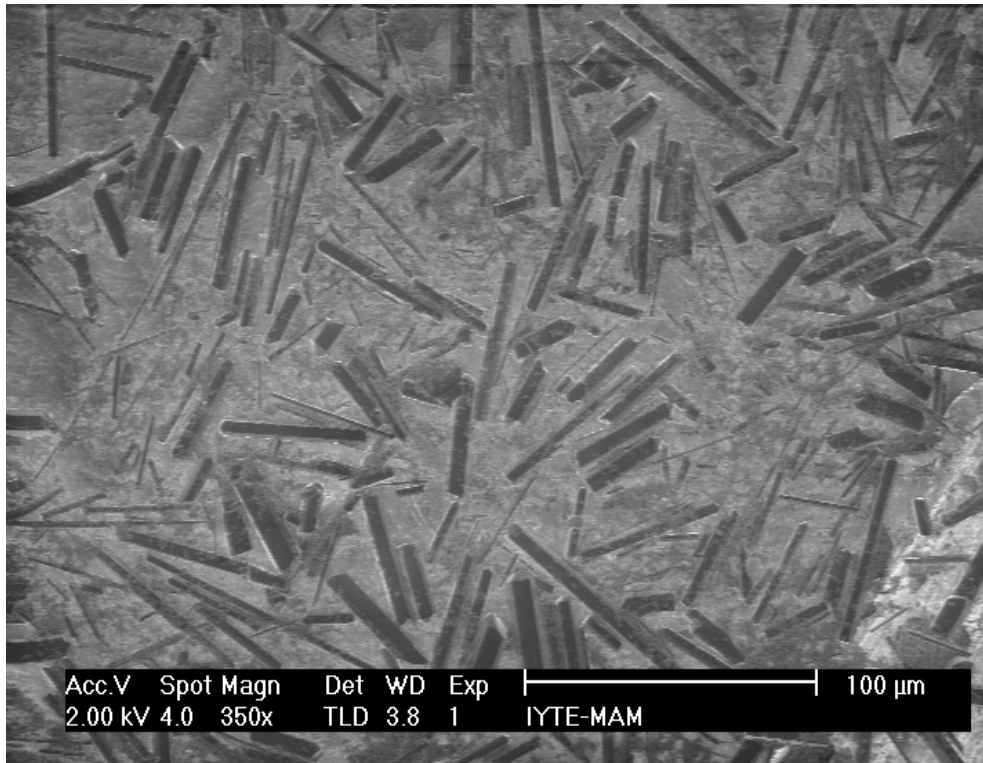


Figure 5.29 (a). SEM image of KNW4 whiskers synthesized at 875°C for 2 h where salt mixture/HA ratio during preparation was 3/1.

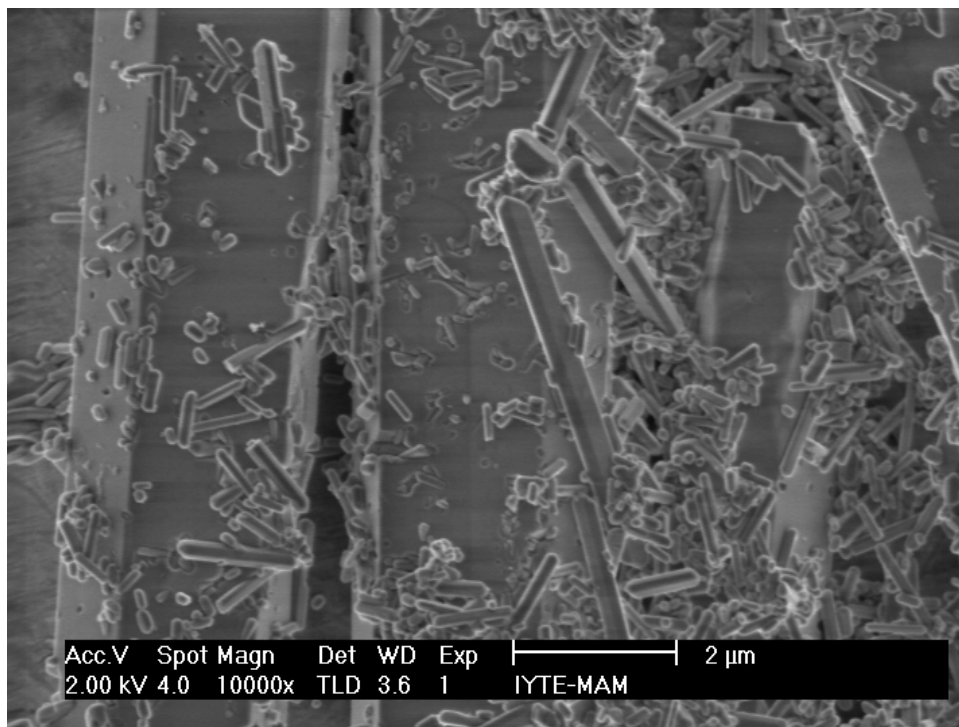


Figure 5.29 (b). SEM image of KNW4 whiskers synthesized at 875°C for 2 h where salt mixture/HA ratio during preparation was 3/1.

KNW4 whiskers produced at 875°C exhibited similar morphology and size distribution with the KNW2 and KNW3 samples. General view of whiskers and small crystals are shown in Figures 5.29 (a) and (b). The length, diameter and aspect ratio of those whiskers were in the range of 10-95  $\mu\text{m}$ , 0.7-10  $\mu\text{m}$  and 10-15, respectively.

The whiskers synthesized at 900°C are shown in Figure 5.30. The whisker size increase is mainly responsible for the sharpness of KNW5 peaks (Figure 5.25). Specifically, the diameters of some of whiskers were much greater than the other KWN samples. The length and diameters distributed from 12 to 100  $\mu\text{m}$  and 0.8 to 25  $\mu\text{m}$ , respectively. The aspect ratios ranged from 4 to 25.

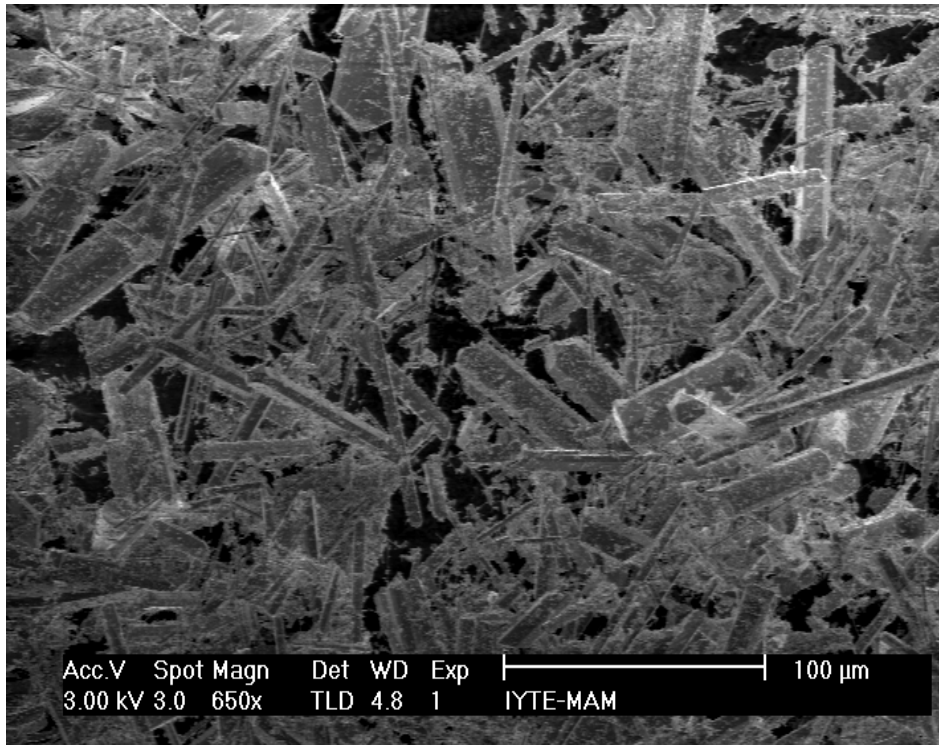


Figure 5.30 (a). SEM image of KNW5 whiskers synthesized at 900°C for 2 h where salt mixture/HA ratio during preparation was 3/1.

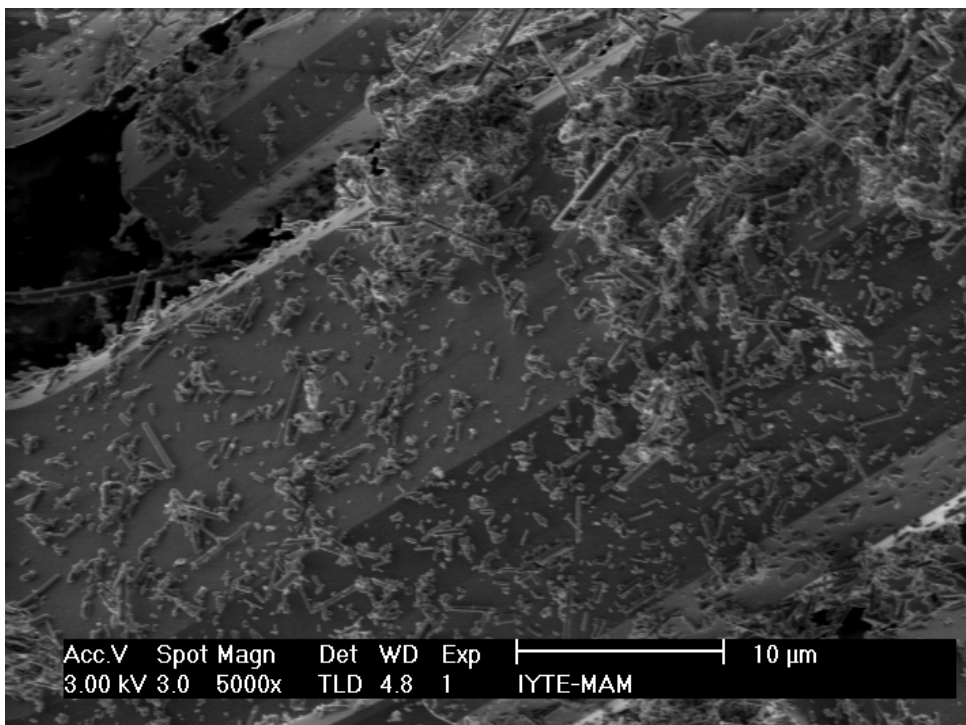


Figure 5.30 (b). SEM image of KNW5 whiskers synthesized at 900°C for 2 h where salt mixture/HA ratio during preparation was 3/1.

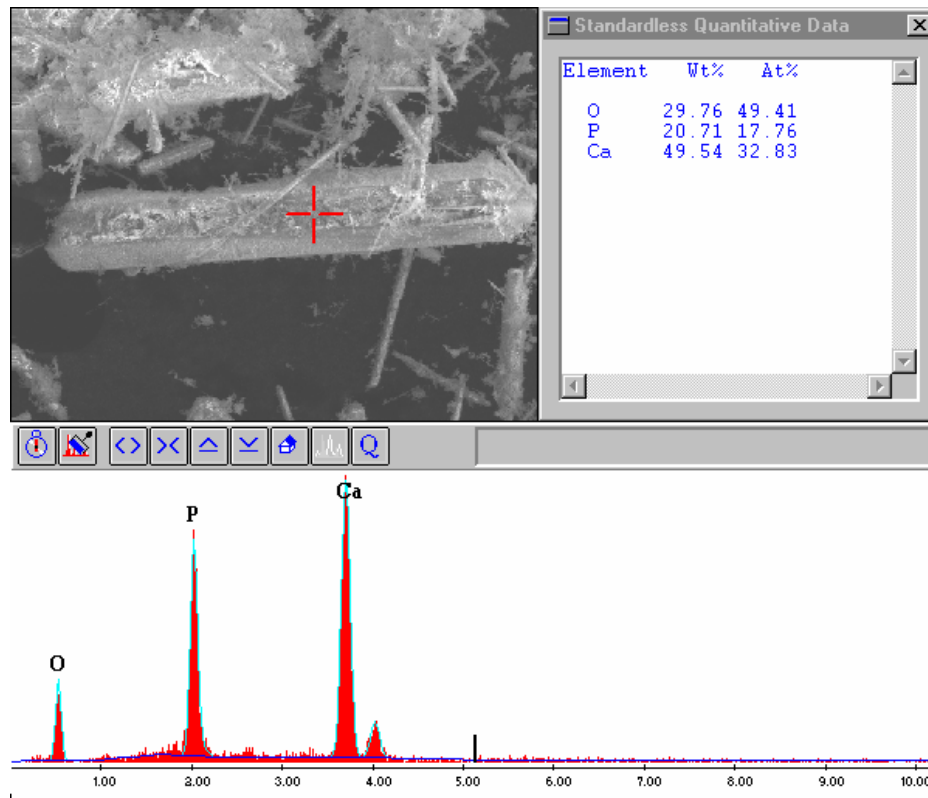


Figure 5.31 (a). EDX results of KNW6 whiskers synthesized at 850°C for 2 h where salt mixture/HA ratio during preparation was 5/1.

The salt mixture/HA powder weight ratio of KNW6 whiskers was chosen as 5/1 in order to investigate its effect on the morphology/size distribution of the samples. All of the processing conditions were kept similar with the previous KNW samples. HA powder and salt mixture were sintered at 850°C for 2 h. The Ca/P ratio was found as approximately 1.9 from the EDX result (Figure 5.31 (a)). Also, the length, diameter and aspect ratio of KNW6 whiskers were in the range of 13-110  $\mu\text{m}$ , 0.5-8  $\mu\text{m}$  and 15-25, respectively. The use of a higher salt content didn't cause any detectable differences in the morphology of the whiskers.

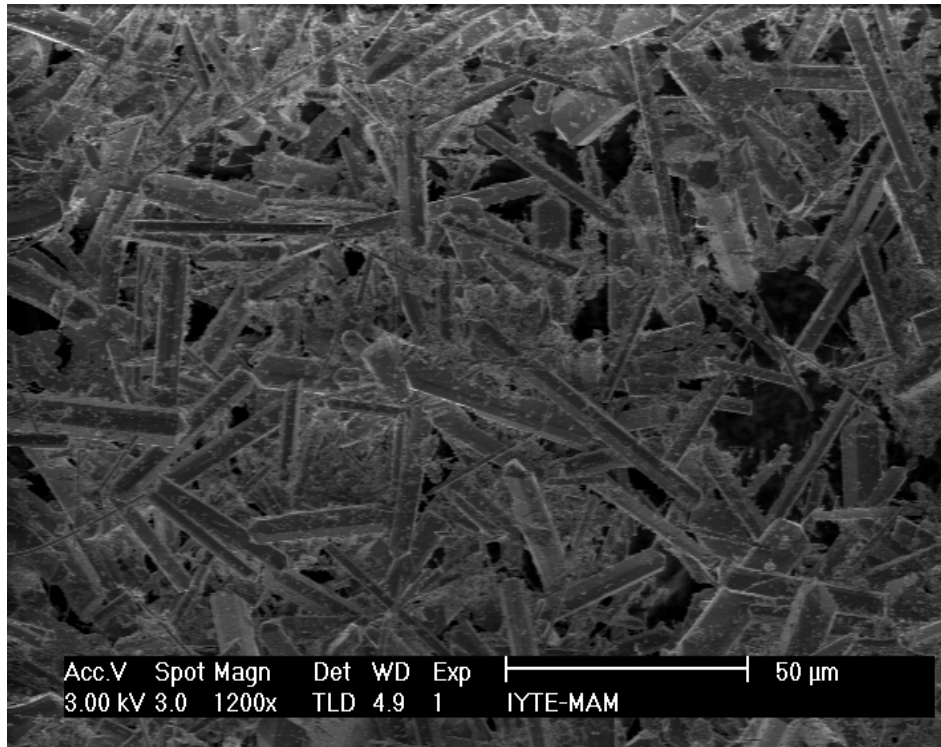


Figure 5.31 (b). SEM image of KNW6 whiskers synthesized at 850°C for 2 h where salt mixture/HA ratio during preparation was 5/1.

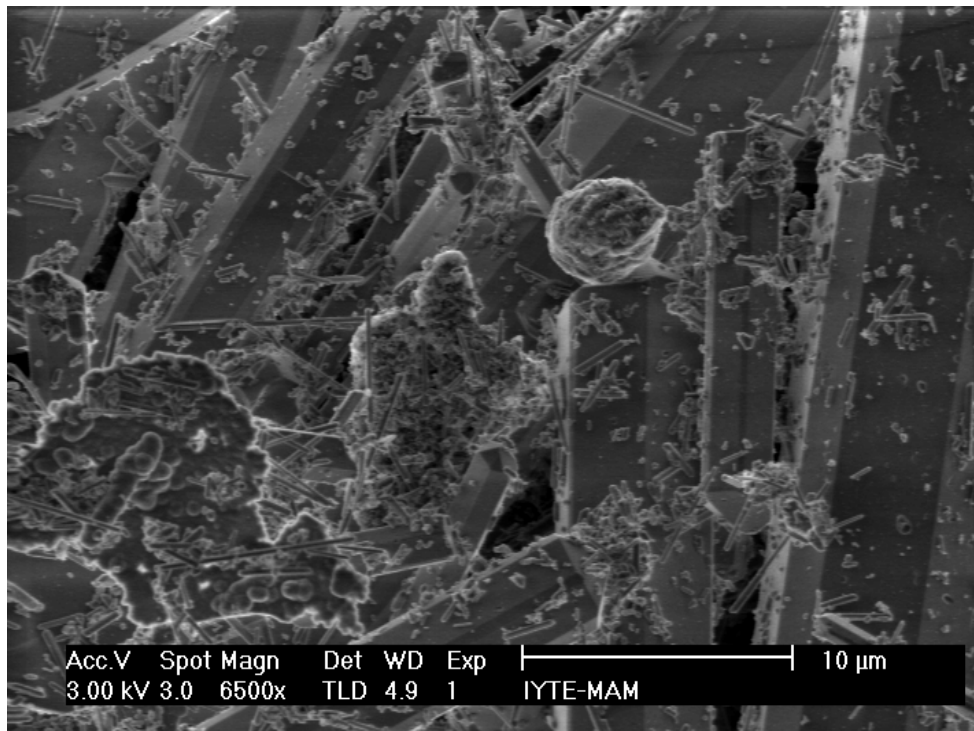


Figure 5.31 (c). SEM image of KNW6 whiskers synthesized at 850°C for 2 h where salt mixture/HA ratio during preparation was 5/1.

## 5.2. The Densification and Sintering Behaviour of Pure HA Powder and HAp/HAW Composites

The whiskers synthesized by using NaCl-K<sub>2</sub>SO<sub>4</sub> salt mixture and commercial HA powder seemed as the most proper whiskers for the composites. The KNW2 was chosen among the similar whiskers. Both pure HA and HAp/HAW composite compacts were sintered at 1200, 1250, 1300 and 1350°C in order to investigate their densification behaviour. The whisker contents of composites were varied from 10% to 50% vol/vol.

The densities of slip cast and dry pressed samples at different sintering temperatures with various whisker contents are shown in Tables 5.5 and 5.6, respectively. P, W, and SC stand for “pure HA”, “whisker” and “slip cast”, respectively in sample coding where the numbers in the codes of WSC show the % whisker content (Table 5.5.). The relative green densities of slip cast samples are given in Figure 5.32. Initially, the 50WSC composite had the highest density (55.1%) whereas commercial pure HAp exhibited the lowest value (46.4%). However, pure HAp shrunk more than the composites at all sintering temperatures and reached to 98.5% theoretical density at 1350°C. The 50WSC composite could only attain to 74.5% density at that temperature. Similar behaviour was also observed for the other HAp/HAW composites. Although the density increases with sintering temperature, the density increase relative to the green structures decreases with whisker content at each sintering temperature. This may be attributed to the hindered shrinkage rate of the composites due to the presence of whiskers during sintering.

Table 5.5. Relative densities of slip cast composites at various sintering temperatures

		<b>(%) Densities at sintering temperatures (°C)</b>				
<b>Whisker Content (%)</b>	<b>Sample Name</b>	<b>Initial</b>	<b>1200</b>	<b>1250</b>	<b>1300</b>	<b>1350</b>
0 (pure HA)	P	46.4	85.8	94.3	98	98.5
10	10WSC	48.8	73	85	91.2	94.2
20	20WSC	51	71.1	80.3	86.4	86.9
30	30WSC	52.3	69	70	77.4	83.6
40	40WSC	53.3	64.5	68.1	76	77
50	50WSC	55.1	63	67.5	72	74.5

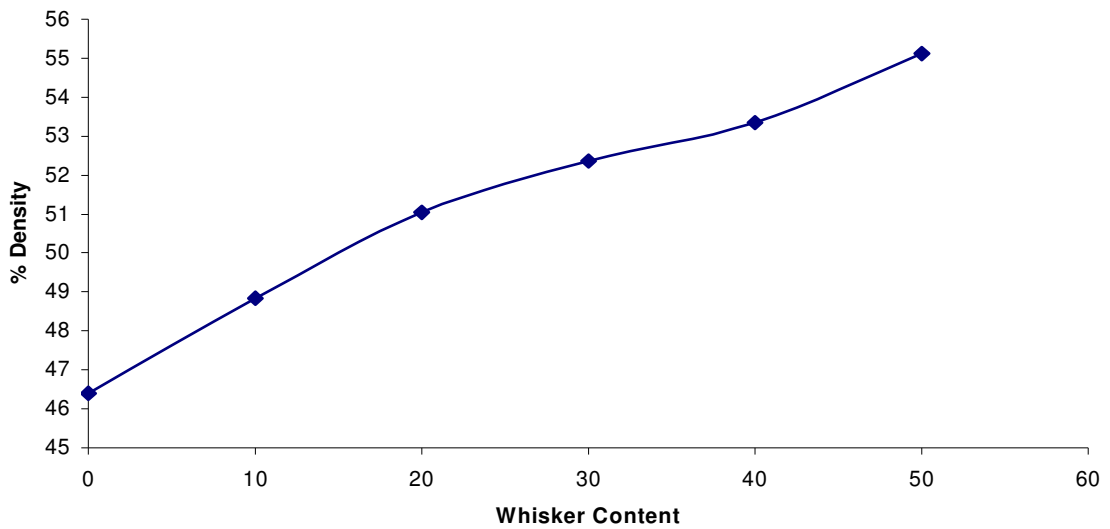


Figure 5.32. The variation of the green densities of slip cast composites with different whisker contents.

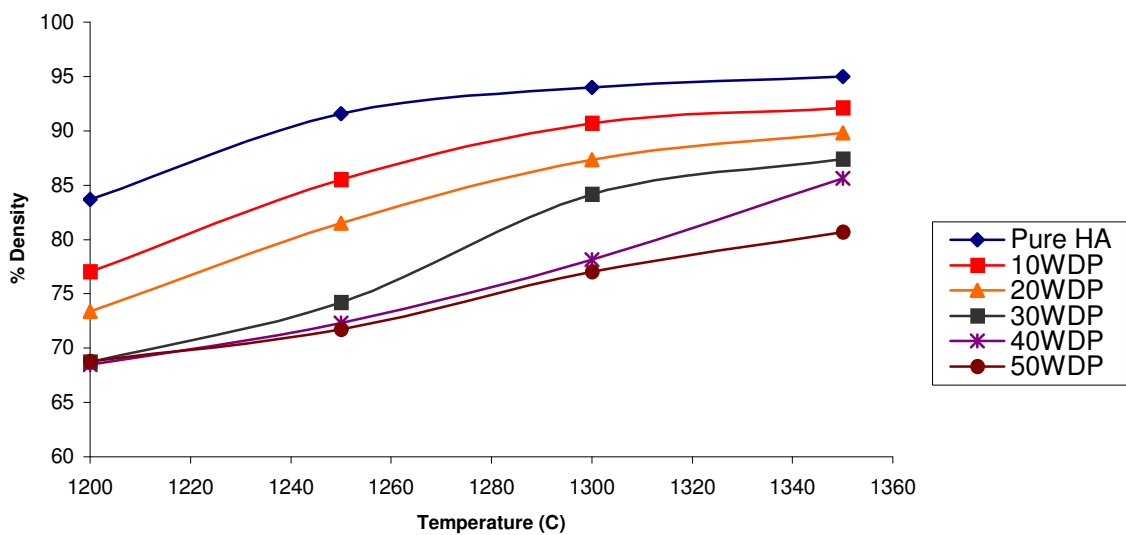


Figure 5.33. Densities of slip cast composites with different whisker contents after sintering.

The densification rates of commercial pure HAp, 10 WSC and 20WSC samples were high at 1200-1300°C range followed by a slight increase at 1300-1350°C range as shown in Figure 5.33. The density values of 30WSC and 40WSC increased continuously at 1250-1350°C and 1200-1300°C, respectively. The variation of the density of 40WSC was found as 1% in the range of 1300-1350°C. However, 50WSC composite displayed a steady density increase at all sintering temperatures.

P, W, and DP stand for “pure HA”, “whisker” and “dry press”, respectively where the numbers represent the % whisker contents in the sample codes given in Table 5.6. The relative green densities of dry pressed samples were slightly higher than the slip cast samples as shown in Figure 5.34. However, their densification behaviour closely resembled to the slip cast composites. For example, commercial pure HA powder had lowest density initially but it reached to 95% of theoretical density at 1350°C. The 10WDP was the most densified sample among the composites (92%) whereas 50WDP could only reach to 80.7% of theoretical density. The presence of whiskers was the reason of low densities similar to the slip cast composites.

Table 5.6. Relative densities of dry pressed composites at various sintering temperatures

		<b>(%) Densities at sintering temperatures (°C)</b>				
<b>Whisker Content (%)</b>	<b>Sample Name</b>	<b>Initial</b>	<b>1200</b>	<b>1250</b>	<b>1300</b>	<b>1350</b>
0 (pure HA)	P	51.2	83.7	91.6	94	95
10	10WDP	52.7	77	85.5	90.7	92
20	20WDP	54.6	73.4	81.5	87.3	89.8
30	30WDP	57.2	68.7	74.2	84.1	87.4
40	40WDP	59	68.5	72.3	78.1	85.6
50	50WDP	62.2	68.8	71.7	77	80.7

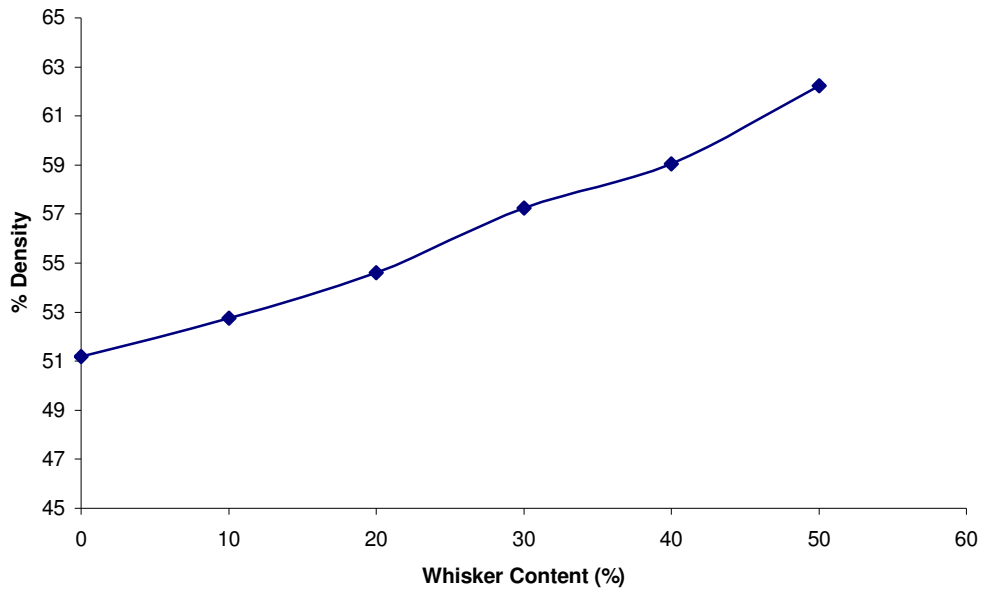


Figure 5.34. The variation of the green densities of dry pressed composites with different whisker contents.

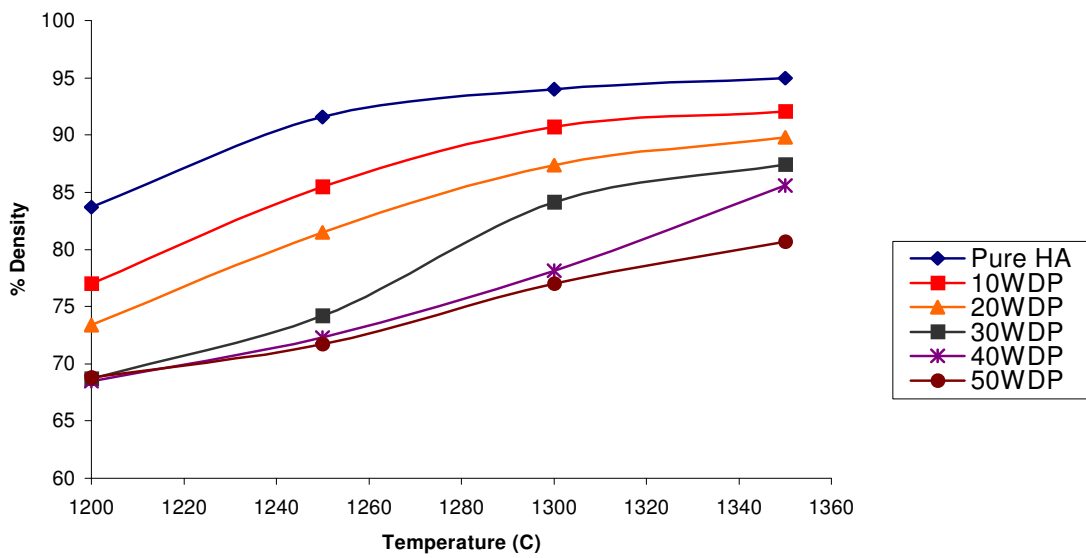


Figure 5.35. Densities of dry pressed composites with different whisker contents after sintering.

The densification rates of commercial HA powder, 10WDP and 20WDP composites were high at 1200-1300°C range followed by a slight increase at 1300-1350°C range as shown in Figure 5.35. The density increases of 30DP and 50WDP composites were high at 1200-1300°C range compared to the increases at 1300-1350°C. A steady density increase was observed for the 40WDP composite at all sintering temperatures.

### **5.3. Characterization of Pure HA Powder and HAp/HAw Composites**

The composites with various whisker content and pure HA powder were characterized by means of X-ray diffraction (XRD) and scanning electron microscopy (SEM) techniques. Both HA and HA composites start to decompose around 1250-1300°C temperature interval (Landuyt et al. 1995). C. Taş and his co-workers also synthesized HA powder which did not decompose even at 1300°C. The TCP (tricalcium phosphate) and tetracalcium phosphate are most common decomposition products for these materials at higher sintering temperatures. In this study, search-match software was used in order to detect the presence of different phases.

The dry pressed samples were subjected to X-rays (with  $\text{CuK}\alpha$ : 1.542 radiation) from 5 to 70°. Neither  $\alpha$ -TCP nor  $\beta$ -TCP was present in the structures of the materials even at 1350°C according to the XRD results. All of the samples seemed as HA at every sintering temperature whether they were stoichiometric or non-stoichiometric. However some impurities/secondary phases might be present in the composite samples which could not be detected.

The crystallinity of composites sintered at 1200°C exhibited resemblance with each other as shown in Figure 5.36. Similar behaviour was also observed for the samples sintered at 1250°C (Figure 5.37). The crystallinity of 50WDP was the highest one among the samples as expected due to its high whisker content. All the samples at 1300°C displayed close crystallinity except the 50WDP which showed the highest peak intensity (Figure 5.38). Both the composites (specifically 50WDP) and pure HA attained high intensities at 1350°C as shown in Figure 5.39.

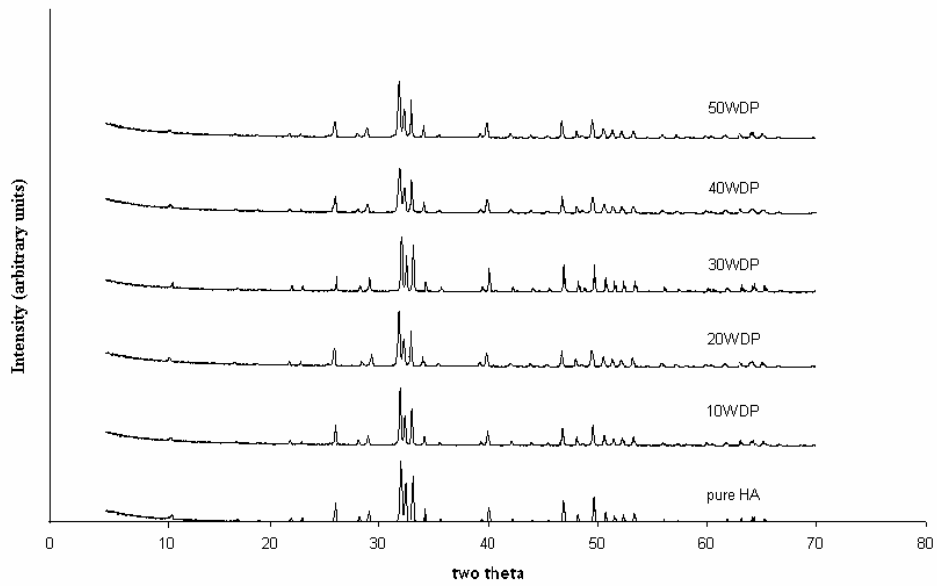


Figure 5.36. XRD patterns of pure HA powder and WDP composites with different whisker contents sintered at 1200°C.

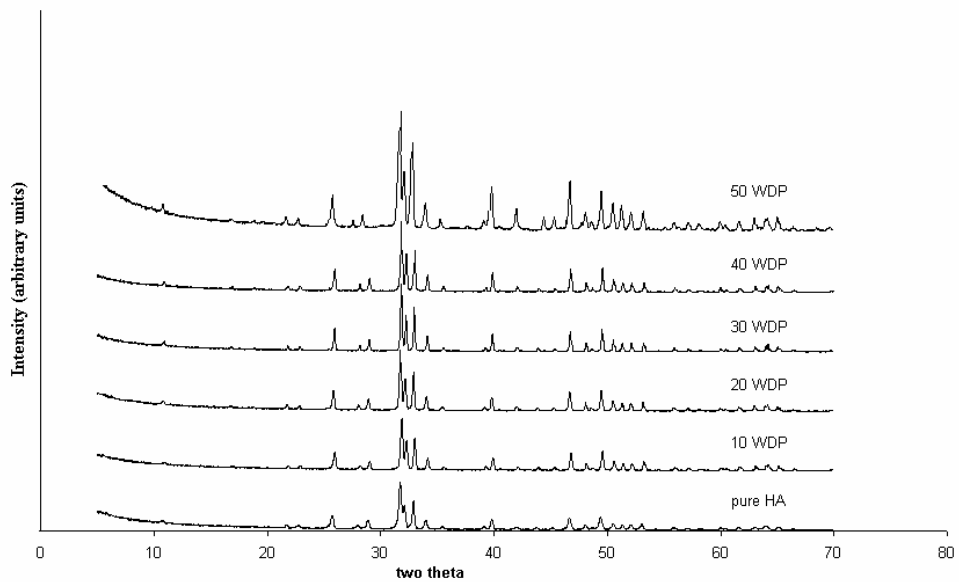


Figure 5.37. XRD patterns of pure HA powder and WDP composites with different whisker contents sintered at 1250°C.

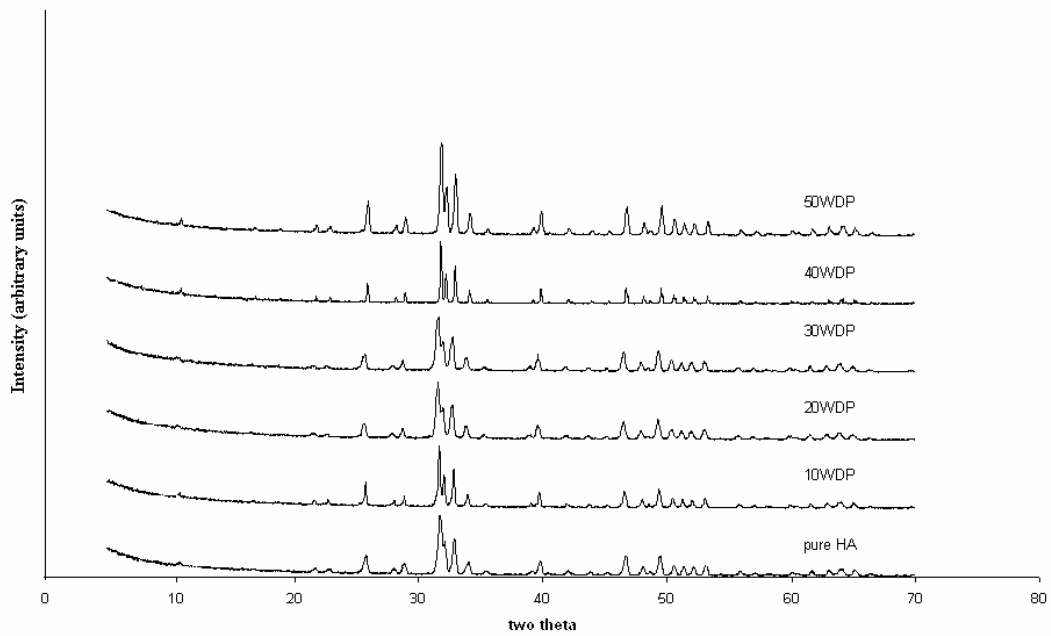


Figure 5.38. XRD patterns of pure HA powder and WDP composites with different whisker contents sintered at 1300°C.

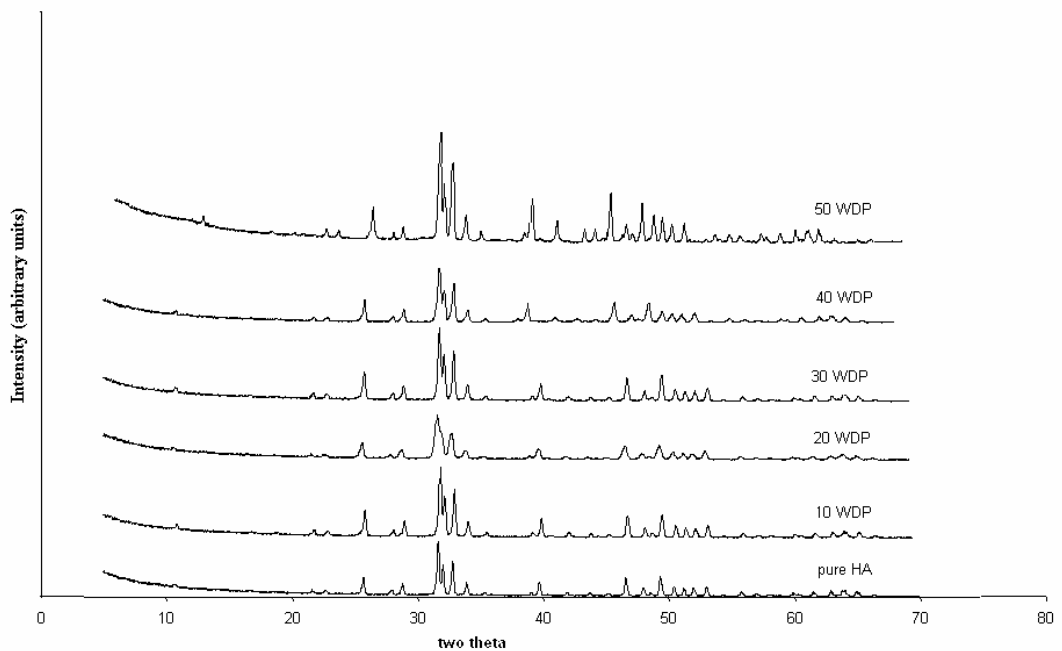


Figure 5.39. XRD patterns of pure HA powder and WDP composites with different whisker contents sintered at 1350°C.

No significant improvement was achieved for the slip cast composites according to the density results obtained after sintering. However, it was estimated that, the whiskers in the composites distributed more uniformly as compared to the dry pressed composites. In order to compare the whisker distributions of the slip cast and dry pressed samples, commercial HA powder and HA whiskers (10%-50 % vol/vol) were dry mixed without applying any mechanical process to any of them. Sintering was carried out at 1250°C for 2 h with the heating rate of 10°C/min and cooling rate of 20°C/min.

The new composites were called as WDP' where W denoted "whisker", DP' was the short form of "dry press" and the numbers in the codes of WDP' represented the "% whisker content" in sample coding. The pellets were fractured and their surfaces were investigated by SEM. The HA whiskers could be observed as embedded in the fine HA matrix for all of the composites. Neck formation were seen in the samples between the HA whiskers-HA particles and HA whiskers-HA whiskers. The size of HA particles in the composites varied from 0.45 to 2.5  $\mu\text{m}$ . The morphology and whisker size distribution of 10WSC and 20WSC composites were similar to those of 30WSC sample.

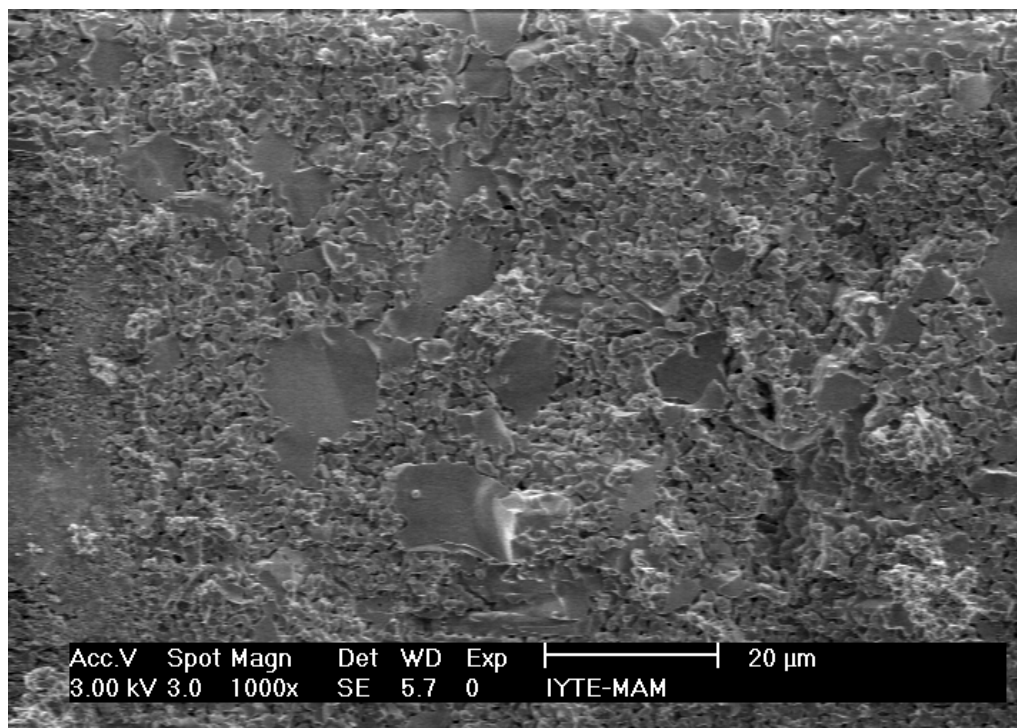


Figure 5.40. SEM image of 30WSC sample sintered at 1250°C for 2 h.

The matrix and the whiskers of 30WSC sample were uniformly blended as shown in Figure 5.40. The HA powder concentration was higher than the whiskers in the morphology of 30WSC composite as expected. However, the whiskers of 30WDP' sample accumulated in a specific region and the concentration of whiskers was higher than that of the matrix as shown in Figure 5.41. Usually, the whiskers were aligned in one specific axis for both 30WSC and 30WDP' samples.

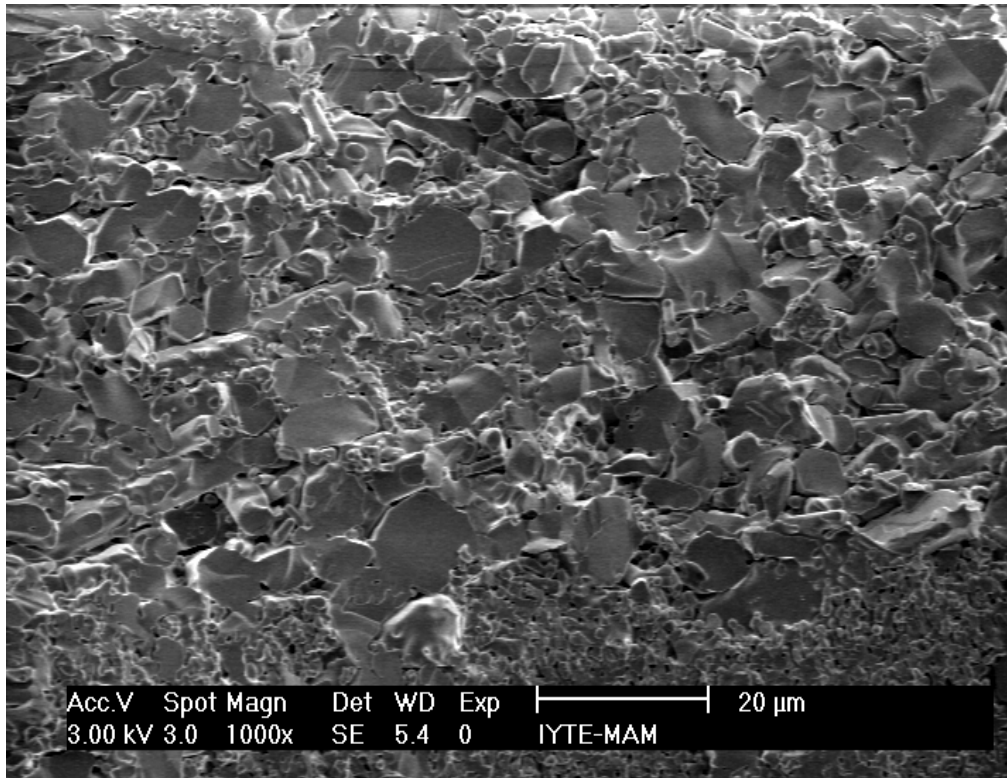


Figure 5.41. SEM image of 30WDP' sample sintered at 1250°C for 2 h.

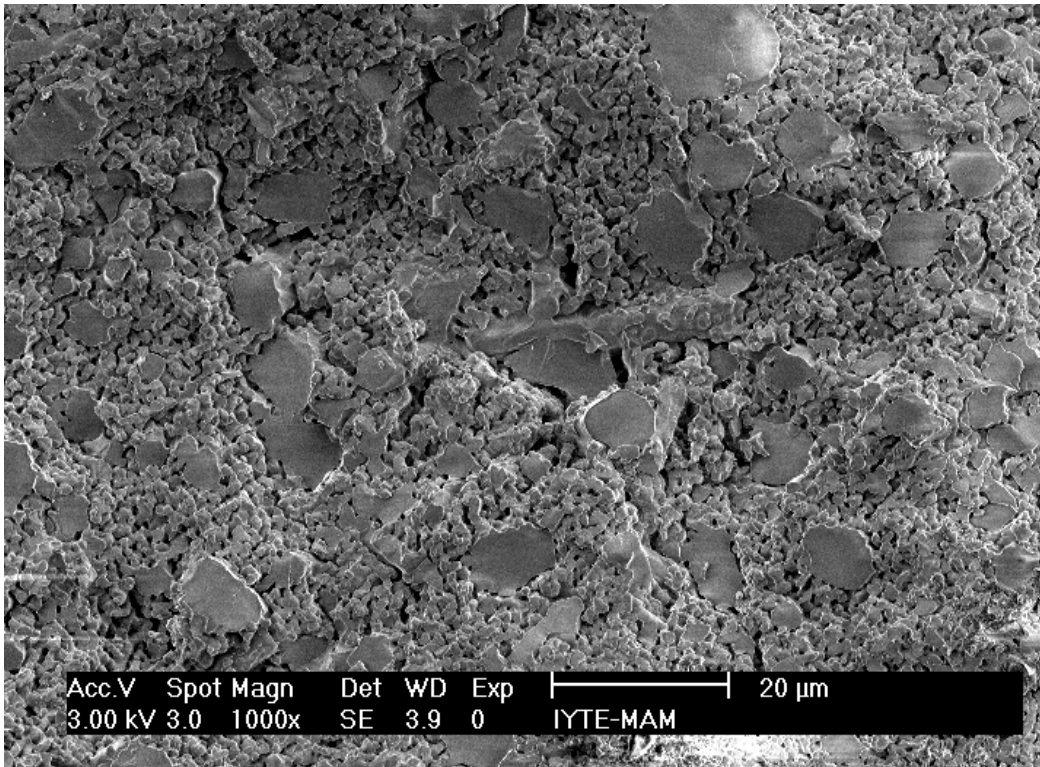


Figure 5.42. SEM image of 40WSC sample sintered at 1250°C for 2 h.

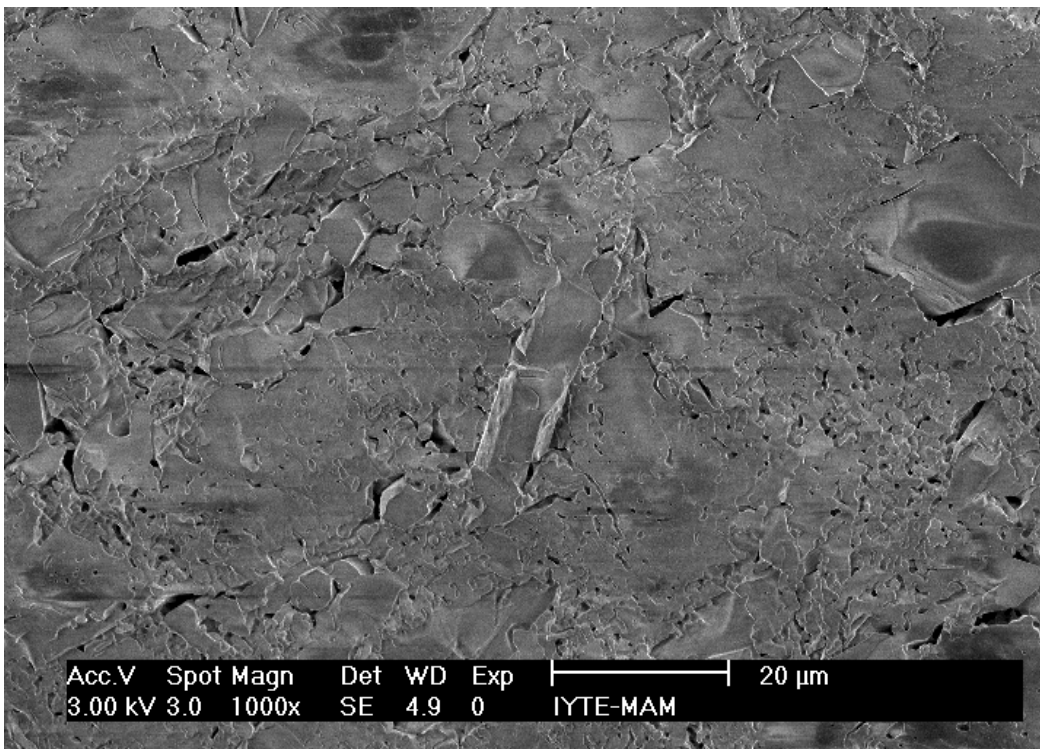


Figure 5.43. SEM image of 40WDP' sample sintered at 1250°C for 2 h.

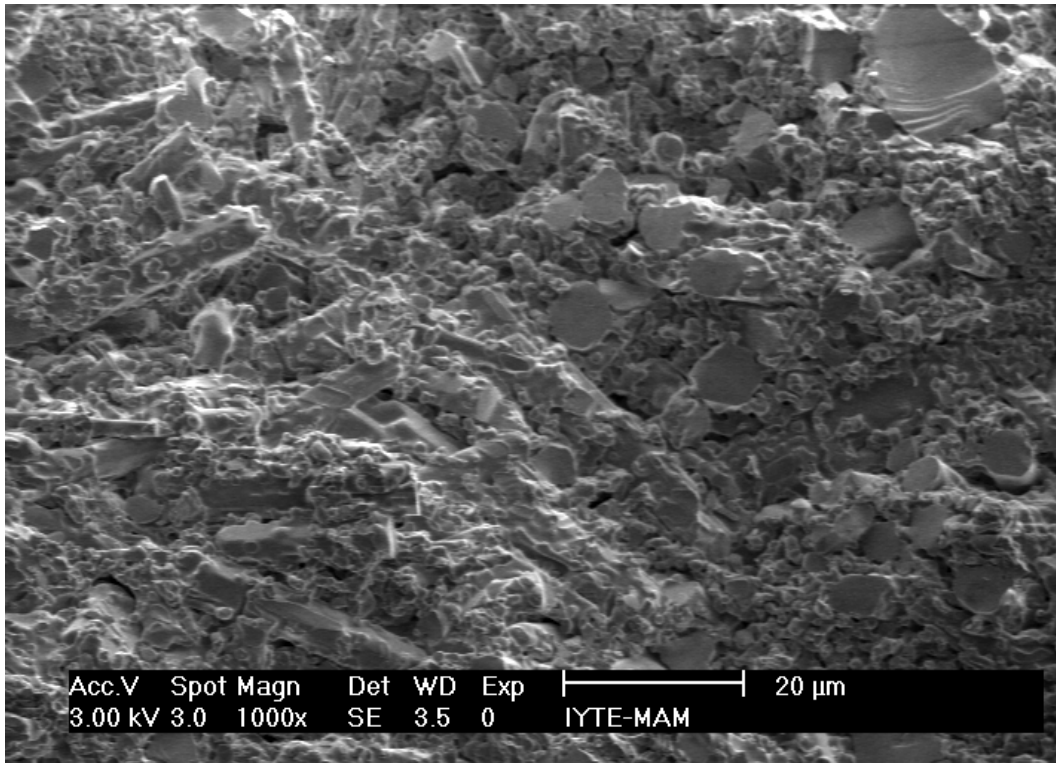


Figure 5.44. SEM image of 50WSC sample sintered at 1250°C for 2 h.

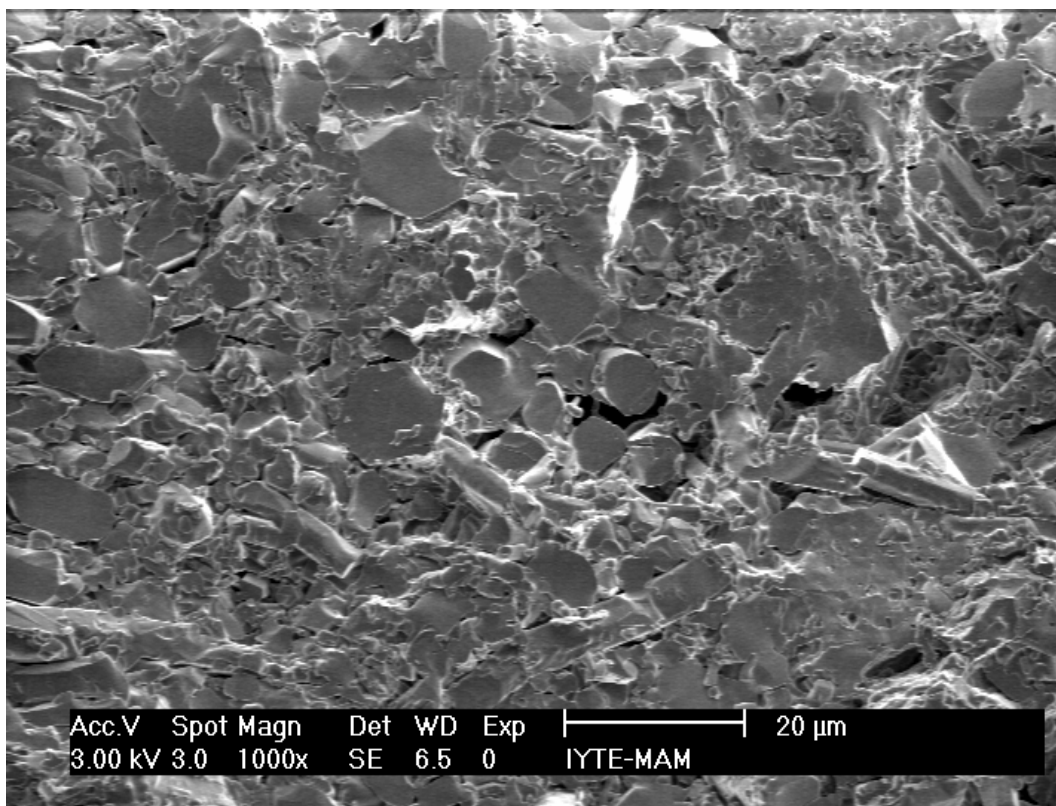


Figure 5.45. SEM image of 50WDP' sample sintered at 1250°C for 2 h.

The matrix and the whiskers were also uniformly blended in the 40WSC composite as shown in Figure 5.42. Generally the whiskers were aligned one specific direction. Unlike the other composites very large and equiaxed particles were observed in the 40WDP' sample as shown in Figure 5.43. The diameters of these whiskers become larger compared to the other samples.

The concentration of matrix and whiskers was equal to each other in the 50WSC composite (Figure 5.44). However, the alignment of the whiskers varied in the 50WSC composite different from the other slip cast samples. The morphologies of 50WDP' and 30WDP' composites showed similarity in terms of whisker distribution. The whiskers accumulated into a specific region in the 50WDP' sample where they were aligned different directions (Figure 5.45). Neck formation between the HA whiskers-HA whiskers and HA whiskers-HA particles were also observed for these composites in Figures 5.46 and 5.47.

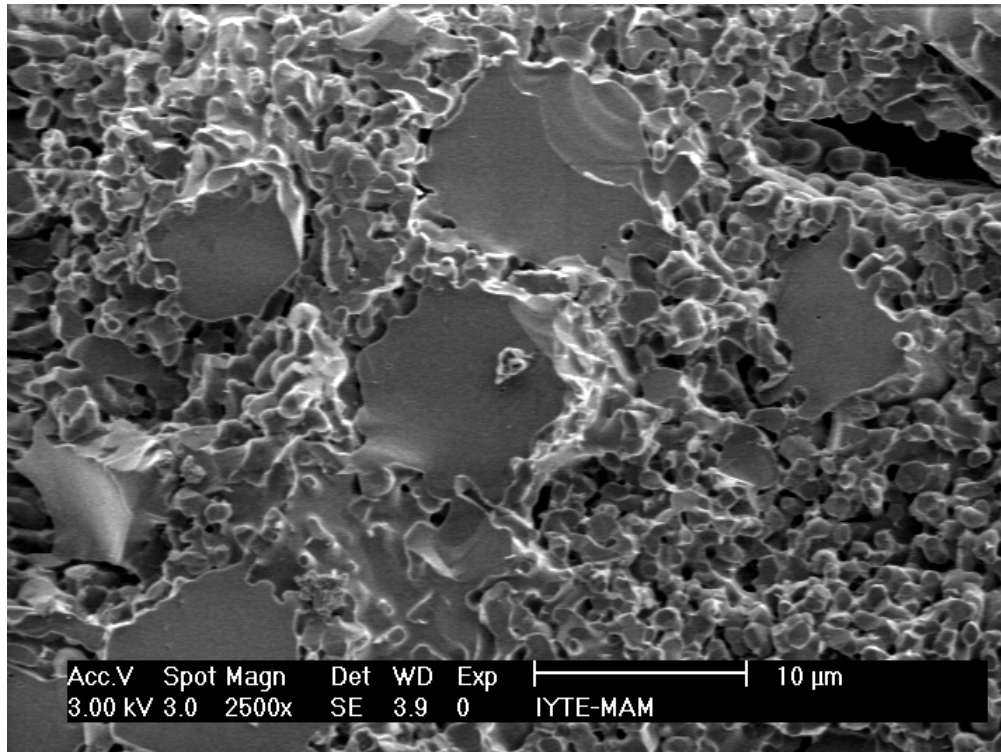


Figure 5.46. SEM image of 50WSC sample sintered at 1250°C.

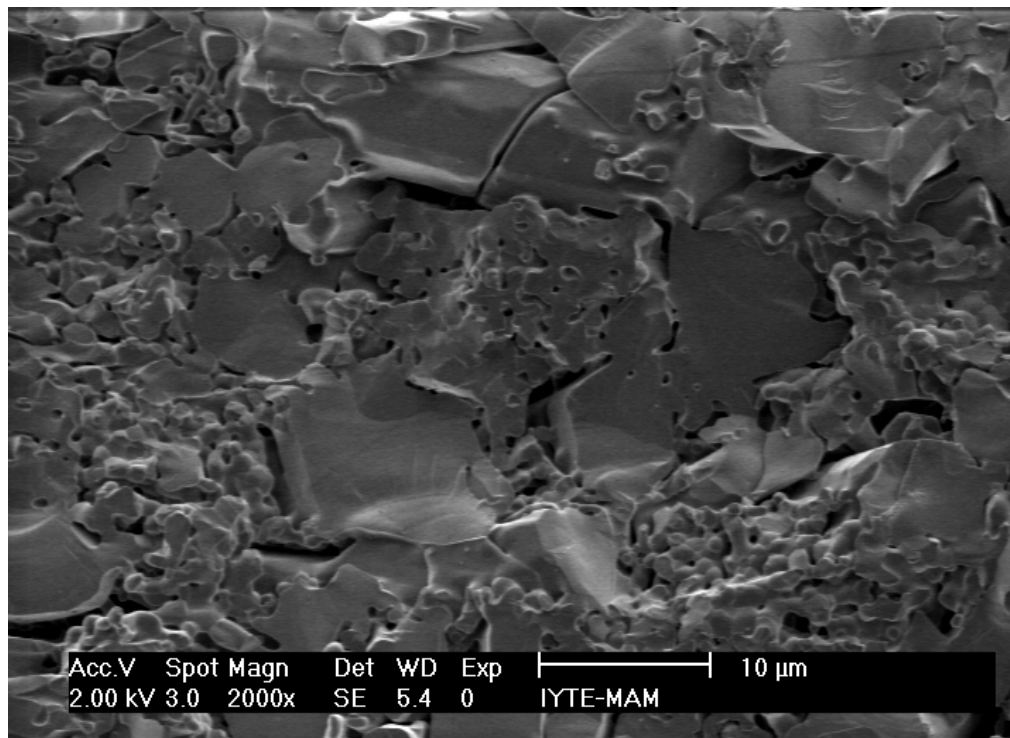


Figure 5.47. SEM image of 50WDP' sample sintered at 1250°C.

## CHAPTER 6

### CONCLUSIONS & RECOMMENDATIONS

In this study, the densification and sintering behavior of hydroxyapatite (HA) matrix reinforced with hydroxyapatite whisker (HAw) composites were investigated. Molten salt synthesis method (MSS) was performed in order to synthesize HA whiskers. The effects on whisker morphology of the alkali salt (flux) selection, the temperatures/time of synthesis, and the salt to HA powder (HAp) ratio were studied. The processing conditions of whisker synthesis were modified throughout the experiments of this work. The parameters effective on the densification behaviour of HAp/HAw composites like whisker content, formation technique and sintering temperature were also studied.

The dimensions of the whiskers synthesized by using NaCl were distributed in a broad range. The length and diameter of these whiskers varied from 0.25 to 40  $\mu\text{m}$  and 0.2 to 15  $\mu\text{m}$ , respectively. The dimensions of the whiskers obtained from  $\text{K}_2\text{SO}_4$ -HA mixture were more uniform compared to the NaCl whiskers. Recrystallization of  $\text{K}_2\text{SO}_4$ , wet mixing of  $\text{K}_2\text{SO}_4$ -HA mixture and ultrasonic treatment with glass balls were the other additional processing steps for the improvement of whisker properties. Uniform and relatively thinner HA whiskers with an aspect ratio of 30 and a typical diameter and length of 2.5  $\mu\text{m}$  and 60  $\mu\text{m}$ , respectively were produced when the salt/HA ratio was selected as 3/1. However, the presence of spherical particles with the diameter of 4-7  $\mu\text{m}$  was also detected which was not desired for the composite preparation.

The whiskers prepared from  $\text{K}_2\text{SO}_4$ -NaCl salt mixture and HA powder was synthesized at relatively low temperatures (800-900°C range). The  $\text{K}_2\text{SO}_4$  to NaCl ratio was fixed as 1:1 and all of the whiskers were synthesized by applying the same processing conditions of  $\text{K}_2\text{SO}_4$  whiskers. The size distribution was very broad, the lengths varied from 12 to 110  $\mu\text{m}$  and the diameters were in the range of 0.5 to 25  $\mu\text{m}$ . Numerous small and thin whiskers were observed to be attached onto the surface of the long whiskers. Many of them were also in the form of coagulates and clusters. It is probable that the HA particles nucleate and form the first generation of crystals when supersaturation is obtained for the first time during the crystallization of whiskers. As they begin to grow and form whiskers, other generations of HA particles nucleate and

start growing. During cooling when the temperature decreases, small HA whiskers precipitate out and are partially attached onto the surface of the larger whiskers without getting enough time for their growth.

The whiskers synthesized by using NaCl-K<sub>2</sub>SO<sub>4</sub> salt mixture and commercial HA powder seemed as the most proper reinforcements for the composites due to their morphologies and their uniformity. The whiskers synthesized at 850°C were selected among the similar whiskers due to their morphology and size distribution. Both pure HA powder and HAp/HAw composites were sintered at 1200-1350°C range in order to investigate their densification behaviour. The whisker contents of composites were varied from 10% to 50% vol/vol and they were formed by slip casting and dry pressing techniques. According to the XRD results no other phases/impurities were detected for the composites and commercial pure HAp when even sintered at 1350°C. Pure HA powder shrunk more than the composites at all sintering temperatures and reached to 98.5% theoretical density at 1350°C. The slip cast composite consisted of 50% whisker could only attain to 74.5% density at that temperature. Similar behaviour was also observed for the other HAp/HAw composites. Although the density increases with sintering temperature, the density increase relative to the green structures decreases with whisker content at each sintering temperature.

The HA whiskers could be observed as embedded in the fine HA matrix for both slip cast and dry pressed samples from the SEM images. As a result of sintering process neck formation were seen in the samples between the HA whiskers-HA particles and HA whiskers-HA whiskers. It was observed that the whiskers generally aligned in one direction except the 50% HAw-50% HAp composites.

For the first time in the MSS technique the HA whisker synthesis temperature was reduced to 800°C by using NaCl-K<sub>2</sub>SO<sub>4</sub> salt mixture. The synthesized whiskers had relatively uniform morphology and higher aspect ratios which were in the 4-25 range. The lengths and aspect ratios of whiskers were expected to be affected by the mobility of the components in the flux, which might be related to the diffusion rate of components and/or the viscosity of the flux during heating. In the future studies related to MSS method and HA, the information about the viscosities of the fluxes will be very essential in order to improve the morphology and dimensional properties. Hardness measurements, compression and fracture toughness tests can be performed for observing the effects of HA whiskers in the composites.

## REFERENCES

- Bonfield, W., 1998. "Composites for Bone Replacement", *Journal of Biomedical Engineering*: Vol. 10, pp.522-526.
- Cheanga, P., Khor, K.K. 2002. "Effect of Particulate Morphology on the Tensile Behaviour of Polymer- Hydroxyapatite Composites", *Materials Science and Engineering*. A345, pp.47-54.
- Cyster, L.A., Grant, D.M., Howdle, S.M., Rose, F.R.A.J., Irvine, D.J., Freeman, D., Scotchford, CA., Shakesheff, K.M. 2005. "The Influence of Dispersant Concentration on the Pore Morphology of Hydroxyapatite Ceramics for Bone Tissue Engineering", *Biomaterials*. Vol.26, pp.697-702.
- Hashimoto, S., Yamaguchi, A., 2000. "Synthesis of needlelike mullite particles using potassium sulfate flux", *Journal of European Ceramic Society*. Vol. 20, pp. 397-402.
- Hayashi, S., Sugai, M., Nakagawa, Z., Takei, T., Kawasaki, K., Katsuyama, T., Yasumori, A., Okada, K. 2000 "Preparation of CaSiO<sub>3</sub> Whiskers from Alkali Halide Fluxes", Vol. 20 pp. 1099-2003.
- Helmus, M. 1991. "Overview of Biomedical Materials", *MRS Bulletin*. pp.33-38.
- Hench, L.L., Wilson, J. 1993. "An Introduction to Bioceramics", *World Scientific*.
- Hench, L.L. 2002. "Biomaterials: A Forecast for the Future", *Biomaterials*. Vol. 19, pp.1423- 1429.
- Kakihana, M., Suchanek, W., Suda H., Yashima, M., 1995. "Biocompatible Whiskers with Controlled Morphology and Stoichiometry", *Journal of Material Research*. Vol. 10 pp. 521-529.

- Keiichi, K., Azuma, Y. 1999. "Molten Salt Synthesis of Single Phase BaNd<sub>2</sub>Ti<sub>4</sub>O<sub>12</sub> Powder", *Journal of Material Science*. Vol. 34, pp.301-305.
- Landuyt, P. Van., Li, F., Keustermans, J.P., Streydio, J.M., Dellanay, F. 1995. "The Influence of High Sintering Temperature on the Mechanical Properties of Hydroxyapatite", *Journal of Material Science*. Vol. 6, pp.8-13.
- Liu, D. 1997. "Preparation and Characterization of Porous Hydroxyapatite Bioceramic via Slip-Casting Route", *Ceramics International*. Vol.24, pp.441-446.
- Nakahira, A., Tamai, M., Miki, S. 2003. "Fracture Behavior and Biocompatibility Evaluation of Nylon Infiltrated Porous Hydroxyapatite", *Journal of Material Science*. Vol. 37, pp.44255-4430.
- Park, J., Lakes, R.S. 1992 "Biomaterials: An Introduction", *Plenum Press*.
- Ramachandro Rao, R., Kannan Thandali, S. 2001. "Dispersion and Slip Casting of Hydroxyapatite", *Journal of American Ceramic Society*. Vol. 84, pp.1710-1716.
- Ramakrishna, S., Mayer, J., Wintermantel, E., Leong, K.W. 2001. "Biomedical Applications of Polymer Composite Materials: A Review", *Composite Science and Technology*. Vol. 61, pp.1124-1189.
- Rodriguez-Lorenzo, L.M., Vallet-Regi, M., Ferreira, J.M.F. 2001. "Colloidal Processing of Hydroxyapatite", *Biomaterials*. Vol. 22, pp.1847-1852.
- Suchanek, W., Yoshimura, M. 1998. "Processing and Properties of Hydroxyapatite-based Biomaterials for Use as Hard Tissue Replacement Implants", *Journal of Material Research*. Vol. 13, pp.94-116.
- Suchanek, W., Kakihana, M., Suda H., Yashima, M. 1996. "Processing and Mechanical Properties of Hydroxyapatite Reinforced with Hydroxyapatite Whiskers", *Biomaterials*. Vol. 17, pp.1715-1723.

- Suchanek, W., Kakihana, M., Suda H., Yashima, M. 1996. "Hydroxyapatite/Hydroxyapatite-Whisker Composites without Sintering Additives: Mechanical Properties and Microstructural Evolution", *Journal of American Ceramic Society*. Vol.80, pp.2805-2813.
- Suchanek, W., Kakihana, M., Suda H., Yashima, M. 1996. "Biocompatible Whiskers with Controlled Morphology and Stoichiometry", *Journal of Material Research*. Vol.10, pp.521-529.
- Suda, H., Yoshimura, M. 1994. "Hydrothermal Synthesis of Biocompatible Whiskers", *Journal of Material Science*. Vol. 29, pp.3399–3402.
- Suetsugu, Y., Tanaka, J. 1999 "Crystal Growth of Carbonate Apatite Using a CaCO<sub>3</sub> Flux", *Journal of Material Science: Materials of Medicine*. Vol. 10, pp.561-566.
- Taş, C. 2001. "Molten Salt Synthesis of Calcium Hydroxyapatite Whiskers", *Journal of American Ceramic Society*. Vol. 84, pp.295-300.
- Thangamani, N., Chinnakali, K., Gnanam, F.D. 2002. "The Effect of Powder Processing on Densification and Mechanical Properties of Hydroxyapatite", *Ceramics International*. Vol. 28, pp.355-362.
- Yoon, K.H., Cho, Y.S., Kang, D.H. 1998. "Review: Molten Salt Synthesis of Lead-based Relaxors", *Journal of Material Science*. Vol. 33, pp.2977–2984.
- Zang, H., Yan, Y., Wang, Y., Li, S. 2002. "Thermal Stability of Hydroxyapatite Whiskers Prepared by Homogeneous Precipitation", *Advanced Engineering Materials*. Vol.4, No:12, pp.916-919.
- Zyan, Z., Ivanov, I., Rochmistrov, D., Glushko, V., Tkachenko, N., Kijko, S. 2001. "Sintering Peculiarities for Hydroxyapatite with Different Degrees of Crystallinity". *Journal of Biomedical Materials Research*. Vol.54, pp.256-263.